cROSstalk
-
Examination of adaptations and signaling interactions between *Hydra* and its main bacterial colonizer *Curvibacter*

Inaugural-Dissertation

zur Erlangung des Doktorgrades
der Mathematisch-Naturwissenschaftlichen Fakultät
der Heinrich-Heine-Universität Düsseldorf

vorgelegt von

Timo Minten
aus Köln

Düsseldorf, Mai 2025

aus dem Institut für Zoologie und Organismischen Interaktionen
der Heinrich-Heine-Universität Düsseldorf

Gedruckt mit der Genehmigung der
Mathematisch-Naturwissenschaftlichen Fakultät der
Heinrich-Heine-Universität Düsseldorf

Berichterstatter:

1. Prof. Dr. Sebastian Fraune

2. Prof. Dr. Martin Beye

Tag der mündlichen Prüfung:

Contents

Contents

Contents

Contents

Abstract

Every multicellular organism coexists with a complex microbial community. Together they form the holobiont, a unified biological system essential for host physiology, immunity, and development. The holobiont concept has redefined animal development as a product of dynamic interactions between a host and its associated microbiota, rather than only an autonomous process of the host. The symbiosis between the freshwater polyp *Hydra vulgaris* and its dominant bacterial colonizer *Curvibacter* lately has emerged as a powerful model to study inter-kingdom interactions.

In this thesis I investigate evolutionary and functional dynamics of this symbiotic relationship and establish a new method to quantify *in vivo* fluorescence signals in *Hydra* polyps.

Phylogenetic analysis using 16S rRNA and GyrB gene sequencing revealed a strong congruence between the phylogenetic trees of *Curvibacter* strains isolated from various *Hydra* species and their corresponding *Hydra* hosts. Taken together with results from prior studies, this suggests a pattern of co-speciation and phylosymbiosis between *Hydra* and *Curvibacter*.

Additionally, I used metatranscriptomic profiling to identify *Curvibacter* genes involved in host colonization. Most of the top upregulated genes during symbiosis are involved in scavenging of reactive oxygen species (ROS), including the *ohrR/ohrA* operon. Examination on the presence of ROS in the *Hydra* holobiont, using a newly established method for high-throughput live cell imaging of *Hydra* polyps, revealed that germ-free polyps exhibit elevated ROS levels. Wild type *Curvibacter* on its own was able to significantly reduce these elevated ROS levels, while a newly created *ΔohrR/ohrA* mutant failed to do so. These initial findings reveal an important role of *Curvibacter* in regulating ROS homeostasis in the *Hydra* holobiont.

Together, these findings demonstrate that host-microbe interactions are shaped by evolutionary history and fine-scale molecular dialogues, reinforcing *Hydra* and *Curvibacter* as a model for unraveling basal principles of holobiont biology.

Introduction

The holobiont concept

Today it is a well-known fact that a comprehensive understanding of an organism's physiological and biochemical processes requires consideration of not only that organism alone, but also its whole environment, be it biotic or abiotic. The importance of inter-species interactions in a given environment and between the organism and the environment itself can be dated back to the theory of "biocenosis" introduced by Karl Möbius, describing a community of organisms and their interactions in their shared habitat (Möbius 1877). The significance of bacteria, and their interactions with certain environments or host-organisms started to attract attention in the late 19th century. Pioneering studies, such as those of Hellriegel and Wilfarth on the endosymbiotic nitrogen-fixing bacteria of legumes (Hellriegel and Wilfarth 1888), of ZoBell on the importance of bacteria for the marine ecosystem (ZoBell 1946) or of Marples from 1969, which described the human skin as a functioning ecosystem (Marples 1969), illustrate the shift in modern research from viewing bacteria only as pathogens, to focusing more on revealing their potential beneficial effects and interactions.

This also led to the realization that organisms do not evolve in complete isolation, but rather in dynamic interactions with other life forms. Already in 1943, German theoretical biologist Adolf Meyer-Abich published his first theory on the topic of "Holobiose" (holobiosis), followed by extensive research on this topic (Meyer-Abich 1943; Meyer-Abich 1948; Meyer-Abich 1950; Meyer-Abich 1963). He acknowledged the fact that no organism lives a sole entity in this world. He argued that the resulting interactions are a base principle for the evolution of higher organisms, stating: "So gibt uns die Theorie der Typensynthese durch Holobiose einen gänzlich neuen umfassenden Ausblick über die Entwicklung der höheren Organismen aus den niederen nach rein biologischen Gesichtspunkten. Niemand kann bezweifeln, dass Parasitosen, Symbiosen und Holobiosen typisch organismische Vorgänge sind, die ständig überall dort vorkommen, wo überhaupt Leben auftritt. Nicht mehr entwickelt

sich nun Höheres aus Niederem nach sinnlos waltenden mechanischen Kräften, sondern in aktiver Schaffenskraft planvoll aus planvollem organismischem Geschehen selbst heraus!“ (The theory of type-synthesis through holobiosis gives us a completely new, comprehensive view of the development of the higher organisms from lower ones, from a purely biological point of view. Nobody can doubt that parasitosis, symbiosis and holobiosis are typical organismic processes that occur constantly wherever life occurs. Higher things no longer develop from lower things according to meaningless mechanical forces, but rather in active creative power in a planned manner from planned organismic events themselves) (Meyer-Abich 1950).

But it was not until the early 1990s, when Lynn Margulis popularized the theory of endosymbiosis, that the importance of symbiotic microbes for a host gained general attention and popularity (Margulis and Fester 1991; Margulis 1993; McFall-Ngai 2002; O'Hara and Shanahan 2006; Baedke, Fabregas-Tejeda, and Nieves Delgado 2020). Through the ever-increasing progress in the development of new technologies and methods to study these interactions, like next-generation-sequencing and multi-omics approaches, new insights into the fundamental frameworks that shape those interactions and their function become available more quickly than ever.

This led up to today’s concept of the “holobiont” as it is defined today: describing a eukaryotic host and all of its associated microorganisms, including eukaryotes, prokaryotes and viruses (Rohwer et al. 2002; Zilber-Rosenberg and Rosenberg 2008; Bosch and McFall-Ngai 2011). The terms “metaorganism” and “holobiont” are often used interchangeably and while an attempt to define a difference between the terms was made, they mostly continue being used with no clear differentiation. I will use the term “holobiont” in this thesis. (Jaspers et al. 2019)

The core feature of the holobiont concept is that the host and its associated microbiota are not just living side-by-side, but are functionally important for each other (**Figure 1**). They interact, influence and protect each other (Bosch and Hadfield 2020). Their genomes are collectively referred to as a “hologenome” (Zilber-Rosenberg and Rosenberg 2008; Rosenberg and Zilber-Rosenberg 2011). When the first animals evolved at least 541 million years ago, bacteria already colonized the earth for around 3 billion years (Knoll 2015; Cunningham et al. 2017; Ros-Rocher et al.

2021). Logically, this means that since the earliest days of animal existence they were already interacting, in some way or another, with bacteria. The hologenome concept tries to integrate this perspective into a combined framework that views the whole holobiont as one evolutionary unit (Rosenberg and Zilber-Rosenberg 2016).

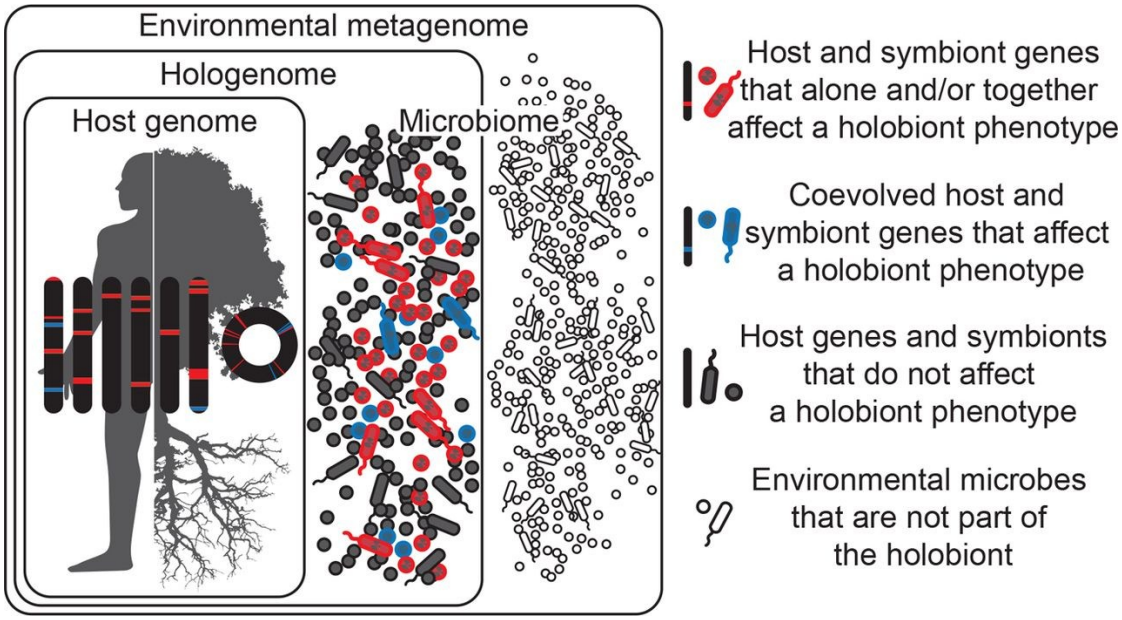

Figure 1: Visualization of the holobiont concept: *Holobiont describes an entity that includes a host and its symbiotic microbiota. Not all members of the microbiota necessarily have an effect on the phenotype of the holobiont or have co-evolved with the host (indicated by the different colors). The hologenome includes host and microbiota genomes, with the same premise that not all necessarily affect holobiont phenotype or evolution at given point in time (Theis et al. 2016).*

It is important to note that these interactions between a host and their symbionts are not necessarily exclusively positive. They can include mutualistic, commensal and parasitic interactions. Depending on the definition, these three terms can all be summarized under the term "symbiosis" (Bary 1879). Similarly to the metaorganism/holobiont characterization, a definition of the term "symbiosis" is still not ultimately set, with some constricting it to only include "an association between different species from which all participating organisms benefit" (Douglas 2010).

In this thesis I will use the term "symbiosis" following the definition of de Bary, to include all persistent biological interactions, and the term "symbiont" to refer to the smaller symbiotic partner in the relationship.

The importance of host-symbiont and symbiont-symbiont interactions for the holobiont is well established (Rosenberg, Sharon, and Zilber-Rosenberg 2009; McFall-Ngai et al. 2013; Koch and McFall-Ngai 2018; Kern et al. 2021; Salem and Kaltenpoth 2022; Voolstra et al. 2024). Holobionts depend on a sensible balance between their partners and proper recognition and communication for a multitude of different functions. These can include production of essential metabolites for the other partner(s), protective function against pathogens or stress, and sometimes the presence of specific microbiota is required for development or reproduction of the host (Zilber-Rosenberg and Rosenberg 2008; Fraune and Bosch 2010; Gilbert, Sapp, and Tauber 2012; Kern et al. 2021; Baldassarre et al. 2022; Carrier and Bosch 2022; Lourenco et al. 2022; Salem and Kaltenpoth 2022; Caballero-Flores, Pickard, and Nunez 2023; Petersen et al. 2023; Zheng et al. 2023; Decaestecker et al. 2024).

One of the most popular and best studied non-human host-symbiont interactions is the symbiotic relationship between the squid *Euprymna scolopes* and *Vibrio fischeri*. The squids are nocturnal and use the bioluminescent *V. fischeri* to camouflage their silhouettes from other predators during the night. The symbiont is taken up by the squid and recruited onto the light-organs surface, a host structure with the sole purpose of harboring *V. fischeri* (Herring 1977; Wei and Young 1989). Each squid generation, a new establishment of this symbiosis takes place through a highly complex and specific process, requiring both host- and symbiont-mediated mechanisms (Nyholm et al. 2000; Visick et al. 2000; Nyholm et al. 2002; Nyholm and McFall-Ngai 2003, 2004). The formation of this symbiosis in newly hatched squids leads to a multitude of behavioral, genetic and physiological changes in both partners, necessary for the stable continuum of this relationship (Nyholm and McFall-Ngai 2021).

An example for a direct protective effect of microbiota on a host was shown for a strain of *Alteromonas* bacteria found on the surface of embryos of the shrimp *Palaemon macrodactylus*. The bacteria protect the embryos against fungal infection by producing and releasing an anti-fungal compound (Gil-Turnes, Hay, and Fenical 1989). A similar interaction between a host and their microbiota can be observed in

polyps from *Hydra vulgaris*. Here, the microbiota is able to protect the host against fungal infection as well, although in this case the synergistic effects of at least two symbionts are required (Fraune et al. 2015). A non-bacterial symbiosis system can be found in another *Hydra* species. *H. viridissima* lives in a symbiotic relationship with a strain of *Chlorella* algae. The photosynthetically active *Chlorella* algae provide the host with fixed carbon, which significantly improves *Hydra* growth and survival during starvation periods (Muscatine and Lenhoff 1963, 1965). In return, the host provides the algae with nitrogen in the form of glutamine (Roffman and Lenhoff 1969; Hamada et al. 2018). Recent findings also suggest that *Chlorella* is involved in shaping the microbiome of the polyps, signifying the importance of multi-species interactions in a holobiont (Bathia et al. 2022).

Wolbachia, a maternally transmitted, strictly intracellular bacterium, is well known for being a reproductive parasite in a multitude of symbiotic relationships with arthropods. To guarantee their transmission to the next generation, *Wolbachia* symbionts are able to manipulate several of the hosts processes, inducing a range of reproductive phenotypes. These include feminization of males, or cytoplasmic incompatibility, which leads to embryo death when uninfected females mate with either infected or uninfected males. Only infected females can successfully reproduce, leading to a reproductive advantage and ensuring the spread of *Wolbachia* (Werren, Baldo, and Clark 2008).

Inter-kingdom communication in the holobiont

To ensure the stable persistence of a functioning symbiosis, the holobiont needs mechanisms that allow some form of communication. This is especially important for extracellular symbioses, where the host-symbiont interface is constantly exposed to the environment. The hosts most common mode of interaction with microbiota, be it symbionts or pathogens, is the innate immune system and, when present, also the adaptive immune system (Boman 2000; Silva et al. 2024). Since the host is in constant contact with microbes from the environment, and microbial colonization always carries a risk for the host in the form of infection, it is logical that the protective

function of the immune system also includes ways to communicate with commensal microbes (Macpherson and Harris 2004; Artis 2008; Belkaid and Hand 2014).

The interactions of the human guts with its colonizing microbiota and their effect on human health have become a central point of interest in health research (Human Microbiome Project 2012). Important interactions include protective functions of the commensal bacteria, i.e. removal of pathogens or production of anti-microbial factors, transfer of stress resistance and several metabolic functions (**Figure 2**) (O'Hara and Shanahan 2006; Nicholson et al. 2012).

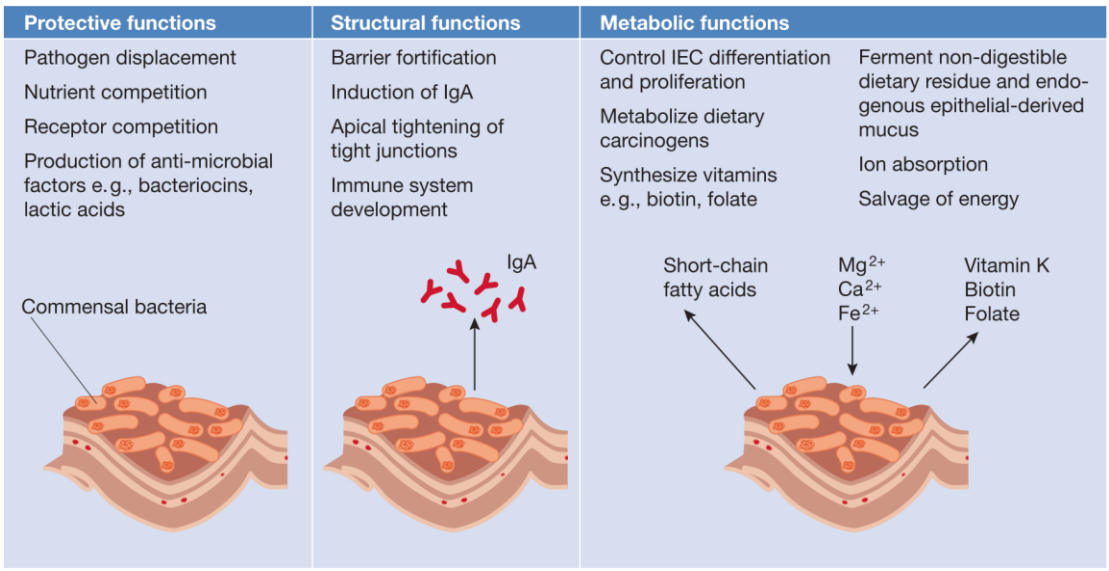

Figure 2: Functions of the human commensal gut microbiota. *Commensal bacteria in the human gut contribute to the maintenance of epithelial integrity, modulation of immune responses, and facilitation of nutrient processing and absorption by exerting a diverse range of protective, structural, and metabolic effects on the intestinal mucosa (modified after O'Hara and Shanahan 2006).*

The gut-microbiota symbiosis relies on an intricate crosstalk between the commensal microbiota and host cells, likely as a result of cospeciation between the human host and its symbionts (Peterson and Artis 2014; Moeller et al. 2016; Davenport et al. 2017; Ruhlemann et al. 2024). Communication is mainly regulated by the innate immune system, especially Pattern recognition receptors (PRRs) on the epithelial surface of the gut. PRRs recognize microbe-associated molecular patterns (MAMPs) like flagellin and lipopolysaccharides (LPS) and induce specific responses to control the commensal population. Some bacterial metabolites can even directly influence metabolism of the host (Cani 2018; Pessione 2020; Rocha and Laranjinha 2020; Daniel, Lecuyer, and

Chassaing 2021; Caballero-Flores, Pickard, and Nunez 2023). An imbalance in this symbiosis can lead to a wide range of pathological conditions, including obesity, autoimmune diseases, cancer and inflammatory bowel disease (O'Hara and Shanahan 2006; Clemente et al. 2012; Cani 2018; Kunst et al. 2023; Sun et al. 2024).

AHL signaling

Inter-kingdom signaling between host and symbionts via hormones and hormone-like compounds also recently became of interest in this field (**Table 1**) (Hughes and Sperandio 2008; Pacheco and Sperandio 2009; Curtis and Sperandio 2011). Especially acyl-homoserine-lactones (AHLs), the regulators of bacterial quorum sensing (QS), have become points of interest for studies on host-microbe interactions, including multi-species bacterial communities (Pacheco and Sperandio 2009; Curtis and Sperandio 2011; Mukherjee and Bassler 2019). AHLs are chemically analogous to eucaryotic lipidic signaling molecules and are known to be able to modulate mammalian cell signaling and immune system (Smith et al. 2002; Sperandio et al. 2003).

Table 1: Hormone signals, receptors and biological functions in procaryotes and eucaryotes (Hughes and Sperandio 2008).

Signal	Prokaryotic receptor	Prokaryotic function	Eukaryotic receptor	Eukaryotic function
Prokaryotic				
Providencia stuartti autoinducer (AI)	Unknown	Peptidoglycan modifications	Unknown	Unknown
AI-3	QseC	Type III secretion system (T3SS) activation, motility, toxin expression, iron uptake and virulence	Unknown	Unknown
Acyl homoserine lactones	LuxR, TraR, LasR and others	Virulence, T3SS regulation, biofilm formation, motility, antibiotic production and others	Unknown	Immunomodulation, intracellular calcium signalling and apoptosis
Eukaryotic				
Adrenaline and noradrenaline	QseC	T3SS activation, motility, toxin expression, iron uptake, virulence, growth and quorum sensing (QS)	Adrenergic receptors	Cyclic AMP levels, phospholipase C activation, stress, cell proliferation, enzyme production and ion channels
Peptide (epidermal growth factor (EGF))	Unknown	Unknown	EFG receptor	Cell proliferation, growth and development
Dynorphin	Unknown	QS and virulence	υ dynorphin opiate receptor	Stress responses
Steroid hormones	Unknown	Unknown	Nuclear receptors	Reproduction and regulated metabolism

In *H. vulgaris* it was shown that AHLs produced by its main colonizer *Curvibacter* can be recognized a modified by the host. Polyps were shown to be able to modify long-chain AHLs via a process called quorum quenching (QQ) (Pietschke et al. 2017). *Hydra's* modification of *N*-(3-oxododecanoyl)-*L*-homoserine lactone (3OC12-HSL) to *N*-(3-hydroxydodecanoyl)-L-homoserine lactone (3OHC12-HSL) appears to be a mechanism to specifically promote its main symbiotic colonizer, *Curvibacter* AEP 1.3. While 3OC12-HSL induces transcriptional responses in *Curvibacter* which negatively affect its colonization ability and growth, the quenching product 3OHC12-HSL induces responses that positively affect host-colonization (Pietschke et al. 2017).

ROS signaling

Recent studies have also highlighted the significant role of reactive oxygen species (ROS) in host-symbiont interactions (Pan et al. 2012; Mone, Monnin, and Kremer 2014; Marciano and Vajro 2017; Ballard and Towarnicki 2020; Kunst et al. 2023; Zhao et al. 2023; Zheng et al. 2023). ROS is used as a collective term for the multitude of different molecules derived from molecular oxygen via redox reactions or electronic excitation (Sies and Jones 2020). The evolution of aerobic organisms and the following oxidation event on earth started the evolution and rise of all higher organisms. While the ability to metabolize glucose using oxygen as an electron acceptor allows organisms to yield significant higher amounts of ATP (~30 ATP for aerobic respiration vs 2 ATP for anaerobic), it also comes with risks. Using oxygen for respiration produces reactive by-products, namely reactive oxygen species. These are highly reactive oxidizers that result from the incomplete reduction of molecular oxygen and can be separated into radical, e.g. superoxide anion ($\bullet O_2^-$), hydroxyl radicals (•OH), and non-radical species, e.g. hydrogen peroxide (H_2O_2) and organic peroxides (ROOH).

$\bullet O_2^-$ is the primary ROS generated, mainly by the mitochondrial electron transport chain and NADPH oxidases (Nox/Duox enzymes). It then reacts with its specific targets, but is mainly rapidly converted to hydrogen peroxide (H_2O_2) by superoxide dismutases (SODs) (McCord and Fridovich 1969). This reaction accounts for most of the H_2O_2 production in eukaryotic cells. H_2O_2 can form harmful hydroxyl radicals if not controlled. Antioxidant systems—including catalase, glutathione peroxidase (GPX), thioredoxins (TRX), and peroxiredoxins (PRDX)—along with redox sinks like glutathione and NADPH, detoxify H_2O_2 to water and oxygen (Lennicke et al. 2015; Smirnoff and Arnaud 2019; Sies and Jones 2020; Andrés et al. 2022; de Almeida et al. 2022). If an imbalance between the generation of ROS and their scavenging occurs, unspecific targeting of redox-radicals can lead to a wide range of pathological effects. This state is termed “oxidative distress” (**Figure 3**) (Sies 2022). Three primary mechanisms are particularly relevant in cell damage induced by a state of oxidative distress: Lipid-, protein- and DNA peroxidation (Marciano and Vajro 2017; Sies et al. 2022; Zhao et al. 2023). Uncontrolled oxidation of these molecules leads to the production of their respective organic hydroperoxides, namely lipid, protein and DNA

hydroperoxides. In contrast to other oxygen radicals like •OH, these can diffuse through membranes and propagate damaging chain peroxidation reactions if not properly reduced by scavenging enzymes (Cadet and Di Mascio ; Girotti and Korytowski ; Dunford 1987; Miyamoto et al. 2007; de Almeida et al. 2022).

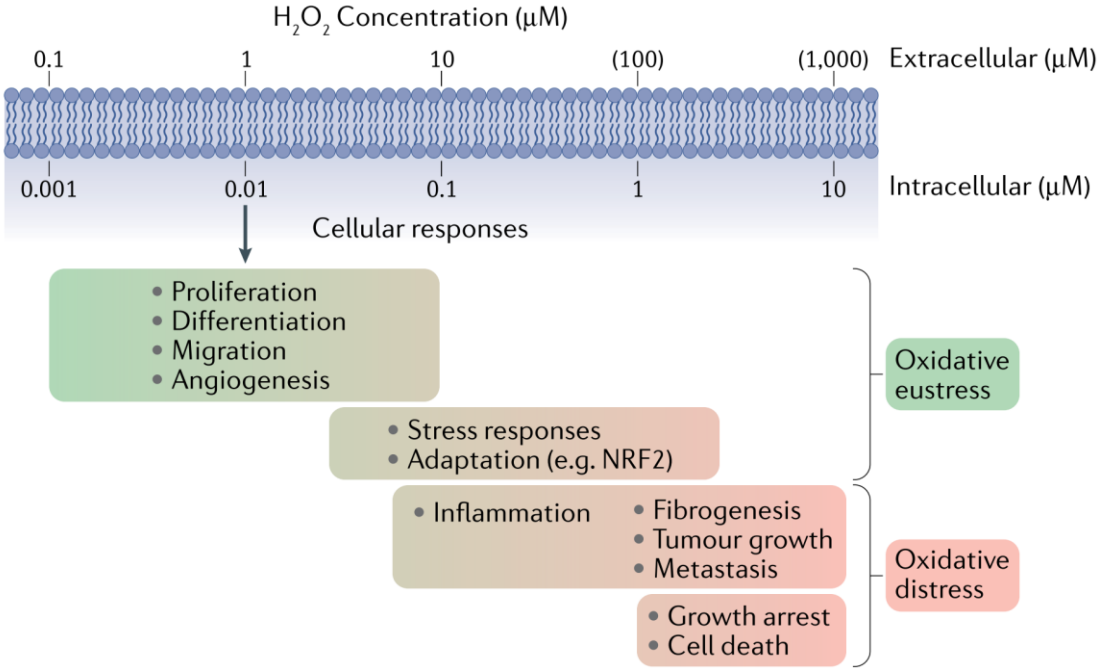

***Figure 3*: Cellular responses to oxidative eustress and distress.** *H_2O_2 is the major ROS involved in the regulation of biological responses via redox pathways. Depending on its concentration H_2O_2 activates either beneficial (green) or pathogenic responses (red) (Sies and Jones 2020).*

Initially only seen as these toxic by-products of respiration, it has now long been established that a permanent base level of oxidants is the normal state under physiological conditions (Sies and Chance 1970). This “Steady-State”-situation is also defined as “oxidative eustress” (**Figure 3**) (Sies 2022). The involvement of ROS in cell signaling, regeneration, and immune responses has since been well-established (Baldridge and Gerard 1932; Babior 1978; D'Autreaux and Toledano 2007; Fisher 2009; Forman, Maiorino, and Ursini 2010; Morgan and Liu 2011; Gauron et al. 2013; Schieber and Chandel 2014; Rudzka, Cameron, and Olson 2015; de Almeida et al. 2022; Sies et al. 2022; Hong et al. 2024; Silva et al. 2024).

Beyond that, ROS are now being investigated as modulators between hosts and their microbiota (Torres 2010; Spooner and Yilmaz 2011; Jones, Mercante, and Neish 2012; Mone, Monnin, and Kremer 2014; Ballard and Towarnicki 2020; Gordon and Hatzios 2020). *Lactobacilli*, prominent members of the gut microbiota, are able to stimulate the production of ROS in intestinal epithelial cells (Jones et al. 2013; Jones et al. 2015; Reedy et al. 2019). This microbial-induced ROS production activates several signaling pathways, such as the ROS-sensitive CncC/Nrf2 pathway, which promotes epithelial cell proliferation and intestinal tissue growth (Reedy et al. 2019).

Commensal bacteria of the gut in general were shown to stimulate the rapid generation of reactive oxygen species (ROS) in host cells, particularly through NADPH oxidases, modulating various cellular processes including proliferation, motility, and immune responses (**Figure 4**) (Jones, Mercante, and Neish 2012; Neish 2013; Lambeth and Neish 2014; Jones and Neish 2017; Perez et al. 2017).

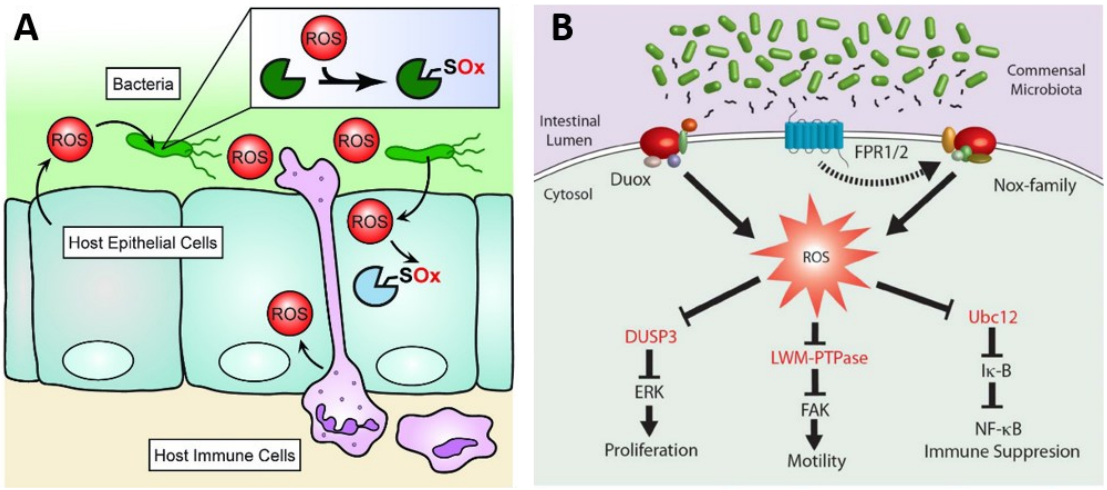

Figure 4: Redox signaling interactions at the host-microbe interface. A: *Reactive oxygen species are produced by host cells as well as the surrounding microbiota. ROS can modulate cell signaling, mostly via site-specific oxidation of redox-sensitive cysteines in proteins. This can lead to significantly altered structure, function or localization of the target proteins (Gordon and Hatzios 2020).* ***B:*** *Receptor-driven activation of NADPH oxidases generates localized ROS, altering the activity of redox-sensitive proteins like DUSP3, LMW-PTPase, and Ubc12. This redox signaling impacts processes such as proliferation, motility, and inflammation. (Jones, Mercante, and Neish 2012)*

DUOX2 was shown to play an important role in maintaining mucosal homeostasis and shaping the gut microbiome in mice (Grasberger et al. 2015). In response to colonization with commensal bacteria as well as a dysbiotic microbiota, DUOX2 expression was upregulated and led to modulation of redox signaling in bacteria, as

well as restricting bacterial translocation to the gut-associated lymphoid tissue (Grasberger et al. 2015).

Studies could also show a link between microbiota and NOX1 modulated redox regulation of Wnt/β-catenin signaling, a critical signaling pathway for tissue homeostasis. NOX1-generated ROS play a crucial role in the redox dependent regulation of Wnt/β-catenin signaling pathways in the colon, maintaining colon homeostasis (Coant et al. 2010; Kajla et al. 2012). NOX1 expression in the colon is upregulated through Toll-like receptor (TLR) signaling in response to intestinal microbiota, suggesting that this microbiota-driven NOX1 regulation contributes to the Wnt/β-catenin–mediated proliferation. (van der Post, Birchenough, and Held 2021; Herfindal et al. 2022).

The holobiont hydra

Phylogeny and physiology of *Hydra*

Hydra is a genus of evolutionary early branching freshwater metazoans belonging to the class Hydrozoa, in the phylum of Cnidaria, a sister group to all Bilateria (**Figure 5A**). The genus *Hydra* can be divided into four major species groups using morphological as well as genetic markers (**Figure 5A**) (Holstein, Campbell, and Tardant 1990; Hemmrich et al. 2007; Martinez et al. 2010; Schwentner and Bosch 2015; Schenkelaars et al. 2020). The earliest diverging group, *H. viridissima*, is easily distinguishable from other *Hydra* species by its green color due to its intracellular symbiotic algae. Only *H. viridissima* is known to stably live in this symbiotic relationship, hence the whole group is also commonly referred to as “green hydra”. The three other groups, namely the vulgaris, braueri and oligactis group, are generally referred to as “brown hydra”.

The life cycle of *Hydra* only consists of a polyp stage, in contrast to most other Hydrozoans who transition from an asexual polyp to a sexually reproductive medusa stage. Under favorable conditions *Hydra* usually reproduces asexually via budding every 2-4 days. Under laboratory conditions, with regular feeding and optimally

controlled living conditions, this allows for the generation and maintenance of large *Hydra* populations, consisting solely of clonal individuals.

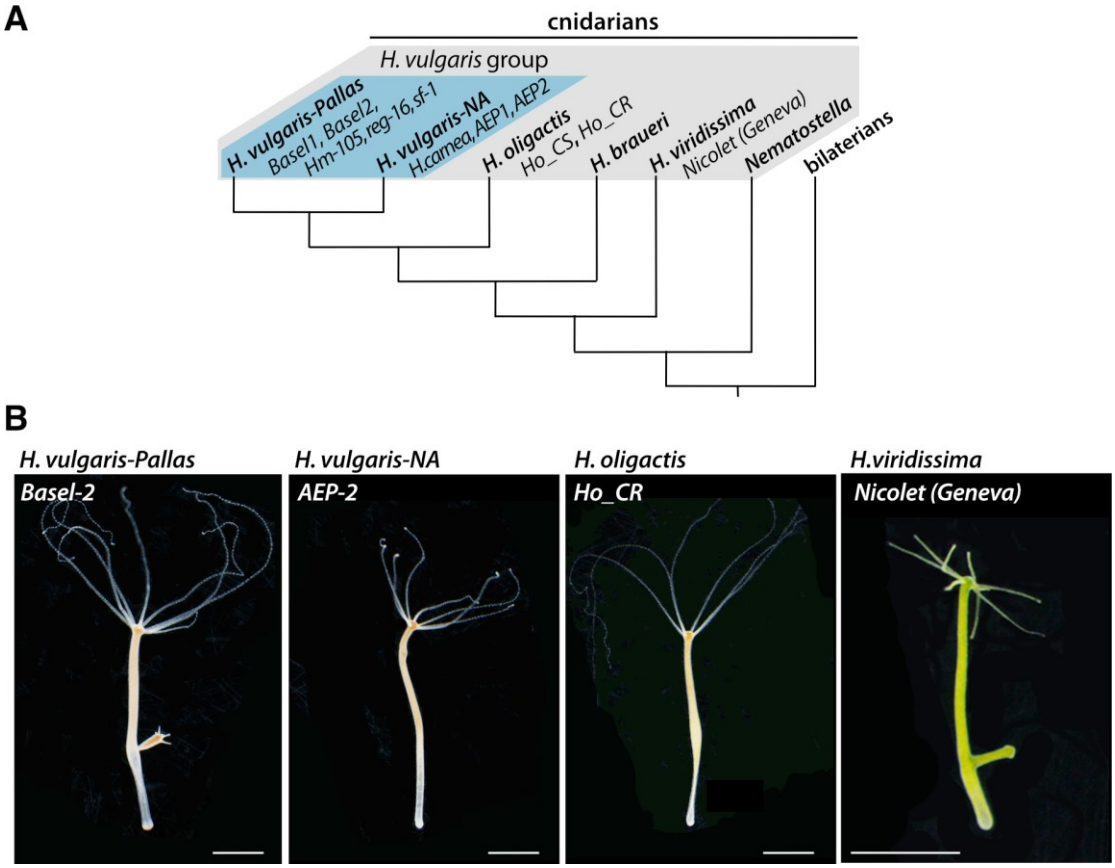

Figure 5: Phylogenetic position and appearance Hydra. **A:** *Phylogenetic position of the four main Hydra groups. Hydra belongs to the phylum Cnidaria, a sister group to all bilaterians.* ***B:*** *Representative images of Hydra laboratory strains. Figure modified after* (Schenkelaars et al. 2020).

Sexual reproduction is possible and mainly induced by environmental cues, like reduced food availability. In response, polyps will then produce either testes or ovaries on the outside of the body wall (Martin et al. 1997). Male polyps release gametes into the surrounding environment which then fertilize the eggs of female polyps. Fertilized eggs detach from the mother polyp and develop independently (Martin et al. 1997). The option to actively switch between sexual and asexual reproduction in the lab is one of the reasons *Hydra* became a well-renowned model organism. Clonal reproduction offers genetic uniformity and high reproducibility for experiments, while sexual reproduction allows the generation of transgenic animals. Fertilized eggs can be injected with a transgenesis vector using a microinjection technique and the following asexual reproduction allows for fast and easy clonal multiplication of those

transgenic lines (Wittlieb et al. 2006; Klimovich, Wittlieb, and Bosch 2019). Other important hallmarks of *Hydra* include its regenerative capacity and lack of senescence (Trembley 1744; Martinez 1998). Polyps are able to regenerate almost all injuries and can even reaggregate into a fully functional polyp after being dissociated into single cells. Tissue grafting between polyps of the same species is not only possible, but straightforward and reliable (Trembley 1744). These traits make *Hydra* an incredible tool for scientific research, especially in the fields of ecological and developmental biology (Steele 2002).

Like all other Cnidaria *Hydra* is a diploblastic organism. Its cylindrical body consists of two true epithelial cell layers, the endo- and ectoderm (Schneider 1890). Endo- and ectoderm are separated by a thin extracellular matrix called mesoglea (**Figure 6A**) (Davis and Haynes 1968; Shostak 1974; Sarras et al. 1991). Along the oral-aboral axis, *Hydra's* body can be separated into three parts: head, body column and foot region. The head has four to twelve tentacles which surround the hypostome, a dome-like structure that contains the mouth of *Hydra*. The structure of the mouth is distinct, as it is not a permanent opening. In its closed state the mouth is a continuous epithelium, with its cells connected via septate junctions (Campbell 1987; Carter et al. 2016). The body column is the region of bud and gonad formation. The foot region with its terminal basal disc is used to adhere to substrates or the water surface (Philpott, Chaet, and Burnett 1966).

Hydra's endo- and ectodermal epithelial cells are continuously dividing, multipotent stem cells that are constantly displaced toward the tentacles and basal disc. Here they give rise to their respective differentiated cell types. A third population of stem cells, the interstitial cells, are precursors to nerve cells, nematocytes, secretory cells and gametes (Marcum and Campbell 1978). Interstitial stem cells are evenly distributed in the body column and not arranged in a separate cell layer.

The ectoderm is covered by the glycocalyx, a multi-layered array of glycoproteins and glycosaminoglycans. Four inner layers are firmly structured and attached to the ectoderm. A fifth layer is only loosely attached (**Figure 6B**) (Holstein, Hess, and Salvenmoser 2010; Bottger and Hassel 2012). The glycocalyx is home to *Hydra's* natural microbiome (Fraune et al. 2015).

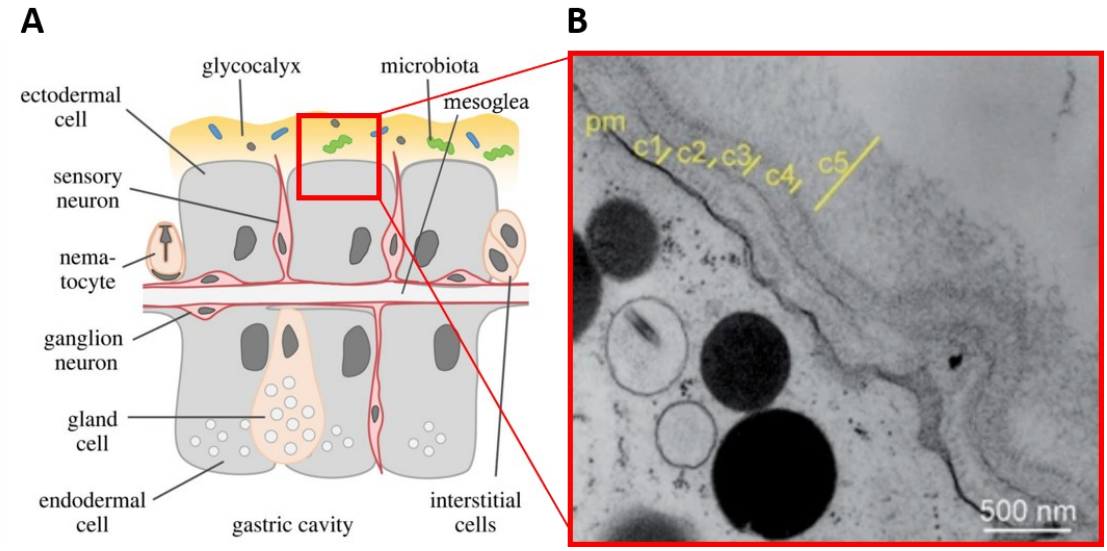

Figure 6: Tissue organization of Hydra polyps. A: *The two epithelial cell layers of endo- and ectoderm are separated by the mesoglea. Interstitial stem cells don't form a distinct cell layer, but are evenly distributed through the body column and embedded within the epithelial cell layers. The same is true for other cells of the interstitial cell lineage, like gland cells, neurons or nematocytes.* ***B:*** *The ectodermal layer of Hydra is covered by the multi-layered glycocalyx and home to Hydra's microbiota (Fraune et al. 2015; Klimovich and Bosch 2024)*

Specific interactions shape the *Hydra* holobiont

With the microbiome in constant contact with the outer epithelia of *Hydra* it presents an interesting challenge for the host. *Hydra* constantly has to differentiate between beneficial, native microbes and possibly harmful, invading species.

For this, *Hydra* uses a range of pattern recognition receptors in combination with effective antimicrobial peptides (**Figure 7**) (Miller et al. 2007; Bosch et al. 2009; Jung et al. 2009; Fraune et al. 2010; Franzenburg et al. 2012; Franzenburg, Walter, et al. 2013; Augustin et al. 2017; Klimovich and Bosch 2024). These not only protect *Hydra* from infection by pathogenic bacteria, but also select, shape and maintain *Hydra's* natural microbiome (Fraune et al. 2010; Franzenburg, Fraune, et al. 2013; Franzenburg, Walter, et al. 2013; Augustin et al. 2017; Klimovich and Bosch 2024). For

example, during early development, polyps produce neuropeptides with specific antimicrobial functions to support the establishment of its main bacterial colonizer, by reducing the bacterial load of undesired species. During later development, they also influence the spatial distribution of the polyp's microbiota (Augustin et al. 2017).

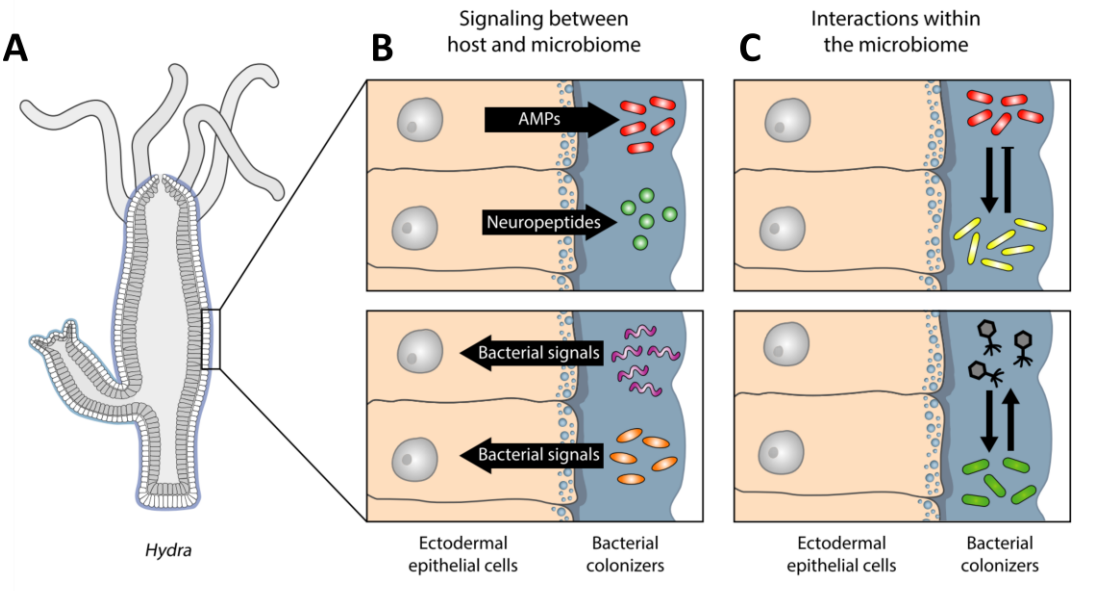

Figure 7: Signaling interactions in the Hydra holobiont: ***A:*** *Cross-section of a Hydra polyp, showing the two epithelial cell layers and the glycocalyx.* ***B:*** *Hydra produces AMPs and neuropeptides to shape and maintain its microbial community. Bacterial colonizers in turn produce signaling molecules like metabolites or hormone-like molecules that act on host targets.* ***C:*** *Interactions between bacteria or bacteria and phages can also contribute to holobiont homeostasis (Deines, Lachnit, and Bosch 2017).*

The selection of its microbiota seems to be highly specific for every *Hydra* species (Fraune and Bosch 2007; Franzenburg, Walter, et al. 2013; Taubenheim et al. 2022). Comparative studies of the microbiota between different *Hydra* species from long-term lab cultures showed that *Hydra* possesses a species-specific microbial composition. This specificity is retained even after decades of culturing these *Hydra* species under identical conditions in the lab (Fraune and Bosch 2007). Even more interesting is the fact that microbial communities of long-term lab cultures were similar to samples collected from the wild, further supporting the idea of a species-specific selection process (Fraune and Bosch 2007; Taubenheim et al. 2022). This is further supported by experiments that used artificially generated, germ-free (GF) *Hydra* polyps. When these polyps are challenged with complex bacterial communities,

they always assemble a microbial community that strongly resembles the natural state, if those complex communities also contained their natural colonizer (Franzenburg et al. 2012; Franzenburg, Walter, et al. 2013). The same effect can be seen when the entire microbiota of homogenized wildtype (WT) polyps is transferred to GF animals (Murillo-Rincon et al. 2017).

Among other things, this selection for a specific, stable microbiome serves as an additional protective function for the polyp. If *Hydra's* colonizing bacteria are removed, the polyp is significantly more susceptible to fungal infection (Fraune et al. 2015). This protective property seems to be mediated by an additive effect of a subset of *Hydra*'s microbiome, since only recolonization with certain combinations of colonizers was able to restore the protective function (Fraune et al. 2015). The microbiome also directly affects *Hydra's* budding, Wnt signalling pathway, nervous system and body contraction rates (Rahat and Dimentman 1982; Bosch et al. 2009; Boehm et al. 2012; Murillo-Rincon et al. 2017; Taubenheim et al. 2020; Giez et al. 2023). Interestingly, the regulation of body contractility seems to be a two-way street. While disrupting or removal of the microbiota results in reduced contraction rates of the polyp, abolishing polyp contraction initially also leads to changes in the microbiota in return (Nawroth et al. 2023).

The main colonizer *Curvibacter*

The microbial community of the commonly used *Hydra* lab strain *Hydra vulgaris* AEP is relatively simple. Only six species make up for 90% of the whole bacterial community, and they all share the same habitat in the glycocalyx of *Hydra* AEP (Franzenburg, Walter, et al. 2013; Fraune et al. 2015). This small community is dominated by *Curvibacter* sp., making up over 75% of the total bacterial community (Fraune et al. 2015). *Curvibacter* species are a common colonizer of *Hydra* cultures in the lab as well as in the wild (Fraune and Bosch 2007; Chapman et al. 2010; Franzenburg, Walter, et al. 2013; Taubenheim et al. 2022).

Curvibacter represents a genus of Gram-negative bacteria in the family of *Comamonadaceae*, belonging to the class *Betaproteobacteria*. They can commonly be

found in freshwater or in freshwater soils, including samples of water treatment plants and bottled water (Ding and Yokota 2004; Dominiak, Nielsen, and Nielsen 2011; Franca et al. 2015; Ma et al. 2016; Lesaulnier et al. 2017; Vandermaesen, Lievens, and Springael 2017; Jakus et al. 2021; Chen et al. 2022; Sun et al. 2022; Feng et al. 2023; Heinze et al. 2023; Le et al. 2023; Yang et al. 2023), but also in association with other freshwater organisms (McKenzie et al. 2012; Gorokhova et al. 2015; Bijnens et al. 2021).

Even though *Curvibacter* is the main colonizer on *Hydra* polyps, and also maintains this dominant position when GF polyps are conventionalized, it is outgrown in direct competition versus other colonizers in liquid culture experiments *(Li et al. 2015)*. In a study using *Curvibacter* and another natural colonizer, *Duganella* sp., it was shown that while *Curvibacter* is able to outcompete *Duganella* on the host, in culture the exact opposite is true (Li et al. 2015). Using a modelling approach, a follow-up study was able to explain this dynamic by introducing a third player as a regulator: bacteriophages (Li et al. 2017). Phages are mostly still an overlooked factor when trying to untangle the web of interactions in the holobiont, even though they can have a variety of effects on their bacterial host (Diaz-Munoz and Koskella 2014; Zhou et al. 2024).

In addition to the more general interactions between *Hydra* and its microbiome, there are also specific interactions between *Hydra* and *Curvibacter*. As already mentioned in the chapter “AHL”, *Hydra* is actively quenching QS signals of *Curvibacter* to promote a positive symbiotic bacterial phenotype (Pietschke et al. 2017). While *Curvibacter* is able to colonize the entire outer epithelia of *Hydra* polyps (Wein et al. 2018), its spatial distribution is regulated by the polyp via AMPs (Augustin et al. 2017; Klimovich and Bosch 2024). Tentacles show a higher density of *Curvibacter* when compared to the body column, while the foot region is only sparsely colonized (Augustin et al. 2017; Wein et al. 2018). *Curvibacter* in turn was shown to impact pattern formation in *Hydra*. Presence of *Curvibacter* led to the upregulation of two small secreted peptides, termed Eco1 and Eco 2, that act as regulators on the *Hydra* Wnt signaling pathway (Taubenheim et al. 2020). A more recent study could also show that presence of

mono-colonized *Curvibacter* influences the eating behavior of polyps by affecting *Hydra's* neuronal activity and reducing opening times of its mouth (Giez et al. 2023).

In an effort to allow for *in vivo* studies of spatial and temporal dynamics between *Hydra* and *Curvibacter*, Wein et al established a first protocol to generate transgenic *Curvibacter* lines (Wein et al. 2018). Using a mobilizable plasmid system, they generated transgenic *Curvibacter* lines expressing different fluorescent proteins to analyse and visualize *Curvibacter* recolonization on the host (Wein et al. 2018). Additionally, they designed and successfully tested a targeted knock-out system in *Curvibacter*, using homologous recombination (Wein et al. 2018). Building on this, Nawroth et al. later created chromosomally GFP-labelled *Curvibacter* (Nawroth et al. 2023). In a previous study I used the mobilizable plasmid system by Wein et al to generate an AHL-responsive *Curvibacter* bioreporter strain (**Figure 8**). In *in vivo* experiments I could show that after 5 days of recolonization, GFP-expressing *Curvibacter* pTM1 could be found all over the polyps, indicating the presence of AHLs, as hypothesized by Pietschke et a. (Minten 2017).

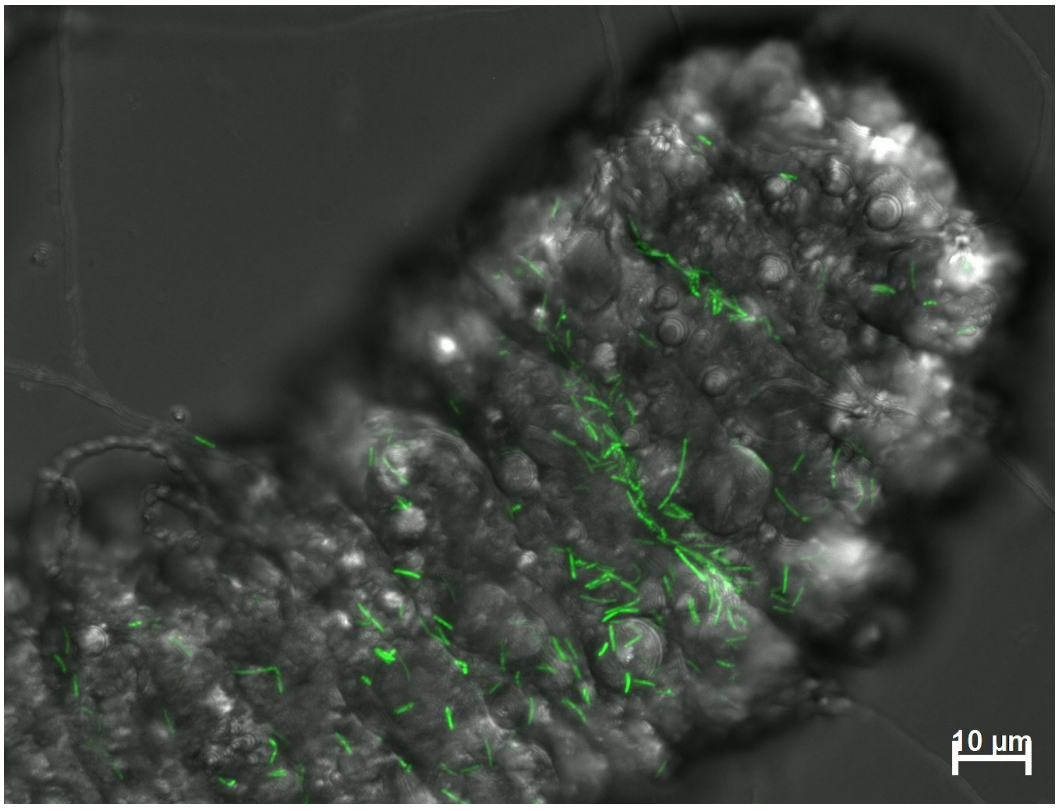

Figure 8: In vivo observation of Curvibacter AHL-bioreporter pTM1. *Tentacle tip of a Hydra polyp recolonized with Curvibacter pTM1, 17 days after recolonization. Green fluorescent cells are clearly visible all over the ectoderm indicating the presence of AHLs (Minten 2017).*

Hydra and *Curvibacter*: A powerful duo

To get a deeper insight into the interactions shaping a holobiont, a good and convenient model system is needed. *Hydra* and *Curvibacter* represent such a system to study inter-kingdom interactions (Minten-Lange and Fraune 2020). The available tools for *Curvibacter* provide the opportunity to create a wide range of *Curvibacter* strains with gene knock-outs, overexpression of specific genes and bioreporter strains. This allows for *in vivo* tracking of gene expression on the host or artificial medium. *Hydra* also presents itself as a prime model organism for the study of host-symbiont interactions in holobionts. As a representative of early branching metazoans with naturally formed microbial symbiotic relationships, any insights gained into the underlying processes of this relationship may offer increased understanding of similar processes in higher developed organisms (Kovacevic 2012; Schröder and Bosch 2016; Koch and McFall-Ngai 2018; He and Bosch 2022). Importantly for this, *Hydra* polyps can be made bacteria-free easily and quickly, allowing to distinguish between host-, environmental- and symbiote-effects (Rahat and Dimentman 1982; Franzenburg et al. 2012). Sequenced genomes for multiple *Hydra* species and a single-cell RNA-seq atlas provide additional important resources to unravel the fundamental processes of host-microbe interactions in the *Hydra* holobiont (Chapman et al. 2010; Siebert et al. 2019; Hamada, Satoh, and Khalturin 2020; Cazet et al. 2023).

In summary, *Hydra* and its symbiont *Curvibacter* form a powerful *in vivo* model for studying inter-kingdom communication in the holobiont. Further research will help to shed light on the molecular mechanisms and key players that shape and maintain holobiont homeostasis and health.

Aims

This study aims to gain deeper insights into the specific adaptations and interactions between *Hydra* and *Curvibacter*. To achieve this, the following objectives will be pursued:

- Isolation of *Curvibacter* strains from all *Hydra* groups, with the aim of testing for cospeciation using a phylogenetic approach. For this, 16S rRNA and GyrB genes of all isolated *Curvibacter* strains will be sequenced
- Analysis of metatranscriptomic data with the goal of identifying single genes or pathways in *Curvibacter* that are important mediators for the successful symbiosis
- Generate *Curvibacter* knockout mutants based on the results of the metatranscriptomic analysis.
- Use these *Curvibacter* knockout mutants to study the effect of these genes/pathways on the holobiont in *in vivo* experiments

Materials

Organisms

Table 2: Bacterial strains

Hydra colonizers	Free-living	Transgenic
Acidovorax sp. AEP1.4	*Acinetobacter* sp. Biofilm4	*Curvibacter sp*. AEP1.3 *ΔohrR-ohrA*
Curvibacter sp. AEP1.3	*Chryseobacterium* sp. Biofilm5	*Escherichia coli* BW29427
Duganella sp. C1.2	*Curvibacter sp.* BG3	*Escherichia coli* DH5α
Pelomonas sp. AEP2.2		
Undibacterium sp. C1.1		

Table 3: Host organisms

Host organism	Feed
Hydra circumcincta	*Artemia salina*
Hydra magnipapillata	*Artemia salina*
Hydra viridissima	*Artemia salina*
Hydra vulgaris	*Artemia salina*
Hydra vulgaris AEP	*Artemia salina*

Chemicals

Antibiotics

Table 4: Antibiotics

Antibiotic	Stock solution	Solvent	Manufacturer
Ampicillin	50 mg/mL	Water	Roth
Chloramphenicol	30 mg/mL	Ethanol	Roth
Kanamycin sulfate	30 mg/mL	Water	Bio Basic
Neomycin sulfate	50 mg/mL	Water	Duchefa Biochemie
Rifampicin	50 mg/mL	DMSO	Duchefa Biochemie
Spectinomycin dihydrochloride pentahydrate	50 mg/mL	Water	TCI Chemicals
Streptomycin sulfate	50 mg/mL	Water	J&K Scientific

Kits

Table 5: Kits

Kit	Manufacturer
Image-iT™ Lipidperoxidations-Kit, for live cell analysis	Thermo Fisher
NucleoBond Xtra Midi	Macherey-Nagel
NucleoSpin Gel and PCR Clean-up	Macherey-Nagel
NucleoSpin Plasmid	Macherey-Nagel
Total Reactive Oxygen Species (ROS) Assay Kit 520 nm	Thermo Fisher
DNeasy Blood & Tissue Kit	Qiagen

Enzymes

Table 6: Enzymes

	Enzyme	Manufacturer
Polymerases	FastGene Taq 2x Ready mix	Nippon Genetics
	Q5 HiFi DNA Polymerase	NEB
Ligases	T4 DNA Ligase	NEB
Kinases	T4 Polynucleotide Kinase	NEB

Restriction enzymes	AleI-v2	NEB
	HpaI	NEB

Chemicals

Table 7: Chemicals

Chemical	Manufacturer
Bacto Tryptone	Gibco
Bacto-Agar	BD
Calcium chloride ($CaCl_2$)	Grüssing GmbH
Calcium chloride dihydrate ($CaCl_2 \cdot 2\ H_2O$)	Honeywell Fluka
D (+)-Saccharose	Roth
2,6-Diaminopimelic acid (DAP)	Sigma-Aldrich
Dimethyl sulfoxide (DMSO)	VWR
Disodium phosphate (Na_2HPO_4)	Roth
Ethanol (EtOH)	Chemsolute
Ethylenediaminetetraacetic acid (EDTA)	Acros Organics

Glycerol	Roth
Hydrogen chloride (HCl)	Sigma-Aldrich
Hydrogen peroxide (H_2O_2)	Fisher Chemical
Magnesium chloride ($MgCl_2$)	Roth
Magnesium sulfate heptahydrate ($MgSO_4 \cdot 7\ H_2O$)	VWR
Magnesiumchlorid Hexahydrat ($MgCl_2 \cdot 6\ H_2O$)	Roth
MIDORI^{Green} Xtra	Nippon Genetics
Peptone ex casein, pancreatic digest	Roth
Potassium Carbonate Anhydrous (CK_2O_3)	Fisher Scientific
Potassium chloride (KCl)	Chemsolute
Potassium dihydrogenphosphate (KH_2PO_4)	Fisher Scientific
Potassium hydroxide (KOH)	Roth
R2A Broth	Neogen
R2A-Agar	Roth
Sodium bicarbonate ($NaHCO_3$)	Sigma-Aldrich

Sodium chloride (NaCl)	Sigma-Aldrich
Sodium hydroxide (NaOH)	Fisher Scientific
Tert-Butyl hydroperoxide (tBuOOH)	Alfa Aesar
TRIS	VWR
Yeast Extract	Roth

Buffer and solutions

Table 8: Buffer and solutions

Solution	Contents / 1l
DAP stock solution	60 mM DAP in 0.1 N HCL
TAE buffer (50x)	242 g TRIS, 57.1 mL Acetic acid, 100 mL 0.5 M EDTA (PH 8)

Media

Table 9: Media

Media	Contents / 1 l
***Artemia salina* artificial seawater**	31.8 g red sea salt
LB agar (Lennox)	5 g NaCl, 10 g tryptone, 5 g yeast extract, 15 g Bacto Agar
LB agar (Luria/Miller)	10 g NaCl, 10 g tryptone, 5 g yeast extract, 15 g Bacto Agar

LB broth (Luria/Miller)	10 g NaCl, 10 g tryptone, 5 g yeast extract
LB broth (Lennox)	5 g NaCl, 10 g tryptone, 5 g yeast extract
R2A agar	18 g R2A agar
R2A broth	3 g R2A broth
S-medium solution 1 (1000x)	42.18 g $CaCl_2 \cdot 2\ H_2O$
S-medium solution 2 (100x)	8.116 g $MgSO_4 \cdot 7\ H_2O$, 4.238 g $NaHCO_3$, 1.0958 g K_2CO_3
S-medium	0.29 mM $CaCl_2 \cdot 2\ H_2O$, 0.5 mM $NaHCO_3$, 0.33 mM $MgSO_4 \cdot 7\ H_2O$, 0.08 mM K_2CO_3
SOC medium	20 g tryptone, 5 g yeast extract, 0.58 g NaCl, 0.19 g KCl, 100 µl $MgCl_2$, 10 mM $MgSO_4$, 100 µl 2 M glucose solution (sterile filtered)

Oligonucleotides

Table 10: Oligonucelotides used in PCRs. All oligonucleotides were ordered from Merck

Name	Nucleotide sequence: 5´ → 3´	Target
Ohr_upstream_fw	GTAACACCAACAACACGGTG TCCATG	Amplification of genomic region upstream of *ohr*
Ohr_upstream_rev	ATCTAGACAAAACACCGTCA GTCAAAGAAGC	
Ohr_downstream_fw	CTTCTAGATAAATTGCGTGC AATTTAATTTAAGAAGC	Amplification of genomic region downstream of *ohr*
Ohr_downstream_rev	AACTTGACACAATGTCGATG TGGTCATGC	
Ohr-KO_verify_fw	CGTGTTGCGTTGGAGTACGG GC	

Ohr_KO_verify_rev	CTATGTGTCGATCGACCAGC AG	Verification of successful genetic knockout

Table 11: Oligonucleotides used for sequencing: All oligonucleotides were ordered from Merck

Name	Nucleotide sequence, 5´ → 3´	Target
pGT42_bla_seq_fw	CAGATCGCTGAGATAGGTGC	Verification of bla-flank insertion
pGT42_seq_bla_R2	TCGACCTCATTCTATTAGACTCTC	
pGT42_nptII_seq_fw	GCGCATCGCCTTCTATCG	Verification of nptII-flank insertion
pGT42_nptII_seq_rev	GCGCAATTAACCCTCACTAAAG	
27_F	AGAGTTTGATCCTGGCTCAG	16S rRNA gene of *Curvibacter* sp.
1492_R	CGGTTACCTTGTTACGACTT	
SF_GyrB_Curvi_F2	GCAAGTTCAACCAGAACAGC	GyrB gene of *Curvibacter* sp.
SF_GyrB_Curvi_R2	TCGGTCATGATGATGATGCG	

Devices

Table 12: Devices

	Device	Manufacturer
Centrifuge	Centrifuge 5415 C	Eppendorf
	Centrifuge 5420	Eppendorf
	Centrifuge 5425 R	Eppendorf
	Centrifuge miniSpin	Eppendorf

	Centrifuge Mini FastGene NG002	Nippon Genetics
	Centrifuge Z 366 K	Hermle
Homogenizer	Homogenizer BeadBug 6	Benchmark
Gel Imaging System	FastGene FAS-DIGI PRO	Nippon Genetics
Microscope	SZX 16	Olympus
Nanophotometer	NP 80	Implen
	P 330	Implen
Plate reader	Spark Cyto	TECAN
	Spark 10M	TECAN
Test tube shaker	RS-VA 10	Phoenix Instrument
Thermal Cycler	peqSTAR 2x Universal Gradient	peqLAB
	SimpliAmp	Applied Biosystems
Thermomixer	compact	Eppendorf
	F 1.5	Eppendorf

Software

Data analysis and statistics	OriginPro
Image analysis	Fiji
In silico cloning	SnapGene
Phylogeny	MEGA X
Transcriptomic data analysis	Rockhopper DESeq2

Methods

Standard procedures

Preparation of chemically competent *E. coli* Dh5α cells

E. coli Dh5α was inoculated in 5 mL LB-medium and grown over night at 37°C and 220 rpm. On the next morning, 1 mL of overnight-culture was used to inoculate 100 mL fresh LB-medium and grown at 37°C and 220 rpm until an OD_{600} between 0.5 to 0.6 was reached. Cells were transferred into two 50 mL centrifugation tubes and kept on ice for 20 minutes. For all following steps, cells were constantly kept on ice. After incubation on ice cells were centrifuged for 5 min. at 3000 rcf and 4°C. The supernatant was discarded and 20ml of ice-cold 100 mM $CaCl_2$ added to each tube. Cells were very carefully resuspended and kept on ice for at least 30 minutes, then centrifuged again at 3000 rcf and 4°C. The supernatant was discarded and each cell pellet very carefully resuspended in 2 mL ice-cold 100 mM $CaCl_2$ containing 15% glycerol. 200 µl of the cell suspension were then pipetted into pre-cooled 1.5 mL tubes and instantly shock-frozen in liquid nitrogen, before being stored at -80°C until they were used. All steps were conducted under sterile conditions.

Preparation of chemically competent *E. coli* BW29427 cells

For *E. coli* strain BW29427, the same protocol as for Dh5α was used, with the addition of 0.1 mM 2,6-Diaminopimelic acid (DAP) into the growth medium.

gDNA extraction

gDNA from *Curvibacter* strains was extracted and purified using the DNeasy Blood & Tissue kit (Quiagen), following the manufacturers protocol for extraction from animal tissue (spin-column protocol). For each strain, 1 mL from an overnight culture was transferred into a microcentrifuge tube and centrifuged for 10 min at 10,000 rcf. Supernatant was removed and 180 µl of buffer ATL and 20µl proteinase K were added onto the pellet. After overnight incubation at 56°C and 550 rpm in a thermomixer, 4

µl RNase A was added to all samples before continuing with the protocol. Samples were finally eluted by using 100 µl buffer AE and reapplying the eluate onto the DNeasy membrane once more.

Polymerase chain reaction

Polymerase chain reaction (PCR) was used for the amplification of DNA fragments. Q5 HiFi DNA Polymerase (New England Biolabs) was used to amplify 16S and GyrB sequences, as well as the flanking regions required for the creation of *Curvibacter* knockout strains, following the manufacturers protocol (**Table 13 + Table 14**). Annealing temperatures were calculated using SnapGene.

Table 13: *Reaction setup for PCR using Q5 HiFi DNA Polymerase*

Component	50 µl reaction	Final concentration
5X Q5 reaction buffer	10 µl	1X
10 mM dNTPs	1 µl	200 µM
10 µM forward primer	2.5 µl	0.5 µM
10 µM reverse primer	2.5 µl	0.5 µM
Template DNA	x µl	< 1,000 ng
Q5 High-Fidelity DNA Polymerase	0.5 µl	0.02 U/µl
Nuclease-free water	to 50 µl	

Table 14: *Thermocycling Conditions for PCR using Q5 HiFI DNA Polymerase*

Step	Temp.	Time
Initial denaturation	98°C	30 seconds
35 Cycles	98°C 50–72°C 72°C	5–10 seconds 10–30 seconds 20–30 seconds/kb
Final extension	72°C	2 minutes

For all other PCRs, FastGene Taq DNA polymerase (Nippon Genetics) was used, following the manufacturers protocol (**Table 15** + **Table 16**).

Table 15: *Reaction setup for PCR using Taq DNA Polymerase*

Component	50 µl reaction	Final concentration
2X FastGene ® Taq ReadyMix (1.5 mM MgCl2 at 1X)2	25 µl	1X
10 µM forward primer	2.5 µl	0.5 µM
10 µM reverse primer	2.5 µl	0.5 µM
Template DNA	x µl	< 1,000 ng
Nuclease-free water	to 50 µl	

Table 16: *Thermocycling Conditions for PCR using Taq DNA Polymerase*

Step	Temp.	Time
Initial denaturation	95°C	3 minutes
35 Cycles	95°C T_m -1°C 72°C	30 seconds 30 seconds 1 minute/kb
Final extension	72°C	10 minutes

Extraction and purification of DNA fragments

Successfully amplified flanking regions for *Curvibacter* knockout generation were isolated from the agarose gel following PCR. The NucleoSpin Gel and PCR Clean-up kit (Macherey-Nagel) was used, according to the manufacturers protocol. Samples were eluted with 25 µl which were reapplied to the column and eluted a second time.

16S and GyrB regions, amplified from *Curvibacter* genomic DNA (gDNA), were purified using the PCR product directly and not extracted from gels. The NucleoSpin Gel and PCR Clean-up kit (Macherey-Nagel) was used, according to the manufacturers protocol. Samples were eluted in 25 µl and the first eluate was reapplied to the column a second time.

Restriction digest of pGT42

To insert the flanking regions into knockout vector pGT42, restriction digests were used to cut the vector at desired positions. *Ale*I-v2 was used prior insertion of the first flank and *Hpa*I for the second. The reaction setup shown in **Table 17** was used. The mixture was incubated for 1 h at 37°C. After incubation, successful digestion was confirmed via agarose gel electrophoresis. Linearized plasmid was then purified directly from the gel using the NucleoSpin Gel and PCR Clean-up kit.

Table 17: *Reaction setup for restriction enzyme digestion*

Component	50 µl reaction
DNA	1 µg
10X rCutSmart buffer	5 µl (1X)
Enzyme	1 µl
Nuclease-free water	to 50 µl

Ligation of flanking regions into vector pGT42

Flanking regions for the *Curvibacter* knockout were inserted into pGT42 using T4 DNA ligase (NEB), following the protocol for blunt-end ligation. The NEBioCalculator was used to calculate molar ratios and volumes of vector and insert DNA for the reaction (**Table 18**). After ligation, 2-5 µl of ligation mix was used for transformation.

Table 18: *Reaction setup for ligation of inserts into pGT42*

Component	20 µl reaction
T4 DNA Ligase Buffer (10X)	2 µl
Vector DNA	x µl
Insert DNA	x µl
T4 DNA ligase	1 µl
Nuclease-free water	to 20 µl

Agarose gel electrophoresis

For separation of DNA, agarose gel electrophoresis was used. 1% agarose was dissolved in 1x TAE buffer by heating. 2 µl of MIDORI^{Green} Xtra were added per 50 mL of agarose gel solution before the gel was cast. Bands were visualized using the FastGene FAS-DIGI PRO system (Nippon genetics).

Plasmid extraction

Plasmids were extracted and purified using the NucleoSpin Plasmid kit (Qiagen), following the manufacturer's protocol for low-copy plasmids. 10 mL of bacteria culture were used in all cases. Plasmids were eluted by applying 25 µl of elution buffer onto the membrane and reapplying the same eluate onto the column once more. DNA concentration and purity were determined using the NP 80 nanophotometer (Implen).

Transformation of *E. coli*

Heat-shock transformation was used to transform *E. coli* with desired Plasmids. Cells were constantly kept on ice, except when stated otherwise. 1 ng of plasmid DNA was added to aliquots of chemically competent *E. coli* cells and incubated for 30 min, followed by a 30 s heat-shock at 42°C. Afterwards, cells were again put on ice for 5 min, before adding 1 mL of pre-warmed SOC medium. Cells were incubated for 1 h at 37°C and 220 rpm before plating on selective plates and overnight incubation at 37°C.

Transformation of *Curvibacter* via conjugation

For transformation of *Curvibacter* with knockout vector pGT42, *E. coli* BW29427 was used as a donor during conjugation. Its DAP auxotrophy allows for convenient counter-selection on DAP-free medium. Overnight-cultures of BW29427 carrying the desired plasmid and *Curvibacter* AEP 1.3 were inoculated and incubated overnight at 37°C and 30°C respectively and 220 rpm.

Cultures were then diluted 1:10 to again grow them to early log phase. Per plasmid, 1 mL of BW29427 and 5 ml of *Curvibacter* were centrifuged for 10 min at 3000 rcf and supernatant removed. Cells were resuspended in 500 µl R2A with 0.1 mM DAP each and both solutions combined in a 1.5 mL microcentrifuge tube. After 1 h incubation at 30°C without shaking, 100 – 250 µl of the cell mixture were spotted carefully onto R2A + DAP plates. Plates were incubated overnight at 30°C.

Using a sterile inoculation loop, the conjugation cell mixture was transferred into a new 1.5 mL tube, containing 1 mL of R2A broth. Cells were washed once with R2A to remove possible traces of DAP and plated on selective R2A plates. Plates were incubated overnight at 30°C.

DNA Sequencing

Sequencing of small DNA regions (< 1 kb) was conducted by eurofins genomics, using their TubeSeq service. Purified 16S and GyrB regions from *Curvibacter* gDNA were sequenced using their respective primer-pairs (**Table 11**). For confirmation of successful insertion of flanking regions into vector pGT42, the the inserted regions were sequenced, using their respective sequencing primer-pair (**Table 11**).

Cultivation

Cultivation of *Hydra* polyps

All *Hydra* cultures were kept under the same conditions, at 18°C with a 12-hour dark/light cycle. Polyps were cultured in plastic containers filled with *Hydra* culture medium (S-Medium). They were fed 3 times a week with first instar larvae of *Artemia salina*. If fed in the morning, cultures were washed after a minimum waiting period of 6 hours, or on the next morning, if fed in the afternoon. Washing included scrubbing of the culture dishes to remove potential algae and biofilm build-up, and full exchange of the S-Medium.

Cultivation of *Artemia salina*

Three teaspoons of *Artemia salina* cysts were added per 1 L of artificial seawater and incubated overnight at 37°C under light. Hatched larvae were collected, washed with S-Medium to prevent salt carry-over into *Hydra* cultures, transferred into fresh S-Medium and subsequently fed to *Hydra*.

Cultivation of *Curvibacter* sp.

All *Curvibacter* strains were grown on either R2A agar or in R2A broth, at 18°C with aeration. Liquid cultures were shaken at 220 rpm. Antibiotics were added to the media when needed.

Cultivation of other *Hydra*-associated bacteria

All other *Hydra*-associated bacteria, including free-living strains, were grown on either R2A agar or in R2A broth, at 18°C with aeration. Liquid cultures were shaken at 220 rpm.

Cultivation of *E. coli*

All *E. coli* strains were grown on LB medium at 37°C. For the DAP-auxotroph strain BW29427, 0.1 mM of DAP was added to all media. Liquid cultures were shaken at 220 rpm. Antibiotics were added to the media when needed.

Generation of germ-free *Hydra* polyps

For experiments requiring germ-free *Hydra, p*olyps of roughly the same size and with no visible gonads or eggs were collected and transferred into sterile 70 mL transparent polypropylene containers with 50 mL of sterile S-Medium. A maximum of 50 polyps was transferred into a single container. An antibiotic cocktail was added, consisting of five antibiotics (ampicillin, neomycin, streptomycin, spectinomycin and rifampicin) with a final concentration of 50 µg / mL each. Over the course of 5 days, the medium was exchanged with fresh, sterile S-medium with added antibiotics every day. After 5 days the medium was exchanged with fresh sterile S-Medium without antibiotics and animals were kept for 2 more days. Before every experiment, 2 polyps from each container were randomly selected and plated on R2A plates to check for sterility. Containers were kept at 18°C in constant dark unless otherwise noted, and all handling steps were done under sterile conditions. Polyps were starved during the whole treatment and the following experiments.

If non-sterile control polyps were required for an experiment, they were subjected to the same treatment in parallel, but instead of the antibiotic cocktail they received 50 µl of DMSO per 50ml of sterile S-Medium.

Experimental procedures

Isolation and identification of *Curvibacter* sp.

Two polyps each of laboratory strain of *Hydra circumcincta*, *Hydra magnipapillata*, *Hydra viridissima*, *Hydra vulgaris*, *Hydra vulgaris* AEP were collected and carefully washed thrice with 1 mL of sterile S-Medium. Polyps were then homogenized and dilution series plated on R2A plates. Plates were incubated at room temperature for at least 3 days. Single bacterial colonies resembling the known *Curvibacter* strain AEP 1.3 were picked and gDNA isolated. The 16S rRNA and GyrB regions were amplified via PCR and subsequently sequenced, using the primer pairs in **Table 11**. Bacterial strains identified as *Curvibacter* were stored at -80°C.

Evolutionary analysis by Maximum Likelihood method

For *Curvibacter*, DNA sequences for 16S rDNA and DNA gyrase subunit B (*GyrB*) were acquired via Sanger-sequencing of the isolates mentioned before. For each isolate both sequences of were combined and used as a single dataset for the analysis. For *Hydra*, Cytochrome c oxidase I (*COI*) DNA sequences of the desired lineages were acquired from the NCBI database.

Evolutionary analysis was conducted in MEGA X (Kumar et al. 2018). All sequences were aligned using the integrated MUSCLE alignment option with default parameters. The evolutionary history was inferred by using the Maximum Likelihood method and Tamura 3-parameter model (Tamura 1992). Initial trees for the heuristic search were obtained automatically by applying Neighbor-Join and BioNJ algorithms to a matrix of pairwise distances estimated using the Maximum Composite Likelihood (MCL) approach, and then selecting the topology with superior log likelihood value. Bootstrap values were calculated based on 100 replicates.

Metatranscriptome

Isolation of bacterial RNA for metatranscriptomic analysis was conducted by Cleo Pietschke. 1,200 H. vulgaris (AEP) polyps were washed for 3 min in 3 mL sterile PBS, to separate the bacteria from the polyps. The supernatant was taken and two volumes of RNAprotect Bacteria Reagent (Qiagen) were added. RNA was subsequently isolated with the RNeasy Mini Kit (Qiagen), following the manufacturer's protocol. Additionally, RNA from *Curvibacter* AEP 1.3 in R2A broth was isolated. For this, cultures were inoculated to OD = 0.1 and grown for 4 more hours. Two volumes of RNAprotect Bacteria Reagent (Qiagen) were added and RNA isolated with the RNeasy Mini Kit (Qiagen).

cDNA libraries were constructed using the TrueSeq Stranded mRNA LT-RiboZero Kit (Illumina) following the manufacturer's protocol. cDNA libraries were sequenced using a NextSeq 500 machine (Illumina) in paired-ends mode and running 150 cycles for high output. The Illumina base caller bcl2fastq2-v2.16.0.10 was used to convert the raw data into FASTQ format.

The reference-based transcript assembly was conducted using Rockhopper, a computational tool developed for analysis of bacterial RNA-seq data (McClure et al. 2013; Tjaden 2015, 2020). Parameters for the reference-based assembly allowed 0.15 mismatches, a minimum seed length of 0.33 and minimum expression of UTRs and ncRNAs at 0.5.

The genome of *Curvibacter* AEP 1.3 (accession nos.: PRJNA320637) was used as the reference genome (Pietschke et al. 2017).

Obtained count data was used for differential gene expression analysis, using the R package DESeq2 (Love, Huber, and Anders 2014). A minimum adjusted p-value requirement of 0.005 was used to filter differentially regulated genes.

KEGG pathway enrichment analysis was performed by Lukas Becker. The proteome FASTA file from the Reference Sequence (RefSeq) database of *Curvibacter* sp. AEP1.3 was utilized as input for BlastKOALA. BlastKOALA is a web-based tool developed by the Kyoto Encyclopedia of Genes and Genomes (KEGG) that assigns KEGG Orthology (KO) numbers to the provided protein identifiers based on sequence similarities with genes in the KEGG GENES database. Subsequently, the KO numbers were merged with the DESeq2 tables of differentially expressed genes. This table was used as input for the pathway enrichment analysis, using the R package clusterProfiler (Yu et al. 2012; Wu et al. 2021; Xu et al. 2024). The clusterProfiler function enrichKEGG was used to conduct the analysis for differentially regulated *Curvibacter* genes.

Cloning strategy for KO

For the creation of *Curvibacter* knockout mutants, the mobilizable gene targeting vector pGT42 was used (Kickstein, Harms, and Wackernagel 2007; Wein et al. 2018). Shortly, two flanking regions, one upstream and one downstream of the desired genomic target sequence are amplified from *Curvibacter* DNA via PCR and inserted into the pGT42 vector (**Figure 9**). After transformation of this KO-vector into *Curvibacter*, the two flanking regions facilitate homologous recombination between vector and genome, leading to a deletion of the desired target sequence via substitution with the *SacB* cassette of the vector. The primer pairs used for amplifying the flanking regions and sequencing of the construct can be found in **Table 10** and **Table 11**.

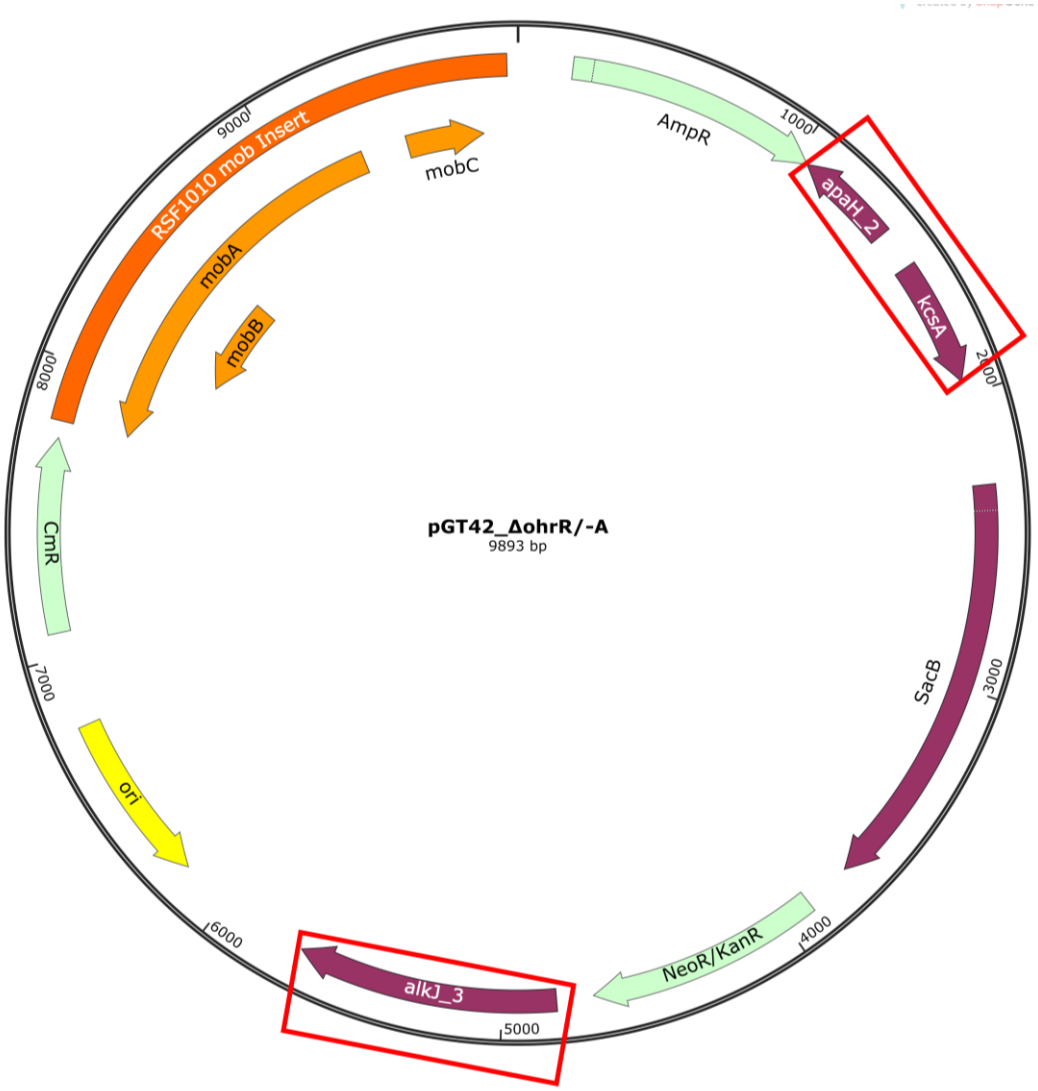

Figure 9: Knockout vector pGT42_ΔohrR/-A. *The flanking regions (highlighted by red boxes) of the ohr cluster, required for homologous recombination, were amplified from Curvibacter AEP1.3 gDNA and cloned into the pGT42 backbone.*

Determination of bacterial growth rates

To determine the growth rate of bacteria, overnight cultures were inoculated by picking single colonies from plates with freshly streaked-put cells. For all experiments, cells were grown at 18°C and 220 rpm. On the day of the experiment, fresh R2A medium was inoculated with 100 µl of overnight culture and grown for roughly 4 hours, until cells reached exponential growth. Cultures were then diluted in fresh growth medium to an OD_{600} of 0.1 and transferred to 96-well plates. Where required, Hydrogen Peroxide (H_2O_2) and *tert*-Butyl hydroperoxide (tBuOOH) were diluted

beforehand in R2A and added to their indicated final concentrations as well. All wells had a final volume of 200 µl with an OD_{600} of 0.1.

Growth rates of colonizers and non-colonizers in response to H_2O_2

Pre-cultures and well-plates were prepared as described before. Growth was determined by measuring absorbance at OD_{600} every 15 min for 12 h at 18°C, using a TECAN Spark 10M.

Growth rates and doubling time were calculated using the ExpGro1 function for one-phase exponential growth in OriginPro, after plotting the growth curves.

Growth comparison and resistance of AEP 1.3 vs ΔohrR-ohrA

Pre-cultures and well-plates were prepared as described before. Growth was determined by measuring absorbance at OD_{600} every 20 min for 12 h at room temperature, using a TECAN Spark Cyto.

Growth rates and doubling time were calculated using the ExpGro1 function for one-phase exponential growth in OriginPro, after plotting the growth curves.

Live cell ROS Assay

Hydra polyps were transferred to 1.5 mL Eppendorf tubes with 5 polyps each and treated with the Total Reactive Oxygen Species (ROS) Assay Kit 520 nm (Thermo Fisher), following the manufacturers protocol. Instead of using the provided assay buffer, S-Medium was used to prepare the 1x staining solution. Incubation was done for 1 hour at 18°C in the dark. After staining, polyps were transferred onto petri dishes with fresh SM and visualized using the Zeiss SZX 16 fluorescence microscope.

Quantification of ROS levels in *Hydra* polyps

Polyps were carefully transferred to 96-well plates using sterile glass pipettes, with one single polyp per well. Excess medium was removed and 1x ROS Detection Reagent

in 100 µl fresh, sterile S-Medium was added to each well. After a one-hour incubation period at 18°C and protected from light, the staining solution was replaced with fresh, sterile S-Medium. Where needed, H_2O_2, tBuOOH or Cumene hydroperoxide (CuOOH) were added to their indicated final concentration after prior dilution in sterile S-Medium. A final volume of 100 µl / well was used for imaging in all cases. Polyps were imaged using the TECAN Spark Cyto fluorescence imaging module. For measurement of ROS in the supernatant, polyps were removed from the wells after imaging. Green fluorescence intensity of the supernatant was measured using the TECAN Spark Cyto Fluorescence Bottom Reading module.

The following settings (**Table 19**) were used for imaging of *Hydra* polyps, stained with the ROS detection kit. For determining lipid peroxidation, fluorescence was additionally measured in the red channel.

Table 19: Settings for imaging of Hydra polyps using the TECAN Spark Cyto

Application:	SparkControl V3.1
Firmware:	LUM:V5.2.4|ABS:V4.3.2|ABS_MEX:V5.1.1|USBCAM:V4.90.34|MTP:V14.2.11|FLUOR:V5.1.4|FLUOR_FP:V5.0.2|FLUOR_BOTTOM:V5.0.2|FLUOR_MEM:V5.1.1|FLUOR_MEX:V5.1.1|FIM:V1.1.9|GCM:V3.0.2|INJ:V3.1.1|PODI:V1.11.2
System	SPARK1922
Plate	[NUN96fb_OpticalBottom]
Lid lifter	No lid
Humidity Cassette	No humidity cassette
Smooth mode	Selected
Mode	Fluorescence imaging
Application	Images-only
Channels	Brightfield, Green
Objective	2x
Pattern	Central
Settle time [ms]	10
Channel	Brightfield

Focus offset [µm]	0
Channel	Green
LED Intensity [%]	100
Focus offset [µm]	150
Exposure time [ms]	60
Cross-talk settings	Blue: 0%, Green: 100%, Red: 0%, Far-red: 0%

Images were analyzed and fluorescence intensity determined using Fiji. All RAW fluorescence images were adjusted for dark background and polyps manually marked as ROI. Mean gray intensity was then measured, with minimum threshold set to 5140 and maximum to 65535.

Influence of light on the hosts ROS-levels

GF and WT polyps were prepared as described before. Following the removal of antibiotics, polyps were separated into two groups, with the same amount of GF and WT polyps in each group. Both groups were kept for one week at 18°C with a 12-hour dark/light cycle. One group followed the regular dark/light cycle of our *Hydra* cultures, while the other one followed an inverted cycle. This allowed for imaging of both conditions, light and dark, at the same timepoint. Imaging and analysis were done as already described.

Recolonization of germ-free *Hydra* polyps

Desired bacterial strains were grown overnight and freshly diluted on the morning of the experiment. After they reached the exponential phase, bacteria were centrifuged for 10 min at 3000 rcf and washed twice with 1 mL of sterile S-Medium, to remove any traces of R2A medium. Cell number was adjusted by diluting bacteria in sterile S-Medium and GF polyps recolonized by adding bacteria to their desired CFU/mL.

To recolonize GF *Hydra* with its natural microbiota (conventionalized), WT polyps were collected and homogenized. For each GF polyp, one WT polyp was collected and

starved for 3 days. On the day of the experiment, polyps were washed twice with 500 µl sterile S-Medium, before being homogenized, using the BeadBug 6. For this, single polyps were placed in sealed tubes with 500 µl sterile S-Medium and ~15 Triple-Pure Zirconium beads with a diameter of 1 mm. After shaking twice for 7 seconds at 3500 rpm polyps were completely homogenized. Each GF polyp was recolonized using the whole lysate of one WT polyp.

Following recolonization, all polyps were incubated for 24 hours at 18°C and no light. After 24 hours the medium was replaced with fresh S-Medium.

Influence of *Hydra* microbiome on the hosts ROS-levels

GF and WT *Hydra* polyps were prepared as described before. GF polyps were separated into four groups. One group was left GF. Each of the other three was inoculated with $25x10^6$ CFU of either *Curvibacter* AEP1.3, *Curvibacter* AEP1.3 *ΔohrR-ohrA* or conventionalized. ROS levels of whole polyps were determined 4 days after recolonization.

Recolonization in mono association

GF polyps were prepared as described before. For each treatment and replicate, 3 polyps were placed in a single 1.5 mL microcentrifuge tube in 1 mL of S-Medium. 128 CFU / polyp of either *Curvibacter* AEP 1.3 or *Curvibacter* AEP1.3 *ΔohrR-ohrA* was used for recolonization. At 1 dpr, 2 dpr and 7 dpr one polyp from each tube was collected. After the collection step at 2 dpr, the SM in the tube with the remaining polyps was exchanged with fresh, sterile S-Medium. Collected polyps were washed in fresh S-Medium, homogenized and a dilution series of the lysate was plated. Polyps recolonized with WT *Curvibacter* were plated on R2A plates. Polyps recolonized with *ΔohrR-ohrA* were plated on R2A plates with added 5 µg /mL of kanamycin. Plates were incubated at RT for 3 days and CFUs counted afterwards.

For di-association, the same basic experimental setup as before was used. Only this time, each polyp was inoculated with 128 CFU / polyp of a cell mixture, containing equal amounts of *Curvibacter* AEP 1.3 and *ΔohrR-ohrA*. Polyps were sampled at 1 dpr, 2 dpr and 9 dpr.

Results

Phylogenetic signals of cospeciation in the *Hydra–Curvibacter* symbiosis

Studies in the past have revealed the close relationship and interactions between *Hydra* and its microbiome. *Curvibacter* is not only the main colonizer of the laboratory strain *Hydra vulgaris* AEP, but can also be found on most other *Hydra* species in high abundances. Because of this, I chose *Curvibacter* for an evolutionary analysis to assess the congruence between phylogenetic trees of *Hydra* and *Curvibacter*.

As they are publicly available, I used sequences of the cytochrome c oxidase I (*COI*) gene from different *Hydra* species, acquired from the NCBI database. For the phylogenetic tree of *Curvibacter* I sequenced the 16S and DNA gyrase subunit B (*gyrB*) gene regions of strains isolated from most of those *Hydra* species used, and one free-living strain.

The phylogenetic trees of *Hydra* and *Curvibacter* show a high congruence (**Figure 10**). The relationships between the *Curvibacter* strains (**Figure 10A**) mirror the relationships between the three *Hydra* groups represented in this tree, namely the vulgaris group (*H. carnea*, *H. vulgaris* AEP, *H. magnipapillata* and *H. vulgaris*), the braueri group (*H. circumcincta*) and the viridissima group (*H. viridissima*) (**Figure 10B**). Also, as previously shown in other studies, *H. carnea* and *H. vulgaris* AEP constitute a single species, separate from the actual *H. vulgaris*.

Within the vulgaris group, the relationship between *Curvibacter* isolates from *H. vulgaris* AEP, *H. magnipapillata* and *H. vulgaris* mirrors the relationships between the corresponding *Hydra* species.

Additionally, *Curvibacter* strains that were isolated from separate cultures of the same *Hydra* species are virtually identical to each other; all of them forming a single taxon, matching the one of their host species. The free-living *Curvibacter* species BG 3 forms its own taxon.

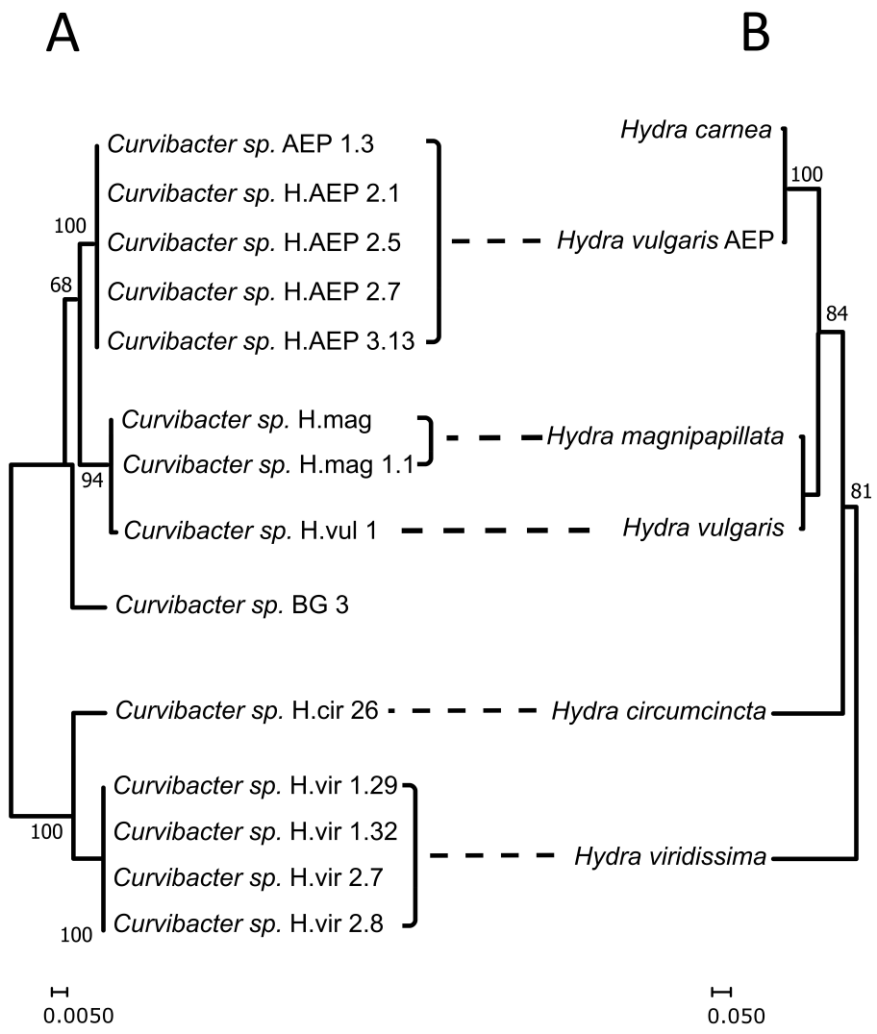

Figure 10: Evolutionary relationship between Hydra and Curvibacter: *The percentage of trees in which the associated taxa clustered together is shown next to the branches. Trees are drawn to scale, with branch lengths measured in the number of substitutions per site.* ***A:*** *Analysis of a combined Curvibacter dataset, containing 16S and GyrB genes. The tree with the highest log likelihood (-3662.55) is shown. A discrete Gamma distribution was used to model evolutionary rate differences among sites (5 categories (+G, parameter = 0.0579)). This analysis involved 14 nucleotide sequences. There were a total of 2027 positions in the final dataset.* ***B:*** *Analysis of Hydra mitochondrial CO1 gene. The tree with the highest log likelihood (-1531.11) is shown. A discrete Gamma distribution was used to model evolutionary rate differences among sites (5 categories (+G, parameter = 0.1342)). This analysis involved 6 nucleotide sequences. There were a total of 573 positions in the final dataset. Analyses were conducted in MEGA X.*

The observed pattern of mirroring phylogenies between individual *Curvibacter* species and their corresponding host could be a first indicator for potential co-speciation of the two species. A previous study could already show that closely related *Hydra* species share a more similar microbiota than more distantly related ones (Franzenburg, Walter, et al. 2013). This pattern is a recurring phenomenon across host-symbiont systems, termed phylosymbiosis (Lim and Bordenstein 2020). Taken

together with my result, this provides further evidence for a close evolutionary relationship between *Curvibacter* and *Hydra*.

Metatranscriptomic analysis of *Curvibacter* genes reveals colonization-specific adaptations

To get deeper insights into the interactions between *Curvibacter* and *HydraI*, the microbiome of WT *Hydra* was washed off the polyps with PBS and total RNA was isolated from this supernatant. The total RNA was sequenced to create a metatranscriptome. As reference, RNA from *Curvibacter* grown in liquid monoculture was isolated and sequenced as well. Following this, I analyzed the transcriptomic data to identify differentially expressed genes of *Curvibacter* between its colonizing state on the polyp and the pelagic R2A culture.

On average, 65% of the total reads could be successfully aligned to the *Curvibacter* reference genome for pelagic samples, and 1.6% for samples from the metatranscriptome. A total of 889 *Curvibacter* genes were significantly regulated when host-associated, with 529 genes upregulated and 360 downregulated. Principal component analysis revealed that the samples are separated depending on their source, with samples from the same source clustering together (**Figure 11**).

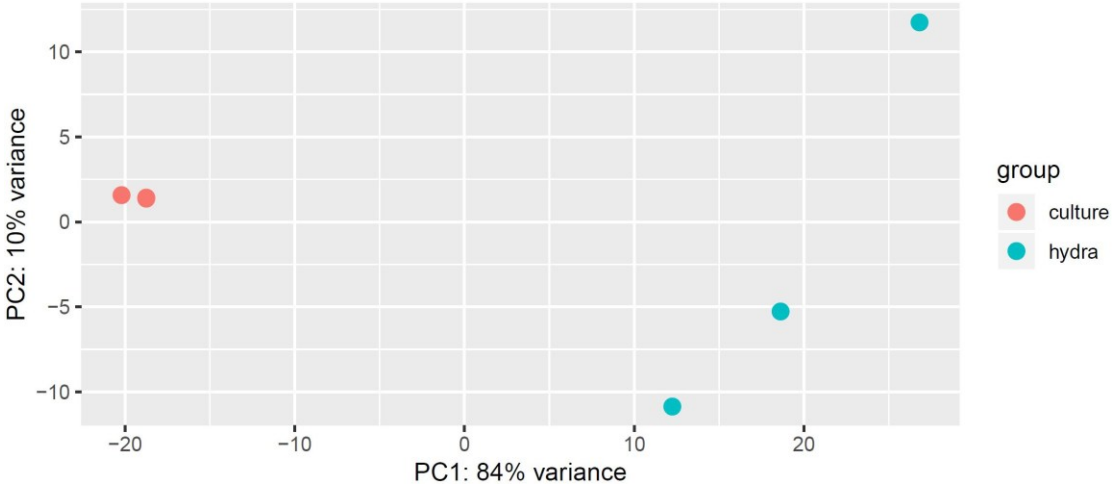

Figure 11: Principal component analysis: *Shows the distribution of the samples isolated from Curvibacter mono-culture and from hydra-associated Curvibacter, spanned by their first two principal components. The percent variation explained by the first two principal coordinates is 94%. Samples cluster depending on their source with a clear differentiation between samples isolated from Curvibacter mono-culture (culture) and the metatranscriptome (hydra).*

KEGG pathway enrichment analysis revealed an upregulation of genes belonging to clusters of ATP-binding cassette (ABC) transporters and ribosomes during host colonization, while some metabolism clusters are downregulated (**Figure 12**). This might indicate adaptations to the host environment, enabling *Curvibacter* to interact with and utilize host metabolites. Motility and chemotaxis genes are downregulated, indicating a potential role of these clusters in finding a suitable host that is not required during host-association. Similar results were observed in studies using mono-colonized *Curvibacter* as well as *Curvibacter* treated with a host-modified AHL, that is suspected to be involved in supporting its host-colonizing ability (Pietschke et al. 2017; Giez et al. 2023).

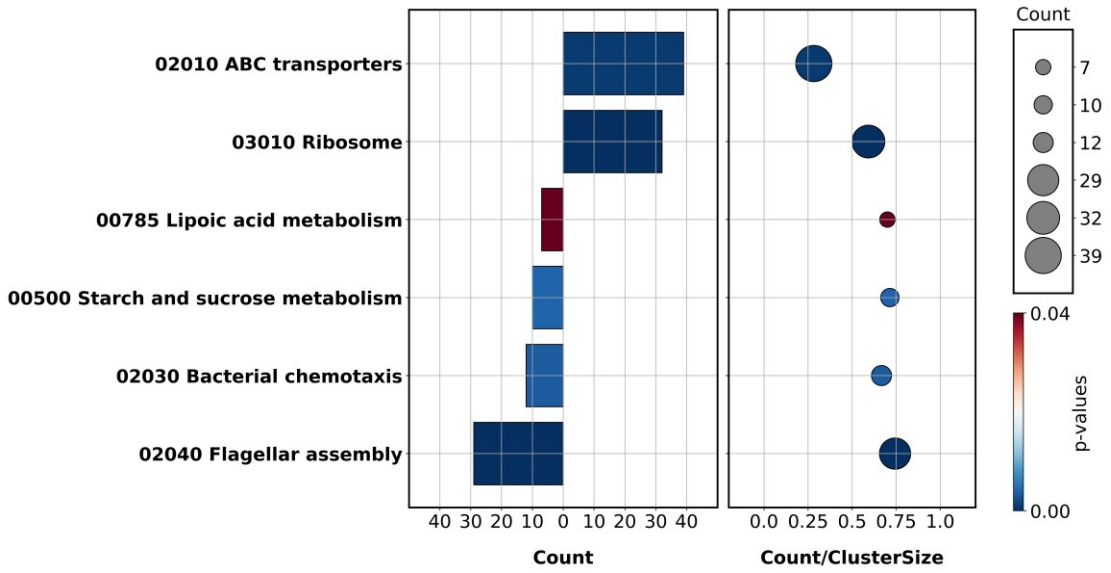

Figure 12: KEGG pathway enrichment analysis: *The bar plots show the regulation of significantly enriched KEGG clusters of differentially regulated Curvibacter genes between host association and liquid mono culture. Count numbers indicate the number of individual regulated genes associated with the respective KEGG cluster. Dots show the ratio of counts to the total size of the corresponding cluster. Dot size indicates the number of counts. Analysis was done by Lukas Becker.*

The top 10 most up-regulated genes of *Curvibacter* in its colonization state on *Hydra* are shown in **Table 20**. Interestingly, out of those 10 genes, 7 are involved in bacterial antioxidant defense system as scavengers of ROS (highlighted by gray background).

Table 20: Strongest upregulated Curvibacter genes: *Top 10 upregulated genes of Curvibacter while colonizing Hydra with its natural, complex microbiome. Genes highlighted by gray background are known ROS scavengers in bacteria. The amount of upregulation compared to Curvibacter grown in liquid mono-culture is shown as log2 fold change (Log2 fc), padj <= 0.005 for all genes.*

Gene ID	Log2 fc	annot
AEP_02913	7.92	Organic hydroperoxide resistance transcriptional regulator; **ohrR_2**
AEP_02912	6.89	Organic hydroperoxide resistance protein; **ohrA**
AEP_02386	6.37	Phosphoenolpyruvate carboxykinase [GTP]; **pckG**
AEP_01802	6.15	hypothetical protein
AEP_00733	5.79	Cysteine desulfurase; **nifS**
AEP_02692	5.41	Rubredoxin; **rubA**
AEP_01736	4.85	Catalase-peroxidase; **katG2**
AEP_02693	4.84	Nigerythrin; **ngr**
AEP_01283	4.64	Alkyl hydroperoxide reductase subunit F; **ahpF**
AEP_01284	4.37	Alkyl hydroperoxide reductase subunit C; **ahpC**

The two strongest upregulated genes, *ohrR* and *ohrA*, encode the organic hydroperoxide resistance (Ohr) transcriptional regulator OhrR and /- protein OhrA, respectively. In most cases, OhrR acts as a repressor of *ohrA*, and the whole operator complex mainly confers resistance against organic hydroperoxides (OHPs), and only rarely against other ROS (Mongkolsuk et al. 1998; Fuangthong et al. 2001; Ochsner, Hassett, and Vasil 2001; Rince et al. 2001; Cussiol et al. 2003; Chuchue et al. 2006). OhrR belongs the family of MarR (Multiple Antibiotic Resistance) transcription factors, which act as sensors and regulators for a wide range of redox-active species (Deochand and Grove 2017; Meireles et al. 2022). MarR family transcription factors

are critical for bacterial cells, as they are involved in a wide range of protective stress responses (Deochand and Grove 2017). The expression profile and function of the *ohr* complex seems to be conserved in bacteria, while it is absent in vertebrates and vascular plants (Meireles et al. 2022). Naturally occurring examples for possible substrates in biological systems include OHPs like lipid hydroperoxides, cholesterol hydroperoxides or protein hydroperoxides, but also peroxynitrite and sulfane sulfur (Miyamoto et al. 2007; Alegria et al. 2017; Xu et al. 2022).

Rubredoxin and Nigerythrin are not well understood, but there is mounting evidence from several microorganisms that proteins of those families are involved in scavenging of H_2O_2 (Lumppio et al. 1997; Alban et al. 1998; Jenney et al. 1999; Lumppio et al. 2001; Sztukowska et al. 2002; Iyer et al. 2005; Kawasaki et al. 2009; Sato et al. 2012; Cardenas, Quatrini, and Holmes 2016; Hancock et al. 2024).

Catalase-peroxidase (katG) and the NADH peroxidase AhpCF (Alkyl hydroperoxide reductase CF), consisting of the two subunits AhpC/AhpF, are well-known and -researched ROS scavengers, principally of H_2O_2. They are regulated by the transcription factor OxyR, a common bacterial redox regulator (Mongkolsuk and Helmann 2002; Imlay 2019). AhpCF is additionally known to be involved in the detoxification of organic hydroperoxides (OHPs) in bacteria (Poole and Ellis 1996; Wang et al. 2013).

This significant upregulation of ROS scavenging genes might represent an important factor that enables *Curvibacter* to successfully colonize *Hydra*. As mentioned in the introduction, *Curvibacter* is the most abundant colonizer of *Hydra*, even though it is readily outgrown in culture by other bacteria. The increased expression of ROS-scavenging genes during colonization could be indicative for a higher ROS resistance of *Curvibacter*, compared to other bacteria. As ROS are a common defense mechanism, a strong ROS-resistance might play a role in its status as main colonizer.

Oxidative stress tolerance among symbiotic bacteria of *Hydra*

To verify this, I tested *Curvibacter* and five other natural bacterial colonizers of *Hydra* for their growth under increasing concentrations of H_2O_2., as it is the most common ROS used in immune responses and most of the upregulated ROS-responsive genes of *Curvibacter* are H_2O_2 scavengers. Additionally, three non-colonizers were tested that can be found in the environment of laboratory cultures, but not on polyps themselves.

All bacteria showed a resistance to concentrations of up to 0.157 mM of H_2O_2 (**Figure 13**). Surprisingly however, *Curvibacter* AEP1.3 showed the least resistance of any tested bacteria against H_2O_2, with a lethal concentration of 0.313 mM (**Figure 13**). *Duganella* sp., the second most abundant colonizer of *Hydra*, and *Undibacterium* sp. were resistant to H_2O_2 until a concentration of 1.25 mM. *Acidovorax* sp. and *Pelomonas* sp. also showed a stronger resistance against H_2O_2 than *Curvibacter*, with a lethal concentration of 0.625 mM. The three non-colonizers showed the strongest resistance against H_2O_2, with a lethal concentration of 2.5 mM.

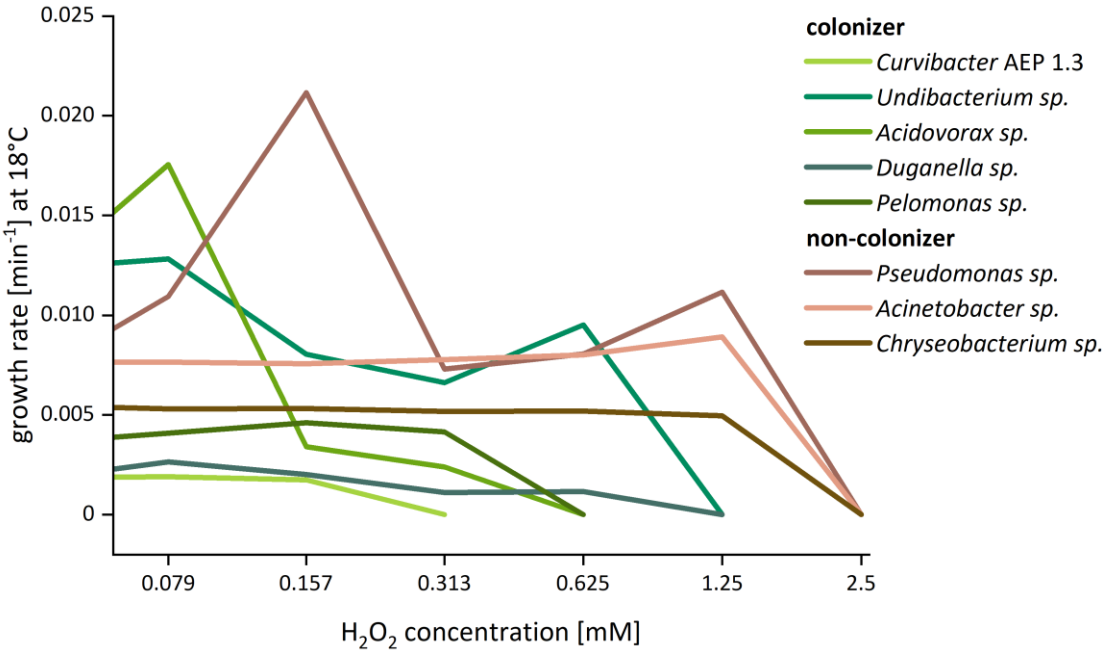

Figure 13: Growth of bacterial Hydra colonizers and non-colonizers in response to H_2O_2. *Resistance of natural bacterial colonizers of Hydra to increasing concentrations of H_2O_2 was compared to that of non-colonizers, isolated from Hydra culture dishes. H_2O_2 was added to the growth medium before the start of the experiment. Cells were grown at 18°C for 24 h. Growth was determined by measuring OD_{600} every 15 min and growth rates calculated afterwards. n = 4*

Although *Curvibacter* shows a strong upregulation of genes involved in scavenging of H_2O_2, in culture this does not translate into increased protection against H_2O_2 when compared to other colonizers and non-colonizers of *Hydra*. Since the upregulation of ROS-scavenging genes in *Curvibacter* during colonization still indicates the presence of ROS in its micro-environment on the polyp, I wanted to confirm the presence of ROS in *Hydra in vivo*.

Hydra polyps show distinct endogenous ROS levels *in vivo*

For this, I used the Total ROS Assay Kit (520 nm) to stain total ROS in live polyps. After staining, I transferred the polyps to petri dishes filled with S-Medium and visualized green-fluorescence signals using a stereo microscope.

Distinct ROS signals were visible, indicating the presence of ROS in WT polyps under standard lab conditions. While I could observe ROS signal in the endoderm (**Figure 14C**), I could not observe any distinct ROS signal at the ectodermal layer. Additionally, it seems that the fluid inside of the body cavity of *Hydra* polyps, including the tentacles, contains a comparatively high amount of ROS (**Figure 14A-C**). Polyps also seemed to be able to regulate the flow of this fluid. At first a uniform distribution of ROS signal in the gastrointestinal tract and the endoderm over the whole polyp was visible (**Figure 14A**). During body contractions, polyps would release the stained fluid in their gastrointestinal tract via their mouth opening into the surrounding medium (**Figure 14B**). After expulsion events and prolonged exposure, I could observe isolated clouds of ROS moving inside of *Hydra´s body cavity* (**Figure 14B-C**). I could also observe this pattern in buds still attached to the parent polyp (**Figure 14A**).

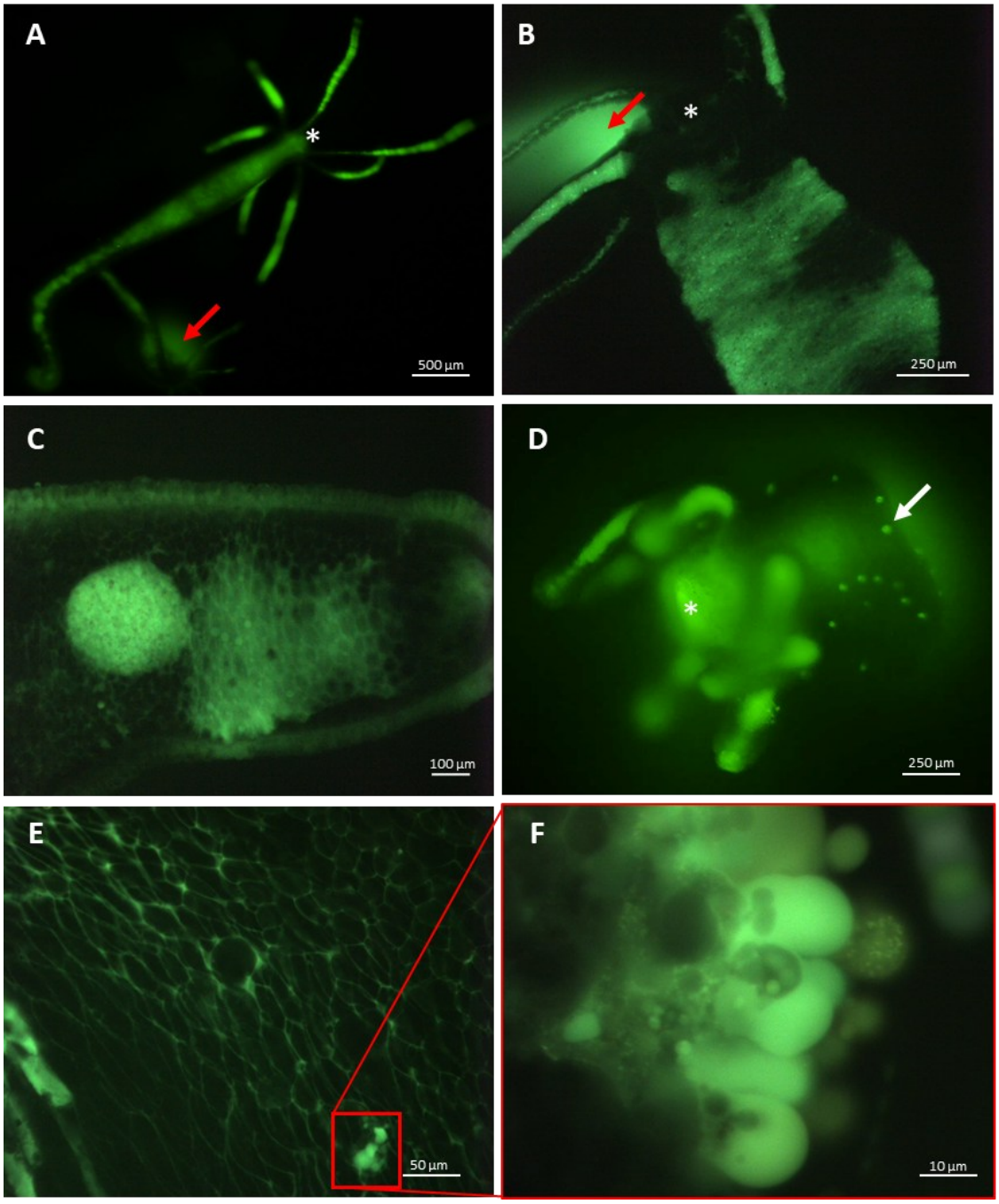

Figure 14: In-vivo ROS assay of Hydra polyps. *Polyps treated with the Total ROS Assay Kit (520nm) and imaged using a fluorescence microscope.* ***A:*** *Hydra polyp with attached bud, showing universal ROS signal in all body cavities, including inside the tentacles.* ***B:*** *Hydra polyp showing a patchy ROS-pattern with unstained areas, after expelling medium out of the mouth-opening.* ***C:*** *Clouds of ROS moving through Hydras body cavity. A distinct signal in the endodermal layer of the polyp is also visible.* ***D:*** *Polyp after elongated exposure to the light. Vesicles that began to form in response are clearly visible.* ***E-F:*** *Magnification of an area where vesicles have formed. * marks the mouth-opening of polyps; white arrow marks an exemplary vesicle; red arrows mark clouds of ROS released into the environment.*

When polyps were observed for a prolonged time under the microscope, they started to form vesicle-like structures (from now on simply called vesicles) all over the body

column. These vesicles showed a strong ROS signal and would detach after some time (**Figure 14D-F**).

Overall, the natural presence of ROS in *Hydra* polyps could be confirmed. Due to the microscope and sample setup, the capacity for fast and reproducible imaging was significantly limited. Live polyps exhibit phototactic avoidance behavior in response to light, which made the fluorescence imaging slow and tedious. Additionally, polyps started to show signs of potentially heat-induced ROS stress due to the prolonged imaging process under the fluorescent lamp. These constrains limited the potential of this setup for further *in vivo* experiments

High-throughput *in vivo* detection of microbe-dependent changes in *Hydra* ROS levels

To allow for faster and simultaneous observation and quantifiable measurement of ROS in *Hydra* polyps, I established a high-throughput assay using a TECAN Spark Cyto equipped with a fluorescence imaging module. I transferred a single polyp into each well of a 96-well plate and stained all samples using the Total ROS Assay Kit (520nm), as described before. After staining, I used the TECAN Spark Cyto plate-reader for convenient and automated imaging of all wells. Following image acquisition, I transferred the supernatant from each well to a new plate and measured the fluorescence intensity of the supernatant, this time using the fluorescence intensity measurement feature of the TECAN Spark Cyto.

To investigate if bacteria have an impact on the ROS-levels in *Hydra* polyps, I compared the ROS levels of WT polyps to GF polyps. As a positive control, I used WT polyps treated for 1 hour with 0.4 mM tBuOOH.

The imaging worked well for almost all replicates, resulting in sharp and focused images, with the fluorescence signal clearly visible (**Figure 15)**. A clear difference in signal intensity between the three treatments was visible, with GF polyps showing a stronger fluorescence signal than WT polyps (**Figure 15A-D**).

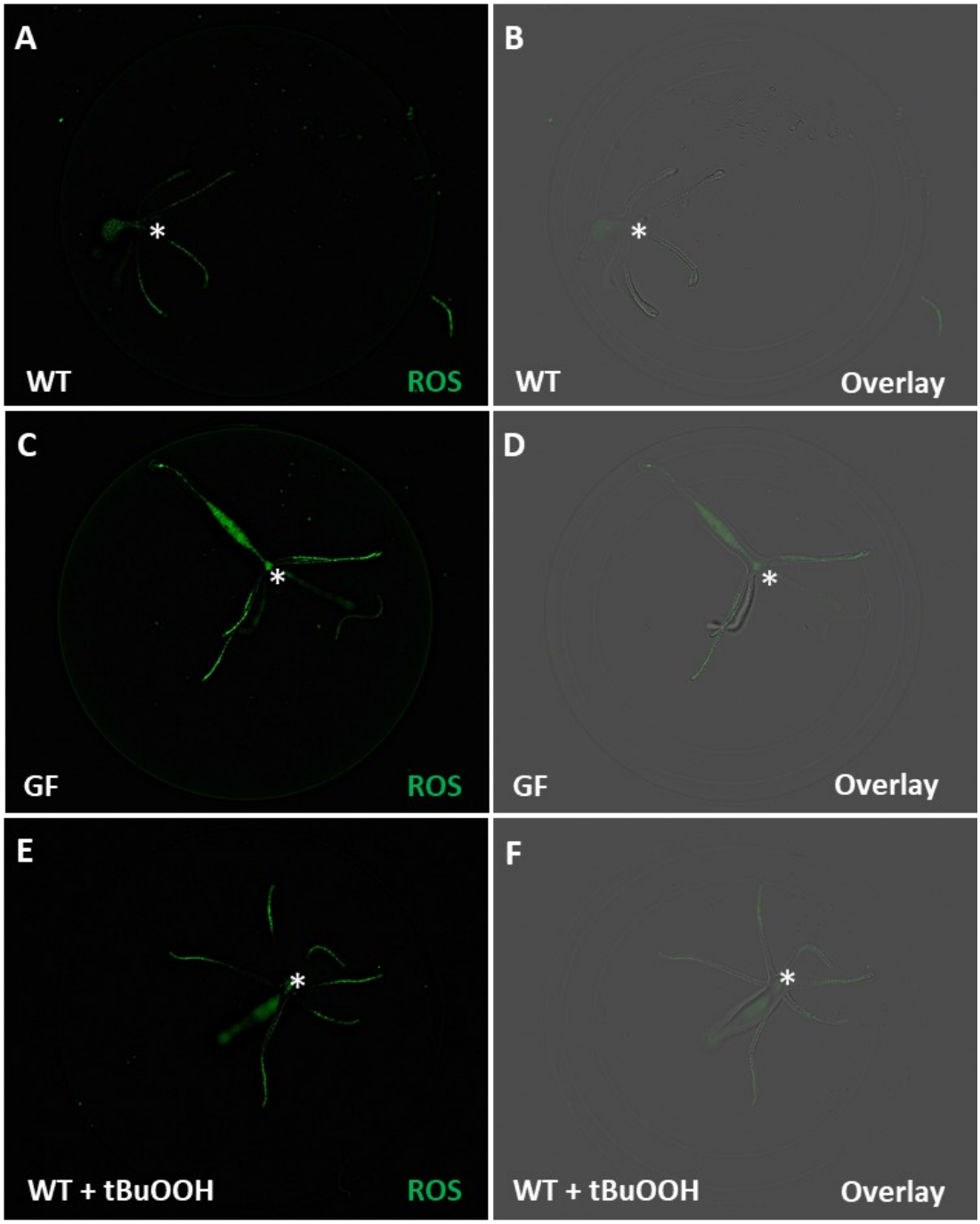

Figure 15: High-throughput In-vivo ROS assay of Hydra polyps. *Polyps labeled with the Total ROS Assay Kit (520 nm) and imaged using the TECAN Spark Cyto.* ***A, C, E:*** *Fluorescence images of a WT polyp, GF polyp and WT polyp treated with tBuOOH, respectively.* ***B, D, F:*** *Overlay images of the fluorescence and phase-contrast channels of the same polyps shown in images* ***A, C, E****. * marks the mouth opening of polyps.*

Quantitative analysis of fluorescence intensity confirmed this and revealed a significant difference in between the treatments (**Figure 16)**. GF polyps showed a significantly stronger signal than WT polyps, in both the imaging analysis of live polyps as well as in the supernatant (**Figure 16A + B**). Interestingly, removal of the natural microbiota of *Hydra* polyps even leads to a stronger increase of ROS levels than the treatment with tBuOOH (**Figure 16B + C**).

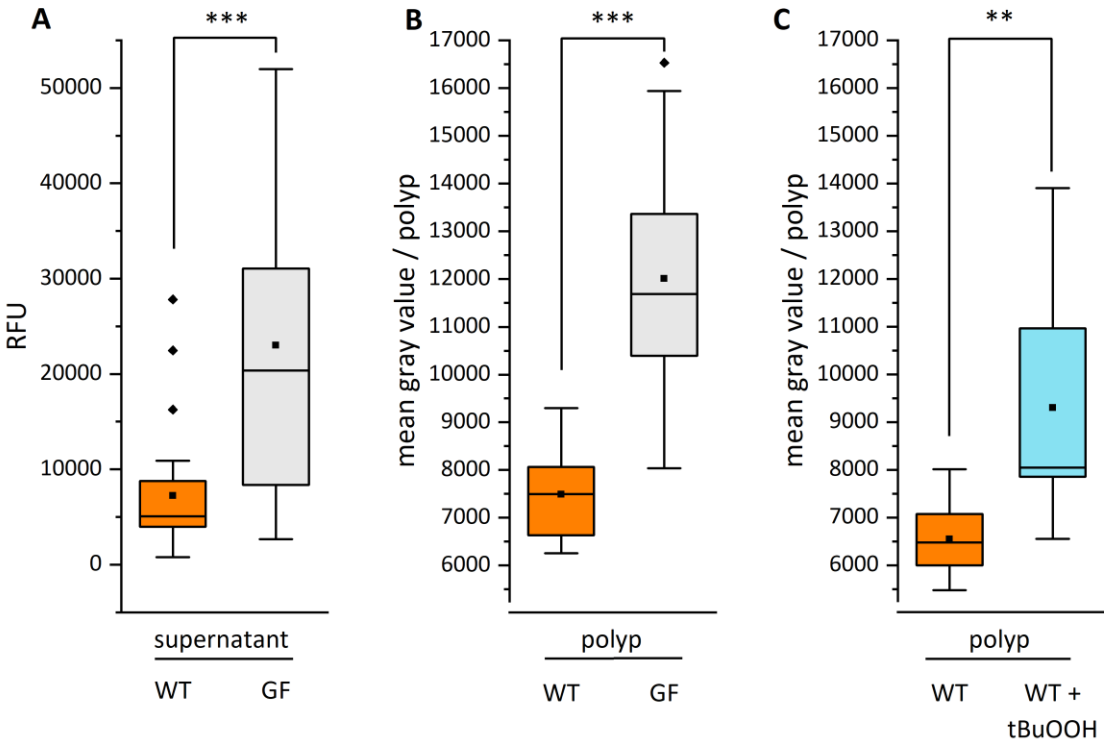

Figure 16: Quantification of ROS levels in Hydra polyps. *Quantification of ROS levels in Hydra polyps, labeled with the Total ROS Assay Kit (520 nm), using the TECAN Spark Cyto.* ***A:*** *Amount of ROS measured in the supernatant of WT and GF polyps. Signal intensity is measured in relative fluorescence units (RFU); n > 24.* ***B:*** *ROS levels of WT and GF polyps, measured as mean gray value / polyp; n > 24.* ***C:*** *mean fluorescent intensity of untreated WT polyps and WT polyps treated with 0.4 mM tBuOOH, measured as mean gray value / polyp; n = 12, two-sample t-test with Welch Correction, *** p <= 0.001, ** p <= 0.01*

These results confirm the efficiency of this method for high-throughput quantification of *in vivo* fluorescence intensity analysis in *Hydra* polyps. It showed that GF polyps exhibit a significantly higher total ROS level then WT polyps, indicating a functional role of the microbiota as ROS scavengers to maintain redox homeostasis in the *Hydra* holobiont.

Hydra's microbiota modulates light-induced ROS

As mentioned before, light is known to affect the behavior and activity levels of *Hydra* polyps and can have strong effects on all living organisms. It also effects ROS production in cells, depending on wavelength and intensity (Kumar Rajendran et al. 2019).

Because of this, I analyzed the potential effect of light on *Hydra* ROS levels. I used the same setup as in the previous experiment, only this time I separated the polyps into two groups. One group was sampled during light conditions and one under dark conditions, as described in the method section.

I wanted to determine if the presence of the microbiota affects *Hydra* ROS levels differently under light and dark conditions and exclude any possible experimental artifacts due to unwanted photoreactions.

The previously observed difference in ROS levels between WT and GF polyps is not affected by the presence or absence of light. Under both conditions, GF polyps showed significantly increased ROS levels when compared to WT polyps (**Figure 17**).

The results also show microbiota -mediated effect on light-induced ROS levels. GF polyps that were sampled during a light phase showed a significantly stronger ROS signal compared to GF polyps sampled during a dark phase. WT polyps on the other hand show no significant difference in their ROS levels between light and dark phases (**Figure 17**).

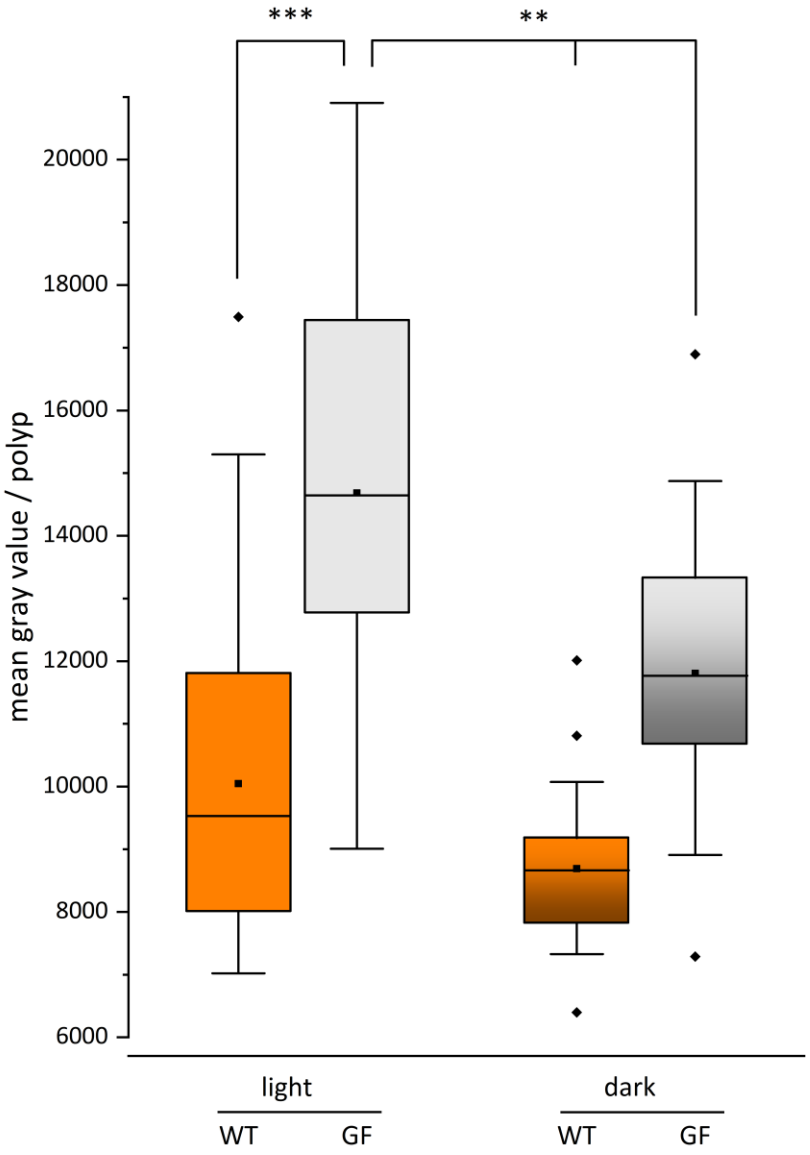

Figure 17: Quantification of ROS levels in Hydra polyps under different light conditions. *ROS levels of WT and GF polyps, sampled either during light or dark conditions, labeled with the Total ROS Assay Kit (520 nm). n > 17, Kruskal-Wallis ANOVA with post-hoc Dunn`s test, *** <= 0.001, ** <= 0.01*

These result support the previous hypothesis that *Hydra's* microbiota is involved in maintaining ROS homeostasis of the holobiont. While WT showed no difference in total ROS levels between light and dark conditions, the GF phenotype of increased ROS levels was even stronger during light conditions than during dark conditions.

To exclude this light-effect from further experiments, all following ROS assay experiments were conducted under dark conditions.

Genetic and structural examination of the *Curvibacter* ohr operon

Since the presence of ROS on *Hydra*, and a significant effect of the microbiota on total ROS levels was now confirmed, I wanted to determine a possible functional role of *Curvibacter's* repertoire of upregulated ROS scavenging genes. I decided to focus on the *ohr* operon for further research, primarily because *ohrR* and *ohrA* were the strongest upregulated genes in the metatranscriptomic analysis, and because these genes are to current knowledge exclusively found in microbiota (Meireles et al. 2022). Additionally, since *Curvibacter* was by far the least-resistant bacterium to H_2O_2 in the *Hydra* ecosystem, I wanted to choose genes that are usually not involved in scavenging of H_2O_2.

Comparison of the *Curvibacter ohr* operon against two of the most studied bacteria in this regard, *Xanthomonas campestris* and *Bacillus subtilis*, revealed a genetic arrangement that is identical to *Xanthomonas campestris* (**Figure 18A**).

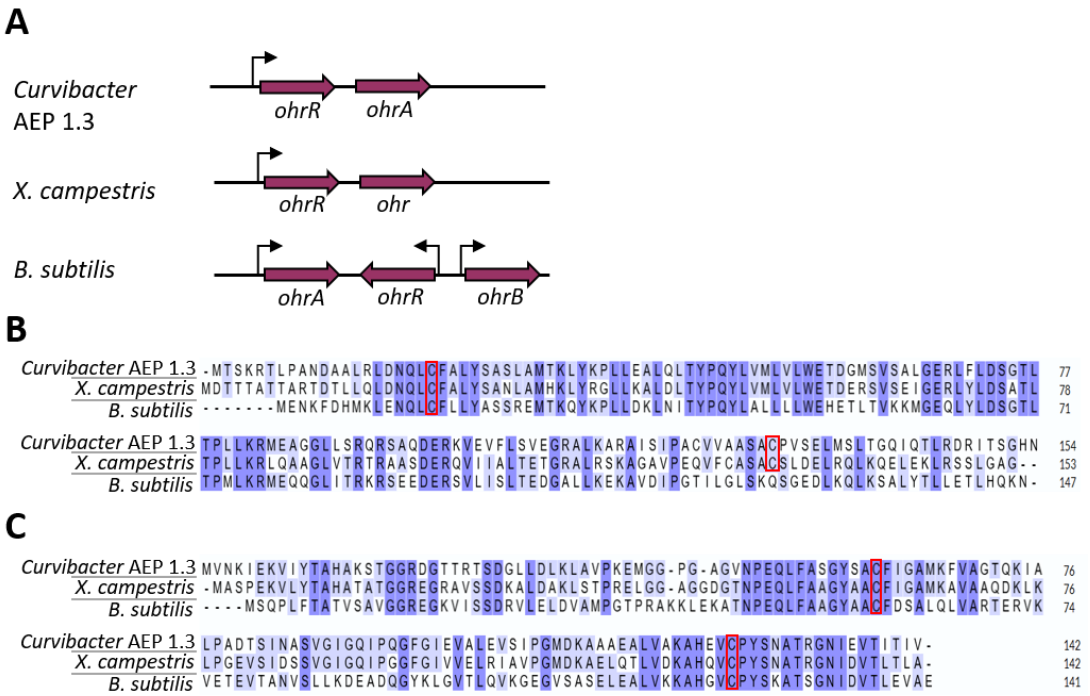

Figure 18: Comparison of the Curvibacter ohr operon with X. campestris and B. subtilis. A: *Arrangements of ohr gene operons in Xanthomonas campestris, Bacillus subtilis and Curvibacter AEP 1.3. Small, bent arrows indicate start and direction of transcription.* ***B:*** *Alignment of OhrR protein sequences.* ***C:*** *Alignment of Ohr protein sequences. Sequences were aligned using CLUSTAL Omega (1.2.4) multiple sequence alignment via UniProt (UniProt 2025). Sequences of X. campestris and B. subtilis were obtain from the NCBI database. Red boxes highlight conserved catalytic cysteine residues.*

Alignment of OhrR protein sequences showed 57.89% similarity between *Curvibacter* and *X. campestris*, compared to 44.90% between *Curvibacter* and *B. subtilis* (**Figure 18B**).

Sequence analysis showed that *Curvibacter* belongs to the multiple-cysteine group of OhrR, with the absolutely conserved sensing cysteine C21 at the N-terminus corresponding to *X. campestris* C22 and C15 of *B. subtilis* (**Figure 18B)**. Two additional cysteines can be found in *Curvibacter* OhrR at positions C123 and C130, with C130 corresponding to X. campestris C131. Comparison of OhrA with the Ohrs from X. campestris and B. subtilis showed the same result, with conserved active sites and a higher overall similarity between *Curvibacter* and *X. campestris*, compared to *B. subtilis* (**Figure 18 C**).

Structure prediction of *Curvibacter* OhrR and OhrA revealed similar overall folds when compared to *X. campestris* and *B. subtilis* (**Figure 19**).

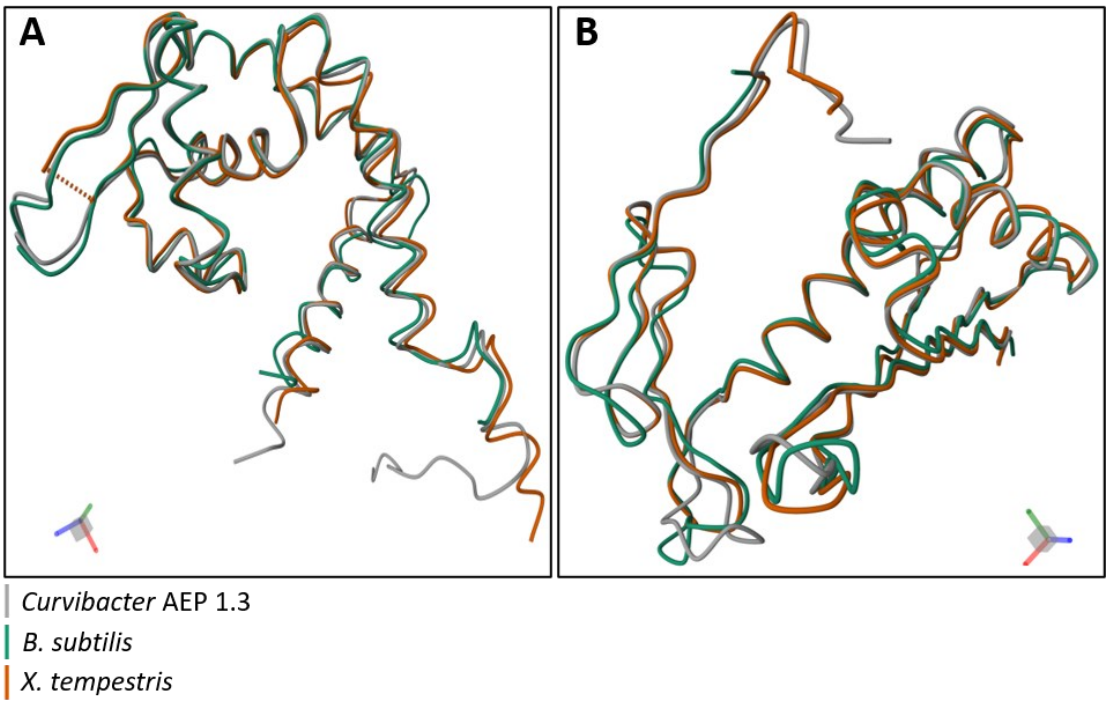

Figure 19: Comparison A: *Superposition of aligned ohrR protein structures of Curvibacter AEP 1.3, X. campestris and B. subtilis.* ***B:*** *Superposition of aligned ohr protein structures of Curvibacter AEP 1.3, X. campestris and B. subtilis. Protein structures for Curvibacter ohrR and ohrA were predicted and overlay figures generated using Alphafold (Jumper et al. 2021; Varadi et al. 2022). Protein structures for X. campestris and B. subtilis were acquired from the Protein Data Bank (PDB) via AlphaFold as well.*

The presence of the conserved cysteines in both OhrR and OhrA as well as the almost identical protein fold predictions indicate a similar function and mechanism for both proteins as those described in *X. campestris* and *B. subtilis*. The *ohr* operon in *Curvibacter* is therefore likely involved in OHP detoxification, with OhrA functioning as a thiol-dependent peroxidase that reduces OHPs to their corresponding alcohols (Cussiol et al. 2003). The strong upregulation of these genes during colonization indicates the presence of OHPs in their environment on *Hydra*.

Generation of *Curvibacter ΔohrR/ΔohrA* mutants for functional analysis

In order to functionally examine the role of the *ohr* operon in the context of the *Hydra-Curvibacter* relationship, I generated a *ΔohrR/-A* double knockout *Curvibacter* strain.

After creation of the cloning vector pGT42_ΔohrR/-A (**Figure 9**), both *ohr* genes were successfully replaced with the SacB/KanR resistance cassette (**Figure 20B**). This was verified by the transference of kanamycin resistance to transformed clones and multiple PCRs targeting the knocked-out region, as well as areas covering inserted regions and adjacent regions in the chromosome.

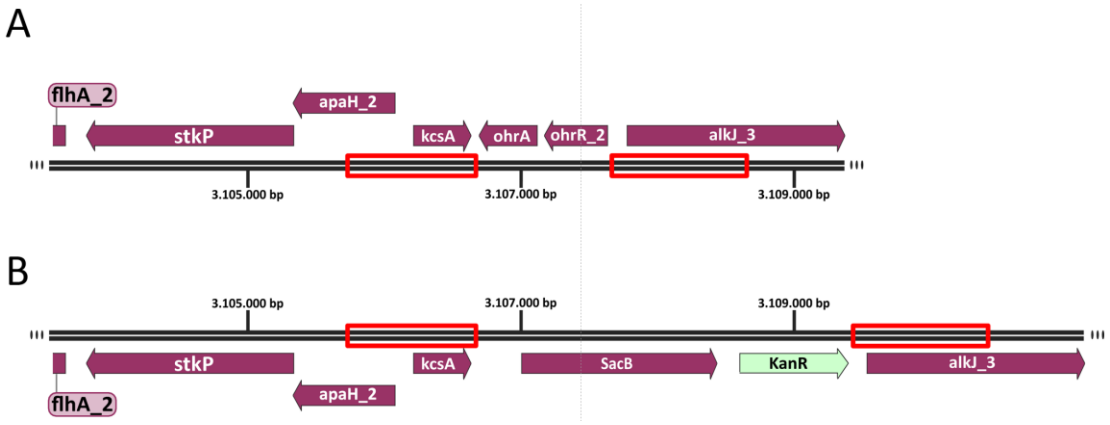

Figure 20: Chromosomal region of ohr genes in the Curvibacter genome. A: *Gene locus of the ohrA and ohrR genes in wildtype Curvibacter.* ***B:*** *The same region after successful knockout of the target genes. The SacB/KanR cassette is inserted via homologous recombination in place of the ohrR/-A cassette, leading to a knockout of both ohr genes. Red boxes highlight the flanking regions used in the creation of knockout vector pGT42_ΔohrR/-A.*

Comparative growth analysis of *Curvibacter ΔohrR/-A*

Following the successful knockout of *Curvibacter ohr* genes, I compared the *in vitro* growth of WT *Curvibacter* AEP 1.3 and the knockout strain *ΔohrR/-A*. Liquid cultures of both strains were diluted to an OD of 0.1 before being transferred to a 96-well plate for growth measurement. The knockout resulted in a significant but very small difference in growth rates between AEP 1.3 and *ΔohrR/-A* (**Figure 21B**). Growth curves of the two strains are almost identical (**Figure 21A**). Overall, the knockout affects growth rate of *Curvibacter* in culture to a negligible amount.

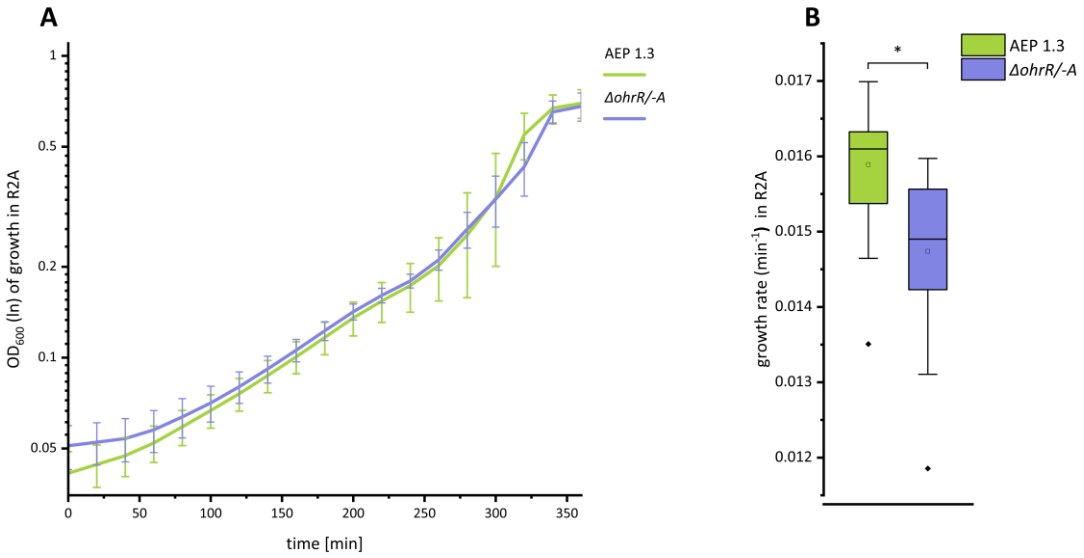

Figure 21: Growth comparison between Curvibacter AEP 1.3 and ΔohrR/-A: *Growth curves of Curvibacter AEP 1.3 and ΔohrR/-A. OD600 was measured every 20 min. Growth rates were significantly different between the two strains. AEP 1.3: growth rate: 0.01589 min-1, ΔohrR/*

Curvibacter ΔohrR/-A shows selective sensitivity to organic hydroperoxides

Next, I wanted to confirm the role of the *ohr* genes in ROS scavenging. For this, I compared growth of AEP 1.3 and *ΔohrR/-A* in culture medium in the presence of either H_2O_2 or *tert*-Butyl hydroperoxide (tBuOOH). tBuOOH is an organic peroxide commonly used for resistance assays against ROS.

The presence of H_2O_2 had no effect on growth of *ΔohrR/-A* when compared to the control. For all concentrations, the knockout only showed the slightly reduced growth rate when compared to WT that I observed before (**Figure 22 + Figure 23**).

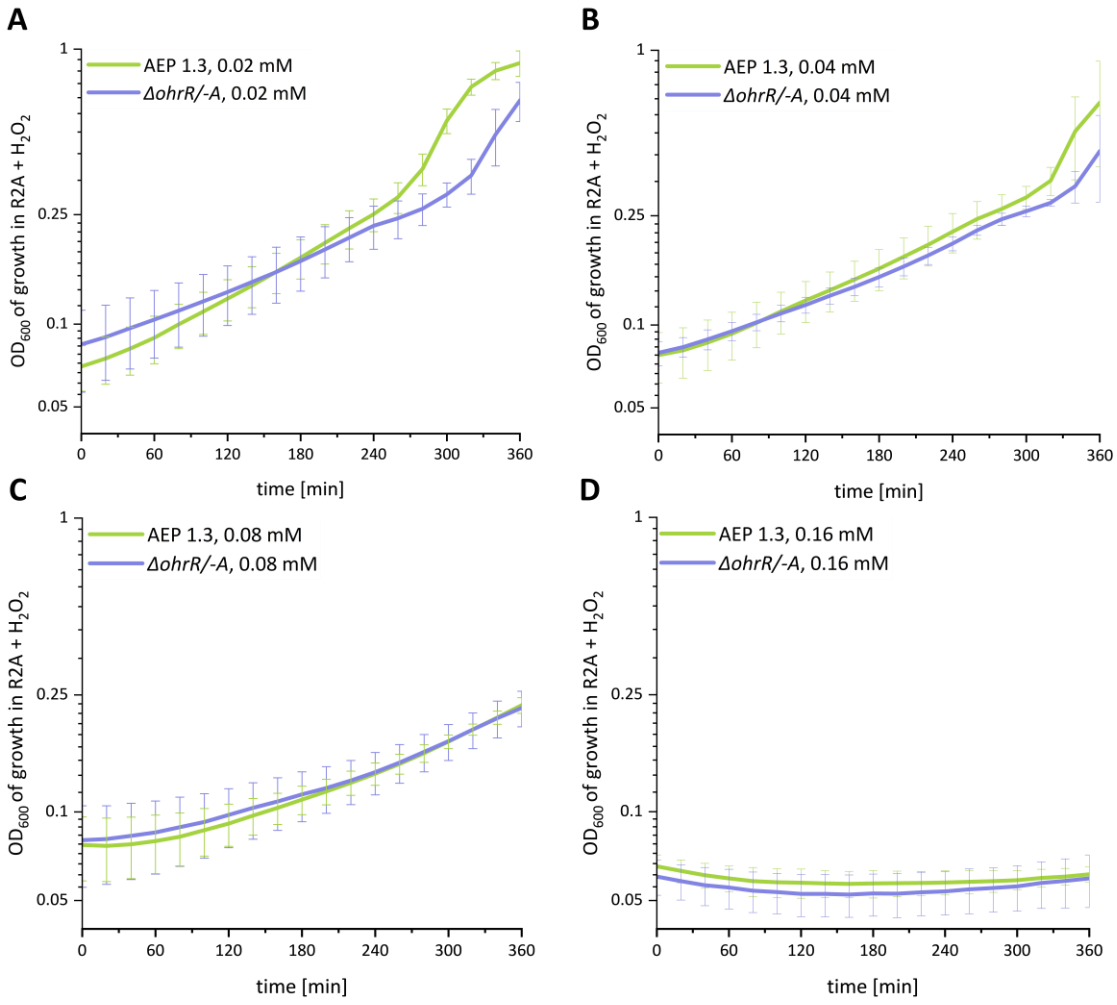

Figure 22: Growth of Curvibacter AEP 1.3 and ΔohrR/-A in the presence of H_2O_2: *Growth curves of Curvibacter AEP 1.3 (green) and ΔohrR/-A (blue) in the presence of 0.02 mM (**A**), 0.04 mM (**B**), 0.08 (**C**) and 0.16 mM (**D**) H_2O_2. All cultures were adjusted to a starting OD of 0.1 in 96-well plates. H_2O_2 was added to the R2A medium immediately before starting the growth measurement. OD_{600} was measured every 20 min. n = 4*

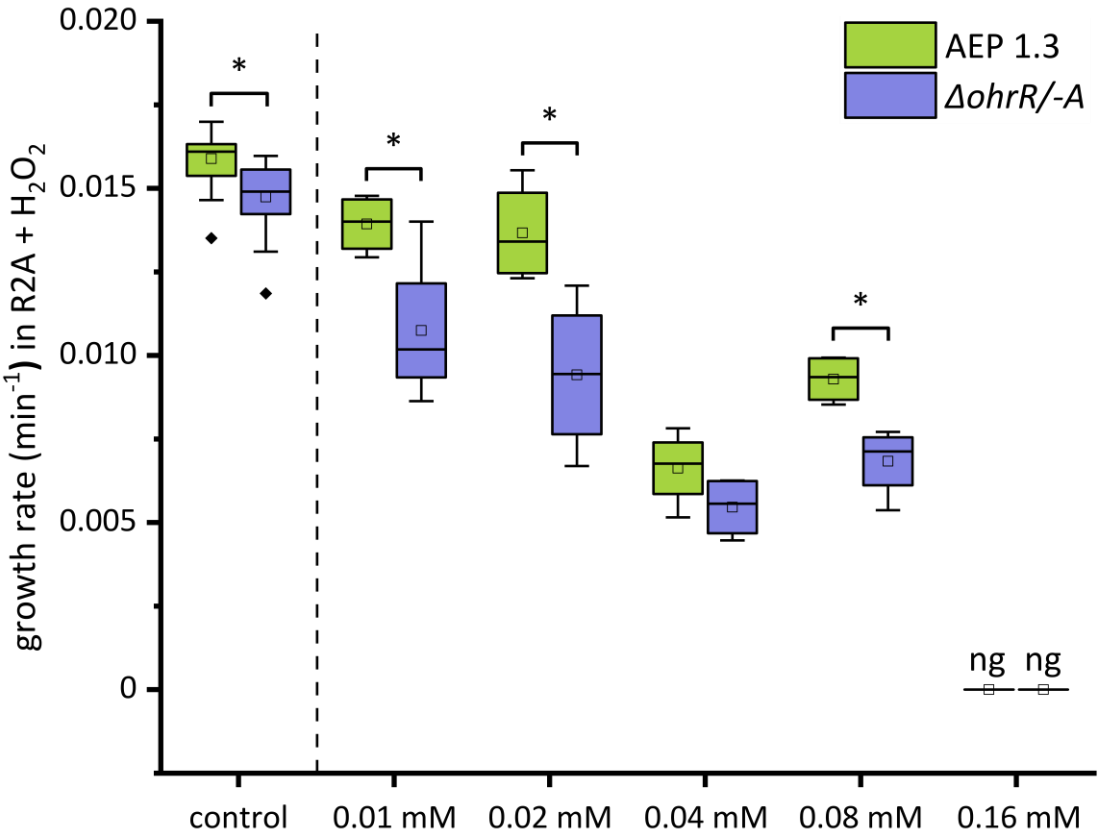

Figure 23: Growth rates of Curvibacter AEP 1.3 and ΔohrR/-A in the presence of H_2O_2: *Growth rates of Curvibacter AEP 1.3 (green) and ΔohrR/-A (blue) in the presence of increasing concentrations of H_2O_2. All cultures were adjusted to a starting OD of 0.1 in 96-well plates. H_2O_2 was added to the R2A medium immediately before starting the growth measurement. OD_{600} was measured every 20 min and growth rates calculated afterwards. ng = no growth. two-sample t-test, * p <= 0.05, n = 4*

Additionally, loss of the *ohr* operon had no impact on resistance against H_2O_2 when compared to AEP 1.3. A concentration of 0.16 mM H_2O_2 was lethal for both strains. This result is in line with most studies on the *ohr* operon. Except for rare exceptions it was shown to have no scavenging function towards H_2O_2 (Meireles et al. 2022).

Treatment of *ΔohrR/-A* with tBuOOH revealed a stronger sensitivity when compared to WT (**Figure 24 + Figure 25**). A concentration of 0.04 mM tBuOOH was lethal for the *ΔohrR/-A* strain, while AEP 1.3 only showed reduced growth.

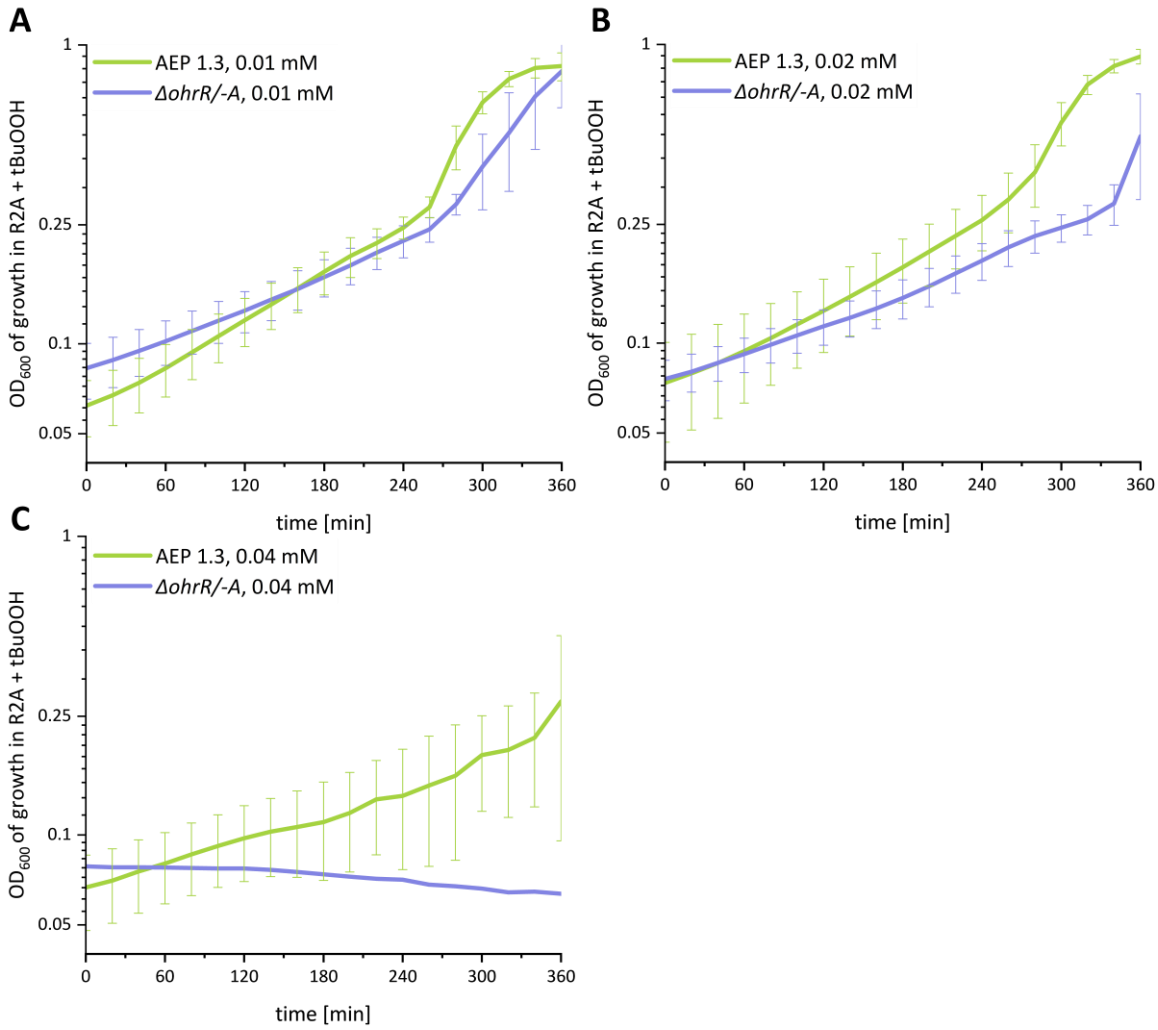

Figure 24: Growth of Curvibacter AEP 1.3 and ΔohrR/-A in the presence of tBuOOH: *Growth curves of Curvibacter AEP 1.3 (green) and ΔohrR/-A (blue) in the presence of 0.01 mM (**A**), 0.02 mM (**B**) and 0.04 (**C**) tBuOOH. All cultures were adjusted to a starting OD of 0.1 in 96-well plates. H_2O_2 was added to the R2A medium immediately before starting the growth measurement. OD_{600} was measured every 20 min. n = 4*

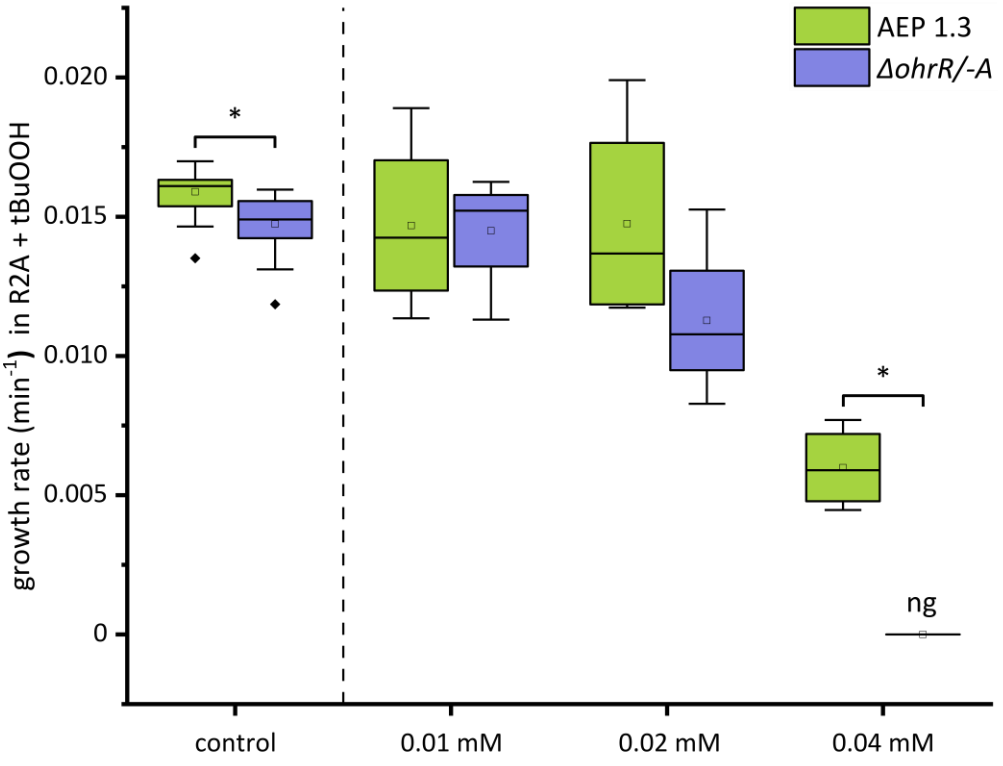

Figure 25: Growth rates of Curvibacter AEP 1.3 and ΔohrR/-A in the presence of tBuOOH: *Growth rates of Curvibacter AEP 1.3 (green) and ΔohrR/-A (blue) in the presence of increasing concentrations of tBuOOH. All cultures were adjusted to a starting OD of 0.1 in 96-well plates. H_2O_2 was added to the R2A medium immediately before starting the growth measurement. OD_{600} was measured every 20 min and growth rates calculated afterwards. ng = no growth. two-sample t-test, * p <= 0.05, n = 4*

This result confirms the functional role of the *ohr* operon as specific scavengers of OHPs, but not H_2O_2, in *Curvibacter*.

Elevated ROS in germ-free polyps is not linked to lipid peroxidation

While previous experiments showed the presence of ROS in the *Hydra* holobiont and the influence of the microbiota on total ROS levels, it is not clear if the increased ROS levels in GF polyps are a sign of ROS distress and are actually detrimental to the polyps. Using a live cell assay, I wanted to determine possible cell damage via oxidative degradation of cellular lipids, a common reaction resulting from distress via OHPs. I compared the amount of lipid peroxidation in WT and GF *Hydra* polyps, using the

Image-iT® Lipid Peroxidation Kit. I labeled WT and GF polyps as described in the method section and used the TECAN Cyto Spark for imaging. As a positive control I used a final concentration of 0.1 mM cumene hydroperoxide (CuOOH) to induce oxidative distress, as provided by the manufacturer. CuOOH is another commonly used artificial organic hydroperoxide to induce oxidative stress.

There was no significant difference in the amount of lipid peroxidation between WT and GF polyps, suggesting that the increased ROS levels of GF polyps do not result in oxidative distress. There was also no significant difference between WT and GF polyps that were both treated with CuOOH, indicating that the microbiota of *Hydra* might not have a direct role in protecting the holobiont against ROS-induced oxidative damage.

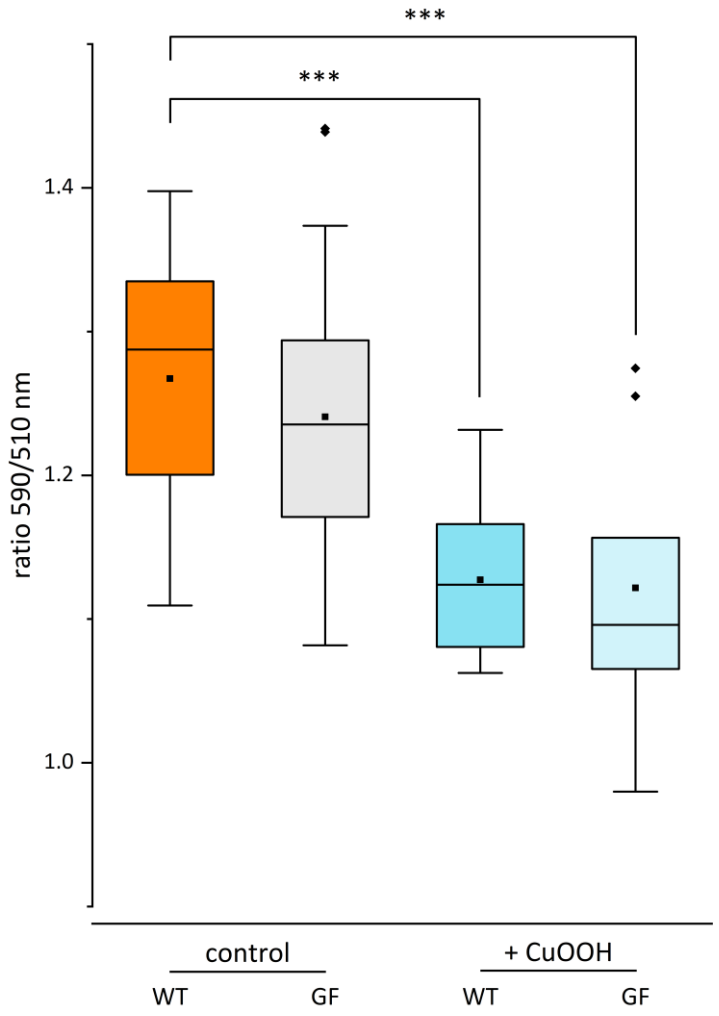

Figure 26: Lipid peroxidation detection assay. *Fluorescence ratios of WT and GF polyps labeled with the Image-iT® Lipid Peroxidation Kit. The given ratio of red to green signal (590/510 nm) gives a read-out for the amount of lipid peroxidation in the polyp's cells. A lower ratio signifies higher lipid peroxidation. 0.1 mM of CuOOH was used as a positive control to induce lipid peroxidation. n = 38 for control groups; n = 9 for CuOOH treatment; One-way ANOVA with post-hoc Tukey test, *** <= 0.001*

Curvibacter ohr operon plays a functional role in maintaining ROS Homeostasis in the *Hydra* holobiont

Even though the increased ROS levels of GF polyps appear not to be inducing any apparent ROS distress, the presence of *Hydra's* natural microbiota still seems to be an important factor for ROS homeostasis of the *Hydra* holobiont. If the previously observed GF phenotype is a direct result of the loss of the polyp's microbiota, simply restoring the microbiota of GF polyps should lead to a reduction of the total ROS level. To test this, I recolonized GF polyps with the full natural microbiome of *Hydra* (conv = conventionalized). I also recolonized polyps with either *Curvibacter* AEP 1.3, or *Curvibacter ΔohrR/-A*, to determine a possible role for the *ohr* operon in maintaining *Hydra´s* ROS levels.

The results show a trend of increasing ROS levels, the more the microbiome differs from its natural state (**Figure 27**).

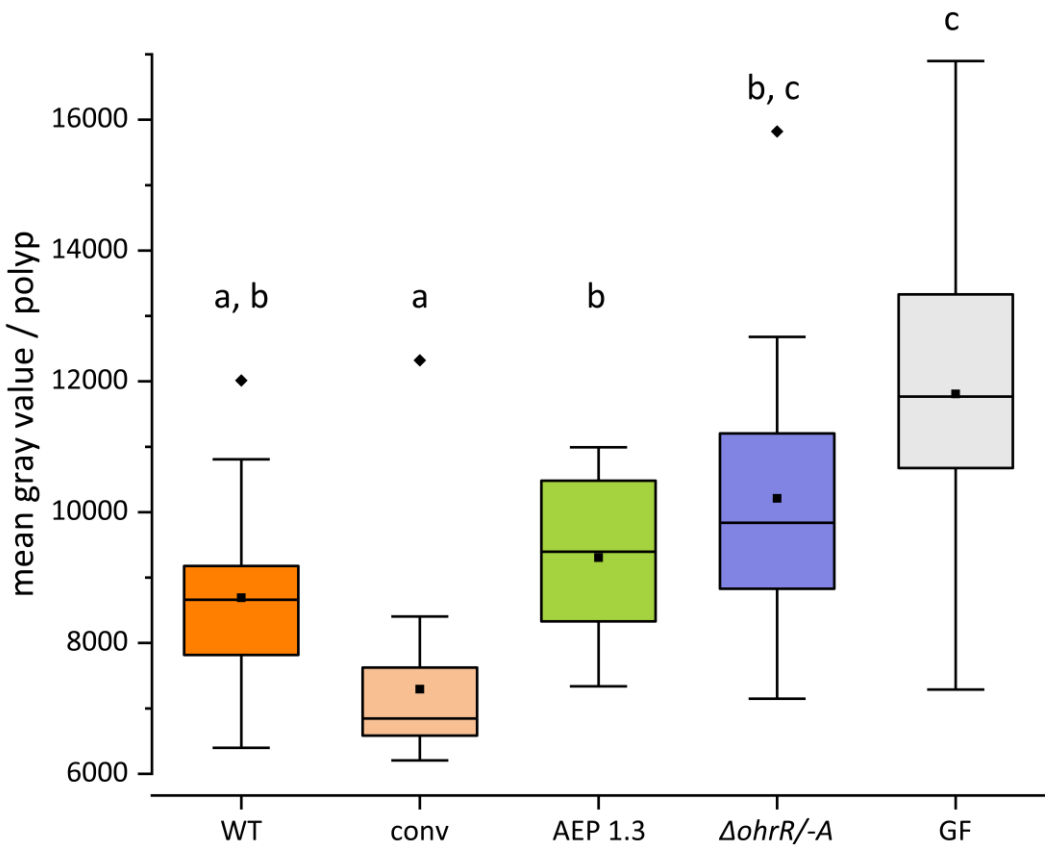

Figure 27: Rescue effect of AEP 1.3. *Quantification of ROS levels in Hydra polyps, labeled with the Total ROS Assay Kit (520 nm). Polyps are recolonized with the full natural microbiota (conventionalized = conv.), mono-colonized with either Curvibacter AEP 1.3 or ΔohrR/-A, and compared to WT or GF polyps. n = 19. Different letters indicate a significant difference measured by Kruskal-Wallis ANOVA with post-hoc Dunn`s test.*

Restoration of the natural microbiota led to significantly reduced ROS levels when compared to GF polyps, restoring them to that of WT polyps. This result also signifies that the GF phenotype is actually due to the loss of the microbiota and not a potential reaction to the AB treatment.

Interestingly, mono-recolonization with WT *Curvibacter* was also able to rescue the GF phenotype, leading to significantly reduced ROS levels when compared to GF polyps and even restoring them to WT levels.

In contrast, recolonization with *ΔohrR/-A* resulted in no significant difference in ROS levels when compared to GF. Although *ΔohrR/-A* showed no significant difference to WT polyps as well, taken together the results of both WT *Curvibacter* and *ΔohrR/-A* indicate an important role of the *Curvibacter ohr* operon in regulating ROS levels in the *Hydra* holobiont. Since *ΔohrR/-A* is not able to scavenge OHPs specifically, the observed differences in ROS levels between WT and GF *Hydra* might be due to an increase of this ROS species.

Despite this apparent regulatory effect, the results from the lipid peroxidation assay showed that the increased ROS levels in GF polyps do not lead to detectable damaging effects (**Figure 26**).

Because of this, I wanted to test if the *ohr* operon is important for *Curvibacter's* colonization efficiency. Since the operon is functionally active, its protective function against OHPs might be required during colonization of *Hydra*.

Curvibacter ΔohrR/-A shows increased colonization ability

To examine a possible effect of the loss of the *ohr* operon on the colonization process, I compared the ability of *Curvibacter* AEP 1.3 and *ΔohrR/-A* to colonize GF *Hydra*.

I recolonized GF polyps with the same number of CFUs of either AEP 1.3 or *ΔohrR/-A*, and determined the amount of CFU that colonized polyps after 1 dpr, 2 dpr and 7 dpr.

Already after 1 dpr, *ΔohrR/-A* showed a significantly higher ability to colonize *Hydra* than AEP 1.3. Both bacteria continuously increased in CFUs over time, however, *ΔohrR/-A* always showed a higher number of CFUs than AEP 1.3 (**Figure 28**).

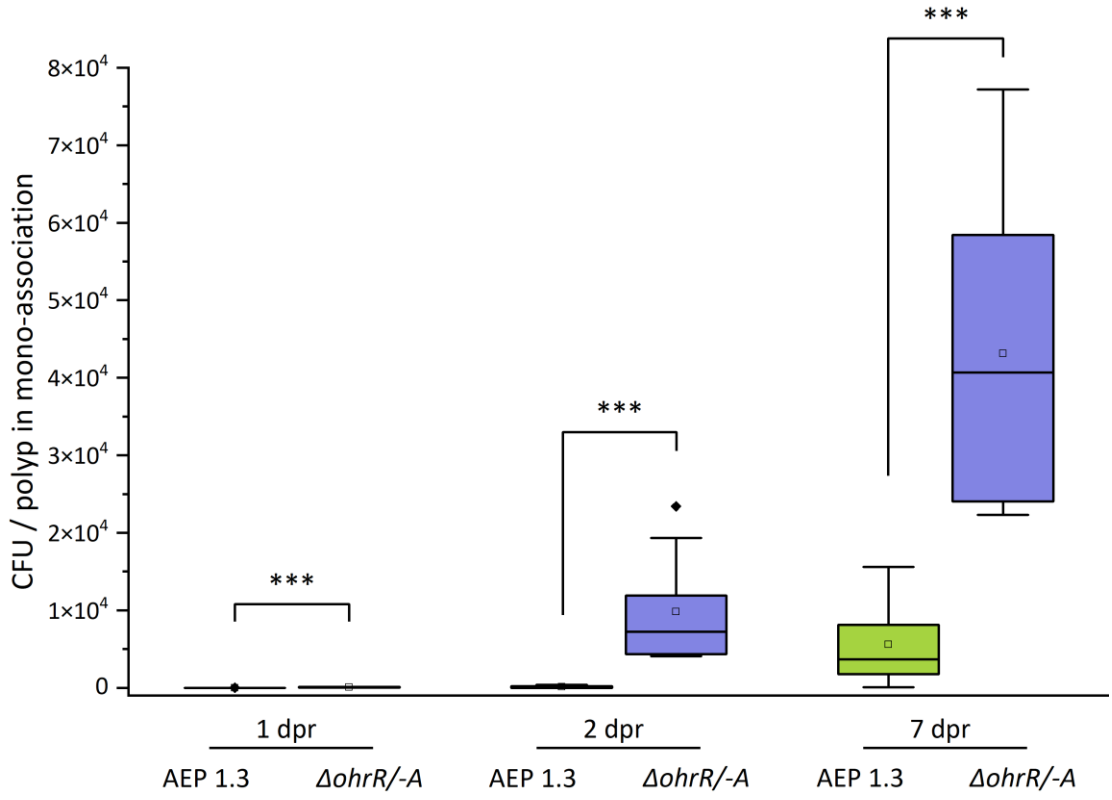

Figure 28: Recolonization efficiency of AEP 1.3 and ΔohrR/-A in mono- association. *CFU / polyp of AEP 1.3 (green) and ΔohrR/-A (purple) at 1 dpr, 2 dpr and 7 dpr in mono- association. n = 10, two-sample t-test with Welch Correction, *** <= 0.001.*

To confirm this result and test the colonization ability of both strains in direct competition, I repeated the experiment. This time I recolonized polyps with equal amounts of both strains in di-association. Even in direct competition, *ΔohrR/-A* was significantly better in establishing and maintaining a stable colonization of *Hydra* than AEP 1.3 (**Figure 29**).

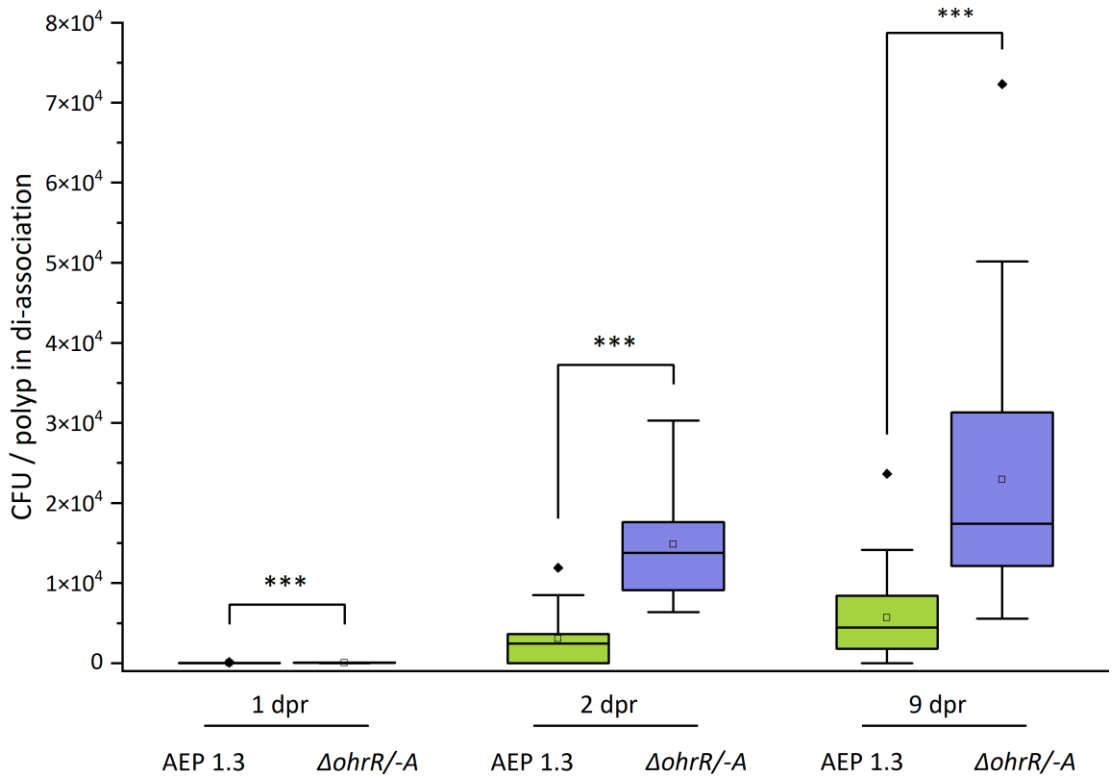

Figure 29: Recolonization efficiency of AEP 1.3 and ΔohrR/-A in di-association. *CFU / polyp of AEP 1.3 (green) and ΔohrR/-A (purple) at 1 dpr, 2 dpr and 9 dpr in di- association. n = 20, two-sample t-test with Welch Correction, *** <= 0.001.*

The result of the recolonization experiments was quite unexpected. The strong upregulation of the *ohr* operon in the metatranscriptomic data, as well as the *ohr* depended rescue effect of the GF phenotype suggested a significant role for those genes for *Curvibacter's* colonization ability. Instead, *ΔohrR/-A* showed a consistent and significant improvement over WT *Curvibacter* in recolonizing GF *Hydra* polyps in mono-colonization, as well as in direct competition. Owing to the nature of *ΔohrR/-A* being a double knockout, it remains unclear if the observed results in the previous experiments result from the loss of OhrA, OhrR, or both. It is possible that OhrR

regulates additional target genes and the observed effects in my experiments are due to the loss of OhrR, leading to a dysregulation of these downstream genes.

Overall, my results show that *Hydra's* microbiota are involved in maintaining ROS homeostasis in the holobiont. The *Curvibacter ohr* operon seems to play an important part in this, although the actual role and function of OhrA and OhrR remains elusive.

Discussion

Hydra and *Curvibacter* share a conserved evolutionary relationship

The bacterial symbiont *Curvibacter* and its host *Hydra* are emerging as a new symbiosis model to study questions of inter-kingdom communication. The goal of this thesis was to find further indications for how important this relationship is and how it is maintained.

I started with an evolutionary analysis to assess the congruence between the phylogenetic trees of *Curvibacter* and *Hydra*. For this, I used *Curvibacter* species isolated from different *Hydra* lab strains and compared their phylogeny to that of *Hydra*.

The phylogenetic tree of *Hydra* was identical to those from several previous studies, supporting the well-established groups and species of *Hydra* (**Figure 10B**) (Martinez et al. 2010; Schwentner and Bosch 2015).

Comparing the phylogenies of *Curvibacter* and *Hydra* showed a strong congruence between the two, with the phylogenetic tree of *Curvibacter* mirroring the one from *Hydra* (**Figure 10**). Congruent phylogenies like this are a hallmark of co-speciation events, where host and symbiont speciate at the same time. This result fits to a previous study, in which it was shown that the composition of the whole microbial communities recapitulates the phylogeny of the *Hydra* hosts as well; a pattern termed phylosymbiosis (Brucker and Bordenstein 2013; Franzenburg, Walter, et al. 2013).

Additionally, all *Curvibacter* isolates from different cultures of the same *Hydra* species clustered together as a single taxon, suggesting that the host selects for, and maintains a specific *Curvibacter* variant (**Figure 10A**). This species-specificity is supported by a previous study as well, where the microbiota composition of long-term *Hydra* cultures was compared to that of polyps collected from the wild (Fraune and Bosch 2007). Even after more than 30 years of culturing, the microbiota composition of lab polyps showed a high similarity to that of wild polyps from the same species (Fraune and

Bosch 2007). In contrast, the microbiota differed significantly when comparing different *Hydra* species, despite having the same living conditions in the lab or living in the same pond (Fraune and Bosch 2007). A later study further confirmed this, using a more advanced sequencing approach (Franzenburg, Walter, et al. 2013).

Similar species-specific host-symbiont relationships with clear signs of co-speciation and/or phylosymbiosis were also found in other holobiont systems. *Nasonia* wasps show a strong phylosymbiosis with their gut microbiome, leading to hybrid lethality even between closely related *Nasiona* species (Brucker and Bordenstein 2012, 2013; Cross et al. 2021). Multiple studies could show a clear congruence between the phylogeny of hominids and their most prevalent bacterial taxa in the gut (Moeller et al. 2016; Groussin et al. 2017; Ruhlemann et al. 2024). Other examples can be found in terrestrial and aquatic systems, including both plants and animals (Lim and Bordenstein 2020).

The co-speciation between *Hydra* and *Curvibacter* shown in this study, as well as their phylosymbiosis (Franzenburg, Walter, et al. 2013), vertical transmission of symbionts (Fraune et al. 2010) and the environment-independent, species-specific microbiome of *Hydra* (Fraune and Bosch 2007), shows the conserved evolutionary relationship between *Hydra* and their microbiota. As *Hydra* is a member of the phylogenetically ancient phylum Cnidaria, it also indicates that co-speciation in general might be an evolutionary conserved phenomenon. Uncovering the underlying mechanisms that determine host-specificity in these evolutionary events will provide a deeper understanding of how inter-kingdom interactions function and how they have influenced reciprocal relationships across the history of life.

In contrast to most other current model organisms, *Hydra's* microbiota consists of only a handful of members which are all readily culturable in the lab (Fraune et al. 2015). In addition, the wide range of available genetic and experimental tools for *Hydra* and its microbiota allows for more convenient analyses to determine the roles of individual members in the *Hydra* holobiont (Fraune et al. 2015; Wein et al. 2018; Klimovich, Wittlieb, and Bosch 2019; Cazet et al. 2023). Using the *Hydra-Curvibacter* symbiosis as

a model for host-symbiont speciation and evolution therefore will allow us to investigate the fundamentals of evolutionary adaptations in holobionts in a low-complex system.

Metatranscriptomic insights into general host-driven symbiotic adaptations of *Curvibacter* during colonization

To get deeper insights into this close association between *Curvibacter* and *Hydra*, I employed a metatranscriptomic approach to identify *Curvibacter* genes important for their relationship.

KEGG analysis of differentially regulated genes showed a downregulation of flagellum and chemotaxis genes during host colonization (**Figure 12**). This makes sense, since chemotaxis and motility via flagellum are not needed by *Curvibacter* when already colonizing its host. The main structural component of the flagellum, flagellin, is also a widely recognized MAMP. It is known that *Hydra* reacts to flagellin-exposure with increased expression of the antimicrobial peptide periculin-1 via a TLR-signaling cascade (Miller et al. 2007; Bosch et al. 2009; Augustin, Fraune, and Bosch 2010). Flagellar expression poses a potential risk to the host, as the motility it confers is, for example, associated with cell invasion or the crossing of epithelial barriers, i.e. actions that can be detrimental to the host (Akahoshi and Bevins 2022). Because of this, suppression of *Curvibacter* flagellin expression is likely to be a necessity during host-colonization.

Interestingly, it was shown before that *Hydra* is able to directly manipulate gene expression of *Curvibacter* to control flagellin expression (Pietschke et al. 2017). The authors could show that *Hydra* is actively quenching homoserine lactones (HSLs), a class of quorum sensing molecules in bacteria (Schauder and Bassler 2001; Pietschke et al. 2017). *Curvibacter* is mainly able to produce and recognize two species of HSLs, namely 3OC12-HSL and 3OHC12-HSL (Minten 2017; Pietschke et al. 2017). *Hydra* is actively quenching 3OC12-HSL and converting it to 3OHC12-HSL via oxidoreductase activity (Pietschke et al. 2017). Both AHLs induce different responses in *Curvibacter*,

with 3OC12-HSL treated *Curvibacter* showing increased expression of flagellum and chemotaxis genes (**Figure 12**). 3OHC12-HSL on the other hand leads to increased expression of several metabolic pathways, similar to the result of my metatranscriptomic data. Additionally, treating *Hydra* polyps with 3OC12-HSL during recolonization experiments leads to a significant reduction of recolonization, when compared to polyps treated with 3OHC12-HSL. The same effect was observed when fully colonized WT polyps were treated with both AHL species. In both experiments, treatment with 3OHC12-HSL had no effect on bacterial colonization. The authors concluded that the quenching-ability of *Hydra* promotes assembly and maintenance of the *Hydra* holobiont by suppressing the unwanted *Curvibacter* phenotype induced by 3OC12-HSL, especially the flagellum (Pietschke 2015; Pietschke et al. 2017). In a more recent study, Ulrich et al. did RNA sequencing experiments on *Curvibacter* AEP 1.3 under different conditions while looking at bacteriophage – bacteria interactions (Ulrich et al. 2022). Their data also shows reduced expression of flagellum genes in mono-colonized *Curvibacter* during host-colonization, while metabolic and ribosomal pathways are upregulated (Ulrich et al. 2022).

Remarkably similar results were observed in a mammalian gut system. Commensal gut bacteria of mice were shown to have the potential to produce flagella, but their expression is suppressed by the host in a healthy gut. If the ability to control flagellar gene expression is disturbed, those members of the community start overexpressing flagellar genes, leading to the invasion and breakdown of the gut mucosal barrier (Cullender et al. 2013). This strongly resembles the situation observed by Pietschke et al. in their study of *Hydra* QQ (Pietschke 2015; Pietschke et al. 2017).

Both studies, by Pietschke et al and Ullrich et al, only used mono-colonized/-cultured *Curvibacter*. Still, they support my results from the metatranscriptomic data and *vice versa*. *Curvibacter* shows a strong adaptation in its gene expression to the host environment. These changes are seemingly not simply reactions to the shift from one environment to the other, but the result of specific interactions between the two partners (Augustin, Fraune, and Bosch 2010; Minten 2017; Pietschke et al. 2017; Ulrich et al. 2022). This in turn indicates that the selection and regulation for a specific

microbiota is an active process by *Hydra* and that the core microbiota is essential for maintaining holobiont homeostasis. Recent experiments in our lab also support this thesis. We could show that *Hydra* is able to differentiate between its native *Curvibacter* species, and closely related but non-native *Curvibacter* from other *Hydra* species (Becker et al. 2025). Recolonization of GF *Hydra* polyps with non-native *Curvibacter* strains led to significantly lower CFUs when compared with the native strain. A similar observation was made in corbiculate bees. Like *Hydra*, they display host-specific microbial composition and diverging lineages of their core microbiota between different hosts (Kwong et al. 2017; Ellegaard et al. 2019; Cornet et al. 2022; Li et al. 2022). In honeybees for example, closely related core bacteria of the same species, but from different hosts, show significantly reduced inoculation success compared to the native strain. The bee reacts to inoculation with this non-native microbiota by increasing ROS levels in their gut, inhibiting growth of the non-native strain and reducing colonization efficiency. The native strain on the other hand does not induce this reaction (Guo, Tang, et al. 2023).

These recurrent similarities between gut systems and *Hydra* are especially interesting, as *Hydra`s* body structure resembles the anatomy of the vertebrate intestine: an ectodermal epithelial cell layer, covered by a multi-layered glycocalyx, which harbors its microbiota (Fraune et al. 2015; Schröder and Bosch 2016; Paone and Cani 2020) . Today it is a well-known fact that a disturbed gut microbiome is linked to a multitude of diseases, metabolic disorders and cancer in humans (Cani 2017, 2018). Co-speciation, controlling gene expression of its symbionts via AMPs and quenching of bacterial communication signals might represent an ancient, evolutionary conserved way to establish and maintain holobiont homeostasis. Studies into these interactions between *Hydra* and its symbionts therefore are a mighty tool to further our understanding of fundamental developmental and evolutionary processes in nature.

Curvibacter contributes to ROS homeostasis in the *Hydra* holobiont through *ohr* dependent mechanisms

Reactive oxygen species are increasingly recognized to play an important role in host–microbe interactions, serving dual functions as antimicrobial agents and signaling molecules (Torres 2010; Mone, Monnin, and Kremer 2014; Diaz et al. 2016; Matziouridou et al. 2018; Ballard and Towarnicki 2020; Kunst et al. 2023; Sun et al. 2024). Recently, host-associated microbiota are getting increased attention as key regulators of redox homeostasis in holobionts, particularly through their influence on ROS-production and -detoxification (Pan et al. 2012; Jones et al. 2015; Wong, Brownlie, and Johnson 2015; Hinzke et al. 2019; Dungan et al. 2021; Martins et al. 2021; Kunst et al. 2023; Voolstra et al. 2024).

On an individual gene level, my metatranscriptomic data showed that multiple ROS scavenging genes are upregulated during *Curvibacter's* colonization state on *Hydra* (**Table 20**). As already mentioned in the introduction, ROS are a natural byproduct of an aerobic metabolism, as well as common signaling molecules and effectors for a range of physiological functions (Sies et al. 2022). A general upregulation of ROS scavenging genes from *Curvibacter* during its colonizing state was therefore not necessarily surprising. Indeed, I could show the distinct presence of ROS in the endoderm and body cavity of WT *Hydra* polyps under standard lab conditions, suggesting a physiological accumulation (**Figure 14**). Polyps also seem to expel accumulated ROS from their body cavity into the environment, seemingly surrounding themself with a cloud of ROS. Even though the colonizing bacteria of *H. vulgaris* AEP are found only in the glycocalyx, this expulsion of ROS by *Hydra* might require its microbiota to protect itself against increased ROS levels.

Previous studies examining the water toxicity of multiple components found similar results regarding ROS production in *Hydra* (Jantzen, Hassel, and Schulze 1998; Murugadas et al. 2016; Zeeshan et al. 2016; Zeeshan et al. 2017). Using the dye 2',7'-Dichlorodihydrofluorescein-diacetat (H_2DCFDA) to stain total ROS, these studies observed fluorescence levels all over the body column of control polyps as well (**Figure 30**).

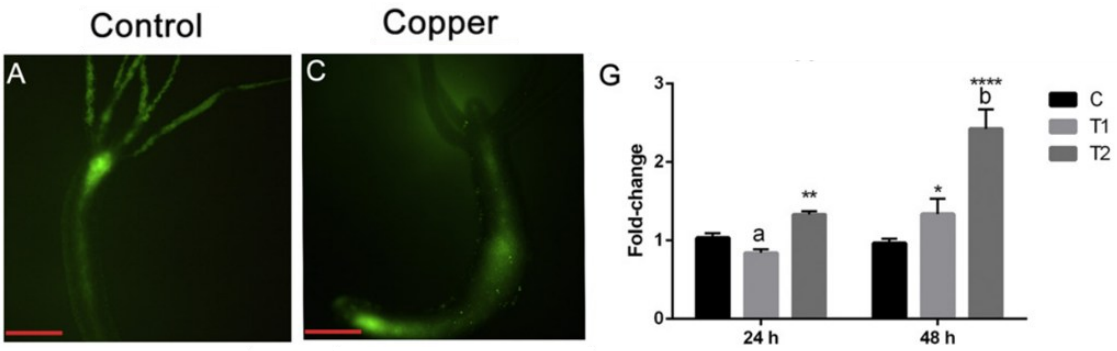

Figure 30: Copper-induced ROS generation in Hydra magnipapillata. *Free radicals were detected using H_2DCFDA.* ***A:*** *Untreated Polyp showing green fluorescence in the endoderm and gastric cavity.* ***C:*** *Polyps treated with copper solution, showing increase fluorescence and vesicles on the ectodermal layer.* ***G:*** *Intracellular ROS levels of cell lysates. T1 = 0.06 mg/L copper solution; T2 = 0.1 mg/L copper solution. **p < 0.01, ****p < 0.0001; ANOVA, Tukey's test. Scale bar A + C: 200 µm. Modified after (Zeeshan et al. 2016).*

Jantzen et al. could show that the fluorescence signal in untreated polyps is likely due to natural mitochondrial formation of ROS and represents the baseline ROS levels in *Hydra* polyps (Jantzen, Hassel, and Schulze 1998). Their treatment of polyps with sodium cyanide, a highly toxic compound that disrupts the electron transport chain in mitochondria, led to the inhibition of fluorescence signals in otherwise untreated polyps (Jantzen, Hassel, and Schulze 1998). Additional treatment with lithium or injury still led to strong fluorescence signals, demonstrating that the fluorescence in control polyps is the result of the respiratory chain (Jantzen, Hassel, and Schulze 1998). Treatment of polyps with toxic compounds led to significantly increased upregulation of antioxidant response genes (Jantzen, Hassel, and Schulze 1998; Zeeshan et al. 2016; Zeeshan et al. 2017). All studies also observed the formation of highly fluorescent dots or vesicles along the body axis, similar to my observations on polyps stressed by long light-exposure (**Figure 14E+F**) (Jantzen, Hassel, and Schulze 1998; Zeeshan et al. 2016; Zeeshan et al. 2017). These results show that increased ROS production can lead to cell damage and death, as a result of a range of exogenous stressors in *Hydra*.

Interestingly, the formation of stress-induced vesicles in those studies coincided with a relative increase in total ROS levels similar to the ones I observed in GF polyps. *Hydra* polyps treated with cobalt or copper showed a 1.5-fold increase in total ROS levels, along with the formation of vesicles and general stress responses (Zeeshan et al. 2016; Zeeshan et al. 2017). I could observe the same relative increase in ROS levels of GF

polyps in my study (**Figure 27**), but no formation of vesicles and no signs of lipid peroxidation (**Figure 26**). This indicates that even though the overall ROS amount in GF polyps is increasing by a relative amount similar to the other studies, it is not an acute stress response. This is also supported by the fact that GF *Hydra* polyps can be maintained over long periods of time, albeit suffering from developmental defects (He et al. 2025). It is known that gut-microbiota are important regulators of ROS homeostasis, playing a vital role in protecting the host against oxidative distress. For example, dysbiosis of the human gut microbiome can lead to oxidative stress, which in turn contributes to the development of several gastrointestinal disorders (Dam, Misra, and Banerjee 2019; Sun et al. 2024). As already mentioned before, both commensal bacteria and pathogens are known to modulate ROS levels of their hosts (Spooner and Yilmaz 2011; Pan et al. 2012; Martins et al. 2021; Kunst et al. 2023). But contrary to my observations, even commensal bacteria usually trigger increased ROS production, and complete removal of bacteria is associated with a decrease in overall ROS production (Jones et al. 2013; Jones et al. 2015; Matziouridou et al. 2018; Sun et al. 2024).

The increased ROS levels I observed in GF polyps, combined with the expression of a range of antioxidant systems in the metatranscriptomic data of *Curvibacter*, indicate that *Curvibacter* is involved in maintaining ROS homeostasis in the *Hydra* holobiont. The two strongest differentially upregulated genes, *ohrR* and *ohrA* (Organic hydroperoxide resistance regulator and protein, respectively) form an operator complex commonly found in bacteria. As their name suggests, they are known to be involved in bacterial resistance against OHPs (Meireles et al. 2022). Consistent with my results that the *Curvibacter ΔohrR/-A* mutant is more susceptible to OHPs, studies in other bacteria show that *ohrR* and *ohrs* are required for protection against artificial OHPs, and expression of these genes is regulated in response to OHPs (Mongkolsuk et al. 1998; Volker et al. 1998; Atichartpongkul et al. 2001; Fuangthong et al. 2001; Ochsner, Hassett, and Vasil 2001; Rince et al. 2001; Shea and Mulks 2002; Previato-Mello et al. 2017; Pande, Veale, and Grove 2018; Si et al. 2018; Sun et al. 2018; Feng et al. 2019; Ruhland and Reniere 2019; Si et al. 2020; Chen et al. 2021; Chen, Shu, and Lin 2021). However, the actual biological function of these genes, as well as their

physiological substrates still remain unclear. While OHPs in the form of lipid hydroperoxides are involved in plant defense reactions against pathogens (Jalloul et al. 2002; Montillet et al. 2002; Gobel, Feussner, and Rosahl 2003), the significance of organic peroxide resistance in animal-associated bacteria remains poorly understood (Meireles et al. 2022). All studies regarding the role of OhrR /Ohrs are based on infection models of pathogenic bacteria and used artificial OHPs; and even these show conflicting results.

In a *B. thailandensis* infection model, a *ΔohrR* mutant showed reduced virulence, while loss of *ohrA* resulted in enhanced infectivity in *C. elegans* (Pande, Veale, and Grove 2018). *Chromobacterium violaceum ΔohrR* showed reduced virulence as well, but here *ΔohrA* mutants had no altered virulence compared to the wild-type (Previato-Mello et al. 2017). Similarly, inactivation of *P. aeruginosa ohrR* led to reduced ability to kill nematodes, with no significant effect of *ohr* inactivation on pathogenicity (Atichartpongkul et al. 2010). In contrast, a *ΔohrR* mutant of *Mycobacterium smegmatis* displayed significantly increased survival within macrophage intracellular compartments, while a *Δohr* and a *ΔohrR/ohr* double mutant again exhibited no differences in intracellular survival when compared to the wild-type strain (Saikolappan, Das, and Dhandayuthapani 2015). In *Brucella abortus*, no effect of either *ohrR* or *ohr* could be detected (Caswell et al. 2012). In my study, the *ΔohrR/ohrA* double mutant of *Curvibacter* showed significantly stronger recolonization than the wild-type, even in direct competition (**Figure 28** + **Figure 29**).

Overall, these results show that loss of the Ohr protein seems to have no negative effect *in vivo* on the ability of bacteria to colonize or infect hosts. Instead, it can actually enhance the ability to effectively colonize the host, as was shown for *B. thailandensis* and possibly *Curvibacter*. OhrR seems to have a more diverse role in this context. Based on the results of these studies, it is likely that OhrR also regulates other target genes. OhrR belongs to the MarR transcriptional regulator family that controls stress responses and virulence in bacteria (Deochand and Grove 2017). Even though OhrR typically acts as a repressor of *ohr*, it may also serve as an activator for other genes that are required for infection. This would explain the reduced virulence of *ΔohrR* mutants in most studies.

Taking these results into consideration, the increased colonization efficiency of the *Curvibacter* knockout mutant in my experiments could be due to the loss of OhrA, similarly to the observation in *B. thailandensis (Pande, Veale, and Grove 2018)*. It is also possible that *Curvibacter* OhrR acts on other targets besides *ohrA*. Depending on the mode of action of OhrR on these target genes, the enhanced growth of colonizing *ΔohrR/ohrA Curvibacter* could be the result of their increased or repressed expression. Since my results are only based on a *ΔohrR/ohr* double mutant, it is not clear which gene is finally responsible for the observed effect on colonization efficiency. Additional experiments using single gene knockout mutants are necessary to get a deeper understanding of their role during colonization.

Nonetheless, the role of *Hydra's* microbiota and especially *Curvibacter* on ROS homeostasis is apparent. Recolonization of GF polyps with their natural microbiome fully restored ROS levels to those of WT *Hydra* (**Figure 27**). Remarkably, recolonization with only *Curvibacter* AEP 1.3 was already sufficient to rescue the GF-effect. In contrast, the *ΔohrR/-A* mutant failed to significantly decrease total ROS levels compared to GF polyps. These results strongly implicate that the *Curvibacter ohrR/-A* operon plays an important role not only for colonization efficiency of *Curvibacter*, but also in microbiota-mediated ROS homeostasis in *Hydra*.

Recent studies have demonstrated that the microbiota of *Hydra* can influence several developmental processes in polyps (Taubenheim et al. 2020; Miklos et al. 2023; He et al. 2025). As already mentioned, long-term GF polyps of *H. vulgaris* exhibit developmental defects. Primarily observable is the temporary loss of budding capability (Rahat and Dimentman 1982; He et al. 2025). Sequencing of non-budding polyps revealed that the absence of bacteria in these polyps led to a downregulation of Wnt, among other developmental factors (He et al. 2025). Wnt signaling pathways are highly conserved and important signaling pathways for development and tissue homeostasis in animals and play a critical role in regeneration and budding initiation events in *Hydra* (Hobmayer et al. 2000; Lengfeld et al. 2009; Hayat, Manzoor, and Hussain 2022; Tursch et al. 2022). In their study of long-term GF polyps, the researchers proposed that: "during long-term absence of the microbiota, factors

accumulate in or on the host that are inhibitory for budding behavior; in the intact holobiont these hypothetical factors would be continuously removed by the bacteria." (He et al. 2025).

The increased ROS levels I observed as a result of removing *Hydras* microbiota could be a missing factor. Due to their reactivity, ROS are known to directly and indirectly modulate a range of developmental pathways under physiological conditions (Sies et al. 2022; Guo, Xing, et al. 2023; Hong et al. 2024). Among others, increased ROS levels can affect the Wnt signaling pathway (Funato et al. 2006; Korswagen 2006; Almeida et al. 2007; Zhou et al. 2010; Staehlke et al. 2020; Chatterjee and Sil 2022; Samatha Jain et al. 2022). The presence of *Hydra's* microbiota, and notably, mono-colonized *Curvibacter*, has already been shown to specifically affect the strength of the Wnt signaling pathway (Taubenheim et al. 2020). Similarly, *Curvibacter* on its own was also able to significantly reduce the increased ROS levels of GF polyps in my study. This also highlights the role of the *ohrR/-A* operon in this context, as the *ΔohrR/-A* mutant was not able to rescue the GF phenotype. This indicates that OHPs might be the main species responsible for the observed phenotype. Without the scavenging ability of its microbiota, ROS homeostasis of GF polyps gets more and more imbalanced over time, possibly leading to inhibitory effects on Wnt signaling and thereby contributing to the inhibition of bud formation. Recolonization of polyps leads to a complete reversal of the budding phenotype, which coincides with my observation that recolonization of GF polyps restores ROS levels to WT levels (**Figure 27**) (He et al. 2025).

It is important to note though, that the Wnt pathway is likely not the only target affected by increased ROS concentrations in GF polyps, nor will ROS be solely responsible for the observed phenotypes. Since the increased ROS levels of GF polyps could be seen along the whole polyp, they would affect other targets as well. Also, the interaction between OHPs and the Wnt signaling pathway is complex and appears to be tissue-dependent. Lipid peroxidation products were shown to activate Wnt signaling as well as suppress it (Funato et al. 2006; Almeida et al. 2007; Chatterjee and Sil 2022). Additionally, Wnt signaling itself can in turn modulate lipid peroxide levels, highlighting a bidirectional relationship (Staehlke et al. 2020; Jia, Bian, and Chang 2025).

Taken together, these results indicate that *Hydra's* microbiota plays an important role in maintaining ROS homeostasis in the *Hydra* holobiont. The *Curvibacter ohrR/-A* operon in particular might be a key regulator in OHP-driven inter-kingdom signaling between *Curvibacter* and *Hydra*. While OHPs potentially act as an important effector on *Hydra* developmental processes, this effect likely involves a highly complex and nuanced regulation that requires further investigation.

Outlook

Traditionally, animal development has been regarded as an autonomous process controlled exclusively by the host genome. Since developmental processes evolved in the context of host-associated microbial communities, it became evident that host development, microbial community composition and signaling, as well as the environmental context are dynamically linked. Still, fundamental questions on the precise signaling molecules and biochemical mechanisms by which the host and its microbiota interact with and influence each other remain largely unresolved.

The cnidarian *Hydra vulgaris* AEP and its main bacterial symbiont *Curvibacter* offer a compelling model system to further our understanding of inter-kingdom communication and how the microbiota can influence host development. Already available functional genetics and cell-type specific *Hydra* reporter lines allow for high-resolution spatiotemporal analyses of gene function and expression *in vivo*. Additionally, the established protocol for the generation of *Curvibacter* bioreporter lines allows for real-time analysis of symbiont gene expression during host-colonization and interaction with other members of the microbiota.

The metatranscriptomic data generated in my study has revealed potential candidate genes involved in the dynamics of host-symbiont adaptation of *Curvibacter*. Combined with targeted gene knockouts this will provide further insights into the function of specific symbiont genes and their downstream effects on colonization success, as well as their potential effects on host development and physiology.

First results provided here indicate that genes commonly involved in scavenging reactive oxygen species play an important role for host-colonization, as well as affecting developmental signaling pathways by regulating ROS homeostasis in the *Hydra* holobiont.

References

Akahoshi, D. T., and C. L. Bevins. 2022. 'Flagella at the Host-Microbe Interface: Key Functions Intersect With Redundant Responses', *Front Immunol*, 13: 828758.

Alban, P. S., D. L. Popham, K. E. Rippere, and N. R. Krieg. 1998. 'Identification of a gene for a rubrerythrin/nigerythrin-like protein in Spirillum volutans by using amino acid sequence data from mass spectrometry and NH2-terminal sequencing', *J Appl Microbiol*, 85: 875-82.

Alegria, T. G., D. A. Meireles, J. R. Cussiol, M. Hugo, M. Trujillo, M. A. de Oliveira, S. Miyamoto, R. F. Queiroz, N. F. Valadares, R. C. Garratt, R. Radi, P. Di Mascio, O. Augusto, and L. E. Netto. 2017. 'Ohr plays a central role in bacterial responses against fatty acid hydroperoxides and peroxynitrite', *Proc Natl Acad Sci U S A*, 114: E132-E41.

Almeida, M., L. Han, M. Martin-Millan, C. A. O'Brien, and S. C. Manolagas. 2007. 'Oxidative stress antagonizes Wnt signaling in osteoblast precursors by diverting beta-catenin from T cell factor- to forkhead box O-mediated transcription', *J Biol Chem*, 282: 27298-305.

Andrés, Celia María Curieses, José Manuel La Pérez de Lastra, Celia Andrés Juan, Francisco J. Plou, and Eduardo Pérez-Lebeña. 2022. 'Chemistry of Hydrogen Peroxide Formation and Elimination in Mammalian Cells, and Its Role in Various Pathologies', *Stresses*, 2: 256-74.

Artis, D. 2008. 'Epithelial-cell recognition of commensal bacteria and maintenance of immune homeostasis in the gut', *Nat Rev Immunol*, 8: 411-20.

Atichartpongkul, S., M. Fuangthong, P. Vattanaviboon, and S. Mongkolsuk. 2010. 'Analyses of the regulatory mechanism and physiological roles of Pseudomonas aeruginosa OhrR, a transcription regulator and a sensor of organic hydroperoxides', *J Bacteriol*, 192: 2093-101.

Atichartpongkul, S., S. Loprasert, P. Vattanaviboon, W. Whangsuk, J. D. Helmann, and S. Mongkolsuk. 2001. 'Bacterial Ohr and OsmC paralogues define two protein families with distinct functions and patterns of expression', *Microbiology (Reading)*, 147: 1775-82.

Augustin, R., S. Fraune, and T. C. Bosch. 2010. 'How Hydra senses and destroys microbes', *Semin Immunol*, 22: 54-8.

Augustin, R., K. Schroder, A. P. Murillo Rincon, S. Fraune, F. Anton-Erxleben, E. M. Herbst, J. Wittlieb, M. Schwentner, J. Grotzinger, T. M. Wassenaar, and T. C. G. Bosch. 2017. 'A secreted antibacterial neuropeptide shapes the microbiome of Hydra', *Nat Commun*, 8: 698.

Babior, B. M. 1978. 'Oxygen-dependent microbial killing by phagocytes (first of two parts)', *N Engl J Med*, 298: 659-68.

Baedke, J., A. Fabregas-Tejeda, and A. Nieves Delgado. 2020. 'The holobiont concept before Margulis', *J Exp Zool B Mol Dev Evol*, 334: 149-55.

Baldassarre, L., H. Ying, A. M. Reitzel, S. Franzenburg, and S. Fraune. 2022. 'Microbiota mediated plasticity promotes thermal adaptation in the sea anemone Nematostella vectensis', *Nat Commun*, 13: 3804.

Baldridge, C. W., and R. W. Gerard. 1932. 'The Extra Respiration of Phagocytosis', *American Journal of Physiology-Legacy Content*, 103: 235-36.

Ballard, J. W. O., and S. G. Towarnicki. 2020. 'Mitochondria, the gut microbiome and ROS', *Cell Signal*, 75: 109737.

Bary, A. de. 1879. *Die Erscheinung der Symbiose* (De Gruyter: Berlin, Boston).

Bathia, J., K. Schröder, S. Fraune, T. Lachnit, P. Rosenstiel, and T. C. G. Bosch. 2022. 'Symbiotic Algae of Hydra viridissima Play a Key Role in Maintaining Homeostatic Bacterial Colonization', *Front Microbiol*, 13: 869666.

Becker, L., L. Fürbach, T. Minten, J. Bathia, M. Karbach, S. Foret, N. M. Winterfeldt, M. Pauly, I. M. Axmann, and S. Fraune. 2025. "Extracelluar polymeric substances drive *Curvibacter* host adaptation and co-speciation with *Hydra*." In.

Belkaid, Y., and T. W. Hand. 2014. 'Role of the microbiota in immunity and inflammation', *Cell*, 157: 121-41.

Bijnens, K., S. Thijs, N. Leynen, V. Stevens, B. McAmmond, J. Van Hamme, J. Vangronsveld, T. Artois, and K. Smeets. 2021. 'Differential effect of silver nanoparticles on the microbiome of adult and developing planaria', *Aquat Toxicol*, 230: 105672.

Boehm, A. M., K. Khalturin, F. Anton-Erxleben, G. Hemmrich, U. C. Klostermeier, J. A. Lopez-Quintero, H. H. Oberg, M. Puchert, P. Rosenstiel, J. Wittlieb, and T. C. Bosch. 2012. 'FoxO is a critical regulator of stem cell maintenance in immortal Hydra', *Proc Natl Acad Sci U S A*, 109: 19697-702.

Boman, H. G. 2000. 'Innate immunity and the normal microflora', *Immunol Rev*, 173: 5-16.

Bosch, T. C., R. Augustin, F. Anton-Erxleben, S. Fraune, G. Hemmrich, H. Zill, P. Rosenstiel, G. Jacobs, S. Schreiber, M. Leippe, M. Stanisak, J. Grotzinger, S. Jung, R. Podschun, J. Bartels, J. Harder, and J. M. Schröder. 2009. 'Uncovering the evolutionary history of innate immunity: the simple metazoan Hydra uses epithelial cells for host defence', *Dev Comp Immunol*, 33: 559-69.

Bosch, T. C., and M. J. McFall-Ngai. 2011. 'Metaorganisms as the new frontier', *Zoology (Jena)*, 114: 185-90.

Bosch, Thomas C. G. , and Michael G. Hadfield. 2020. *Cellular dialogues in the holobiont* (CRC Press: Boca Raton).

Bottger, A., and M. Hassel. 2012. 'Hydra, a model system to trace the emergence of boundaries in developing eumetazoans', *Int J Dev Biol*, 56: 583-91.

Brucker, R. M., and S. R. Bordenstein. 2012. 'The roles of host evolutionary relationships (genus: Nasonia) and development in structuring microbial communities', *Evolution*, 66: 349-62.

———. 2013. 'The hologenomic basis of speciation: gut bacteria cause hybrid lethality in the genus Nasonia', *Science*, 341: 667-9.

Caballero-Flores, G., J. M. Pickard, and G. Nunez. 2023. 'Microbiota-mediated colonization resistance: mechanisms and regulation', *Nat Rev Microbiol*, 21: 347-60.

Cadet, Jean, and Paolo Di Mascio. 'Peroxides in Biological Systems.' in, *PATAI'S Chemistry of Functional Groups*.

Campbell, R. D. 1987. 'Structure of the Mouth of Hydra Spp a Breach in the Epithelium That Disappears When It Closes', *Cell and Tissue Research*, 249: 189-97.

Cani, P. D. 2017. 'Gut microbiota - at the intersection of everything?', *Nat Rev Gastroenterol Hepatol*, 14: 321-22.

———. 2018. 'Human gut microbiome: hopes, threats and promises', *Gut*, 67: 1716-25.

Cardenas, J. P., R. Quatrini, and D. S. Holmes. 2016. 'Aerobic Lineage of the Oxidative Stress Response Protein Rubrerythrin Emerged in an Ancient Microaerobic, (Hyper)Thermophilic Environment', *Front Microbiol*, 7: 1822.

Carrier, T. J., and T. C. G. Bosch. 2022. 'Symbiosis: the other cells in development', *Development*, 149.

Carter, J. A., C. Hyland, R. E. Steele, and E. M. Collins. 2016. 'Dynamics of Mouth Opening in Hydra', *Biophys J*, 110: 1191-201.

Caswell, C. C., J. E. Baumgartner, D. W. Martin, and R. M. Roop, 2nd. 2012. 'Characterization of the organic hydroperoxide resistance system of Brucella abortus 2308', *J Bacteriol*, 194: 5065-72.

Cazet, J. F., S. Siebert, H. M. Little, P. Bertemes, A. S. Primack, P. Ladurner, M. Achrainer, M. T. Fredriksen, R. T. Moreland, S. Singh, S. Zhang, T. G. Wolfsberg, C. E. Schnitzler, A. D. Baxevanis, O. Simakov, B. Hobmayer, and C. E. Juliano. 2023. 'A chromosome-scale epigenetic map of the Hydra genome reveals conserved regulators of cell state', *Genome Res*, 33: 283-98.

Chapman, J. A., E. F. Kirkness, O. Simakov, S. E. Hampson, T. Mitros, T. Weinmaier, T. Rattei, P. G. Balasubramanian, J. Borman, D. Busam, K. Disbennett, C. Pfannkoch, N. Sumin, G. G. Sutton, L. D. Viswanathan, B. Walenz, D. M. Goodstein, U. Hellsten, T. Kawashima, S. E. Prochnik, N. H. Putnam, S. Shu, B. Blumberg, C. E. Dana, L. Gee, D. F. Kibler, L. Law, D. Lindgens, D. E. Martinez, J. Peng, P. A. Wigge, B. Bertulat, C. Guder, Y. Nakamura, S. Ozbek, H. Watanabe, K. Khalturin, G. Hemmrich, A. Franke, R. Augustin, S. Fraune, E. Hayakawa, S. Hayakawa, M. Hirose, J. S. Hwang, K. Ikeo, C. Nishimiya-Fujisawa, A. Ogura, T. Takahashi, P. R. Steinmetz, X. Zhang, R. Aufschnaiter, M. K. Eder, A. K. Gorny, W. Salvenmoser, A. M. Heimberg, B. M. Wheeler, K. J. Peterson, A. Bottger, P. Tischler, A. Wolf, T. Gojobori, K. A. Remington, R. L. Strausberg, J. C. Venter, U. Technau, B. Hobmayer, T. C. Bosch, T. W. Holstein, T. Fujisawa, H. R. Bode, C. N. David, D. S. Rokhsar, and R. E. Steele. 2010. 'The dynamic genome of Hydra', *Nature*, 464: 592-6.

Chatterjee, S., and P. C. Sil. 2022. 'ROS-Influenced Regulatory Cross-Talk With Wnt Signaling Pathway During Perinatal Development', *Front Mol Biosci*, 9: 889719.

Chen, N. X., Y. J. Chu, B. Ni, P. Hsu, and H. C. Wong. 2021. 'Organic Hydroperoxide Resistance Gene ohr (VPA1681) Confers Protection against Organic Peroxides in the Presence of Alkyl Hydroperoxide Reductase Genes in Vibrio parahaemolyticus', *Appl Environ Microbiol*, 87: e0086121.

Chen, S. J., H. Y. Shu, and G. H. Lin. 2021. 'Regulation of tert-Butyl Hydroperoxide Resistance by Chromosomal OhrR in A. baumannii ATCC 19606', *Microorganisms*, 9.

Chen, Y., X. Li, T. Liu, F. Li, W. Sun, L. Y. Young, and W. Huang. 2022. 'Metagenomic analysis of Fe(II)-oxidizing bacteria for Fe(III) mineral formation and carbon assimilation under microoxic conditions in paddy soil', *Sci Total Environ*, 851: 158068.

Chuchue, T., W. Tanboon, B. Prapagdee, J. M. Dubbs, P. Vattanaviboon, and S. Mongkolsuk. 2006. 'ohrR and ohr are the primary sensor/regulator and

protective genes against organic hydroperoxide stress in Agrobacterium tumefaciens', *J Bacteriol*, 188: 842-51.

Clemente, J. C., L. K. Ursell, L. W. Parfrey, and R. Knight. 2012. 'The impact of the gut microbiota on human health: an integrative view', *Cell*, 148: 1258-70.

Coant, N., S. Ben Mkaddem, E. Pedruzzi, C. Guichard, X. Treton, R. Ducroc, J. N. Freund, D. Cazals-Hatem, Y. Bouhnik, P. L. Woerther, D. Skurnik, A. Grodet, M. Fay, D. Biard, T. Lesuffleur, C. Deffert, R. Moreau, A. Groyer, K. H. Krause, F. Daniel, and E. Ogier-Denis. 2010. 'NADPH oxidase 1 modulates WNT and NOTCH1 signaling to control the fate of proliferative progenitor cells in the colon', *Mol Cell Biol*, 30: 2636-50.

Cornet, L., I. Cleenwerck, J. Praet, R. R. Leonard, N. J. Vereecken, D. Michez, G. Smagghe, D. Baurain, and P. Vandamme. 2022. 'Phylogenomic Analyses of Snodgrassella Isolates from Honeybees and Bumblebees Reveal Taxonomic and Functional Diversity', *mSystems*, 7: e0150021.

Cross, K. L., B. A. Leigh, E. A. Hatmaker, A. Mikaelyan, A. K. Miller, and S. R. Bordenstein. 2021. 'Genomes of Gut Bacteria from Nasonia Wasps Shed Light on Phylosymbiosis and Microbe-Assisted Hybrid Breakdown', *mSystems*, 6.

Cullender, T. C., B. Chassaing, A. Janzon, K. Kumar, C. E. Muller, J. J. Werner, L. T. Angenent, M. E. Bell, A. G. Hay, D. A. Peterson, J. Walter, M. Vijay-Kumar, A. T. Gewirtz, and R. E. Ley. 2013. 'Innate and adaptive immunity interact to quench microbiome flagellar motility in the gut', *Cell Host Microbe*, 14: 571-81.

Cunningham, J. A., A. G. Liu, S. Bengtson, and P. C. Donoghue. 2017. 'The origin of animals: Can molecular clocks and the fossil record be reconciled?', *Bioessays*, 39: 1-12.

Curtis, M. M., and V. Sperandio. 2011. 'A complex relationship: the interaction among symbiotic microbes, invading pathogens, and their mammalian host', *Mucosal Immunol*, 4: 133-8.

Cussiol, J. R., S. V. Alves, M. A. de Oliveira, and L. E. Netto. 2003. 'Organic hydroperoxide resistance gene encodes a thiol-dependent peroxidase', *J Biol Chem*, 278: 11570-8.

D'Autreaux, B., and M. B. Toledano. 2007. 'ROS as signalling molecules: mechanisms that generate specificity in ROS homeostasis', *Nat Rev Mol Cell Biol*, 8: 813-24.

Dam, Bomba, Arijit Misra, and Sohini Banerjee. 2019. 'Role of Gut Microbiota in Combating Oxidative Stress.' in Sajal Chakraborti, Tapati Chakraborti, Dhrubajyoti Chattopadhyay and Chandrima Shaha (eds.), *Oxidative Stress in Microbial Diseases* (Springer Singapore: Singapore).

Daniel, N., E. Lecuyer, and B. Chassaing. 2021. 'Host/microbiota interactions in health and diseases-Time for mucosal microbiology!', *Mucosal Immunol*, 14: 1006-16.

Davenport, E. R., J. G. Sanders, S. J. Song, K. R. Amato, A. G. Clark, and R. Knight. 2017. 'The human microbiome in evolution', *BMC Biol*, 15: 127.

Davis, L. E., and J. F. Haynes. 1968. 'An ultrastructural examination of the mesoglea of Hydra', *Z Zellforsch Mikrosk Anat*, 92: 149-58.

de Almeida, Ajpo, Jcpl de Oliveira, L. V. da Silva Pontes, J. F. de Souza Junior, T. A. F. Goncalves, S. H. Dantas, M. S. de Almeida Feitosa, A. O. Silva, and I. A. de Medeiros. 2022. 'ROS: Basic Concepts, Sources, Cellular Signaling, and its Implications in Aging Pathways', *Oxid Med Cell Longev*, 2022: 1225578.

Decaestecker, E., B. Van de Moortel, S. Mukherjee, A. Gurung, R. Stoks, and L. De Meester. 2024. 'Hierarchical eco-evo dynamics mediated by the gut microbiome', *Trends Ecol Evol*, 39: 165-74.

Deines, P., T. Lachnit, and T. C. G. Bosch. 2017. 'Competing forces maintain the Hydra metaorganism', *Immunol Rev*, 279: 123-36.

Deochand, D. K., and A. Grove. 2017. 'MarR family transcription factors: dynamic variations on a common scaffold', *Crit Rev Biochem Mol Biol*, 52: 595-613.

Diaz-Munoz, S. L., and B. Koskella. 2014. 'Bacteria-phage interactions in natural environments', *Adv Appl Microbiol*, 89: 135-83.

Diaz, J. M., C. M. Hansel, A. Apprill, C. Brighi, T. Zhang, L. Weber, S. McNally, and L. Xun. 2016. 'Species-specific control of external superoxide levels by the coral holobiont during a natural bleaching event', *Nat Commun*, 7: 13801.

Ding, L., and A. Yokota. 2004. 'Proposals of Curvibacter gracilis gen. nov., sp. nov. and Herbaspirillum putei sp. nov. for bacterial strains isolated from well water and reclassification of [Pseudomonas] huttiensis, [Pseudomonas] lanceolata, [Aquaspirillum] delicatum and [Aquaspirillum] autotrophicum as Herbaspirillum huttiense comb. nov., Curvibacter lanceolatus comb. nov., Curvibacter delicatus comb. nov. and Herbaspirillum autotrophicum comb. nov', *Int J Syst Evol Microbiol*, 54: 2223-30.

Dominiak, D. M., J. L. Nielsen, and P. H. Nielsen. 2011. 'Extracellular DNA is abundant and important for microcolony strength in mixed microbial biofilms', *Environ Microbiol*, 13: 710-21.

Douglas, Angela E. 2010. *The Symbiotic Habit* (Princeton University Press: Princeton N.J.).

Dunford, H. B. 1987. 'Free radicals in iron-containing systems', *Free Radic Biol Med*, 3: 405-21.

Dungan, A. M., D. Bulach, H. Lin, M. J. H. van Oppen, and L. L. Blackall. 2021. 'Development of a free radical scavenging bacterial consortium to mitigate oxidative stress in cnidarians', *Microb Biotechnol*, 14: 2025-40.

Ellegaard, K. M., S. Brochet, G. Bonilla-Rosso, O. Emery, N. Glover, N. Hadadi, K. S. Jaron, J. R. van der Meer, M. Robinson-Rechavi, V. Sentchilo, F. Tagini, Sage class, and P. Engel. 2019. 'Genomic changes underlying host specialization in the bee gut symbiont Lactobacillus Firm5', *Mol Ecol*, 28: 2224-37.

Feng, C., Z. Yi, W. Qian, H. Liu, and X. Jiang. 2023. 'Rotations improve the diversity of rhizosphere soil bacterial communities, enzyme activities and tomato yield', *PLoS One*, 18: e0270944.

Feng, X., W. Sun, L. Kong, and H. Gao. 2019. 'Distinct Roles of Shewanella oneidensis Thioredoxin in Regulation of Cellular Responses to Hydrogen and Organic Peroxides', *Appl Environ Microbiol*, 85.

Fisher, A. B. 2009. 'Redox signaling across cell membranes', *Antioxid Redox Signal*, 11: 1349-56.

Forman, H. J., M. Maiorino, and F. Ursini. 2010. 'Signaling functions of reactive oxygen species', *Biochemistry*, 49: 835-42.

Franca, L., A. Lopez-Lopez, R. Rossello-Mora, and M. S. da Costa. 2015. 'Microbial diversity and dynamics of a groundwater and a still bottled natural mineral water', *Environ Microbiol*, 17: 577-93.

Franzenburg, S., S. Fraune, P. M. Altrock, S. Kunzel, J. F. Baines, A. Traulsen, and T. C. Bosch. 2013. 'Bacterial colonization of Hydra hatchlings follows a robust temporal pattern', *ISME J*, 7: 781-90.

Franzenburg, S., S. Fraune, S. Kunzel, J. F. Baines, T. Domazet-Loso, and T. C. Bosch. 2012. 'MyD88-deficient Hydra reveal an ancient function of TLR signaling in sensing bacterial colonizers', *Proc Natl Acad Sci U S A*, 109: 19374-9.

Franzenburg, S., J. Walter, S. Kunzel, J. Wang, J. F. Baines, T. C. Bosch, and S. Fraune. 2013. 'Distinct antimicrobial peptide expression determines host species-specific bacterial associations', *Proc Natl Acad Sci U S A*, 110: E3730-8.

Fraune, S., F. Anton-Erxleben, R. Augustin, S. Franzenburg, M. Knop, K. Schröder, D. Willoweit-Ohl, and T. C. Bosch. 2015. 'Bacteria-bacteria interactions within the microbiota of the ancestral metazoan Hydra contribute to fungal resistance', *ISME J*, 9: 1543-56.

Fraune, S., R. Augustin, F. Anton-Erxleben, J. Wittlieb, C. Gelhaus, V. B. Klimovich, M. P. Samoilovich, and T. C. Bosch. 2010. 'In an early branching metazoan, bacterial colonization of the embryo is controlled by maternal antimicrobial peptides', *Proc Natl Acad Sci U S A*, 107: 18067-72.

Fraune, S., and T. C. Bosch. 2007. 'Long-term maintenance of species-specific bacterial microbiota in the basal metazoan Hydra', *Proc Natl Acad Sci U S A*, 104: 13146-51.

———. 2010. 'Why bacteria matter in animal development and evolution', *Bioessays*, 32: 571-80.

Fuangthong, M., S. Atichartpongkul, S. Mongkolsuk, and J. D. Helmann. 2001. 'OhrR is a repressor of ohrA, a key organic hydroperoxide resistance determinant in Bacillus subtilis', *J Bacteriol*, 183: 4134-41.

Funato, Y., T. Michiue, M. Asashima, and H. Miki. 2006. 'The thioredoxin-related redox-regulating protein nucleoredoxin inhibits Wnt-beta-catenin signalling through dishevelled', *Nat Cell Biol*, 8: 501-8.

Gauron, C., C. Rampon, M. Bouzaffour, E. Ipendey, J. Teillon, M. Volovitch, and S. Vriz. 2013. 'Sustained production of ROS triggers compensatory proliferation and is required for regeneration to proceed', *Sci Rep*, 3: 2084.

Giez, C., D. Pinkle, Y. Giencke, J. Wittlieb, E. Herbst, T. Spratte, T. Lachnit, A. Klimovich, C. Selhuber-Unkel, and T. C. G. Bosch. 2023. 'Multiple neuronal populations control the eating behavior in Hydra and are responsive to microbial signals', *Curr Biol*, 33: 5288-303 e6.

Gil-Turnes, M. S., M. E. Hay, and W. Fenical. 1989. 'Symbiotic marine bacteria chemically defend crustacean embryos from a pathogenic fungus', *Science*, 246: 116-8.

Gilbert, S. F., J. Sapp, and A. I. Tauber. 2012. 'A symbiotic view of life: we have never been individuals', *Q Rev Biol*, 87: 325-41.

Girotti, Albert W., and Witold Korytowski. 'Generation and Reactivity of Lipid Hydroperoxides in Biological Systems.' in, *PATAI'S Chemistry of Functional Groups*.

Gobel, C., I. Feussner, and S. Rosahl. 2003. 'Lipid peroxidation during the hypersensitive response in potato in the absence of 9-lipoxygenases', *J Biol Chem*, 278: 52834-40.

Gordon, E. M., and S. K. Hatzios. 2020. 'Chemical tools for decoding redox signaling at the host-microbe interface', *PLoS Pathog*, 16: e1009070.

Gorokhova, E., C. Rivetti, S. Furuhagen, A. Edlund, K. Ek, and M. Breitholtz. 2015. 'Bacteria-mediated effects of antibiotics on Daphnia nutrition', *Environ Sci Technol*, 49: 5779-87.

Grasberger, H., J. Gao, H. Nagao-Kitamoto, S. Kitamoto, M. Zhang, N. Kamada, K. A. Eaton, M. El-Zaatari, A. B. Shreiner, J. L. Merchant, C. Owyang, and J. Y. Kao. 2015. 'Increased Expression of DUOX2 Is an Epithelial Response to Mucosal Dysbiosis Required for Immune Homeostasis in Mouse Intestine', *Gastroenterology*, 149: 1849-59.

Groussin, M., F. Mazel, J. G. Sanders, C. S. Smillie, S. Lavergne, W. Thuiller, and E. J. Alm. 2017. 'Unraveling the processes shaping mammalian gut microbiomes over evolutionary time', *Nat Commun*, 8: 14319.

Guo, L., J. Tang, M. Tang, S. Luo, and X. Zhou. 2023. 'Reactive oxygen species are regulated by immune deficiency and Toll pathways in determining the host specificity of honeybee gut bacteria', *Proc Natl Acad Sci U S A*, 120: e2219634120.

Guo, W., Y. Xing, X. Luo, F. Li, M. Ren, and Y. Liang. 2023. 'Reactive Oxygen Species: A Crosslink between Plant and Human Eukaryotic Cell Systems', *Int J Mol Sci*, 24.

Hamada, M., N. Satoh, and K. Khalturin. 2020. 'A Reference Genome from the Symbiotic Hydrozoan, Hydra viridissima', *G3 (Bethesda)*, 10: 3883-95.

Hamada, Mayuko, Katja Schröder, Jay Bathia, Ulrich Kürn, Sebastian Fraune, Mariia Khalturina, Konstantin Khalturin, Chuya Shinzato, Nori Satoh, and Thomas Cg Bosch. 2018. *Metabolic co-dependence drives the evolutionarily ancient Hydra-Chlorella symbiosis*.

Hancock, T. L., E. K. Dahedl, M. A. Kratz, and H. Urakawa. 2024. 'Synechococcus dominance induced after hydrogen peroxide treatment of Microcystis bloom in the Caloosahatchee River, Florida', *Environ Pollut*, 345: 123508.

Hayat, R., M. Manzoor, and A. Hussain. 2022. 'Wnt signaling pathway: A comprehensive review', *Cell Biol Int*, 46: 863-77.

He, J., and T. C. G. Bosch. 2022. 'Hydra's Lasting Partnership with Microbes: The Key for Escaping Senescence?', *Microorganisms*, 10.

He, Jinru, Alexander Klimovich, Sabine Kock, Linus Dahmke, Sören Franzenburg, and Thomas C. G. Bosch. 2025. 'The microbiota affects stem cell decision making in Hydra'.

Heinze, B. M., K. Kusel, N. Jehmlich, M. von Bergen, and M. Taubert. 2023. 'Metabolic versatility enables sulfur-oxidizers to dominate primary production in groundwater', *Water Res*, 244: 120426.

Hellriegel, Hermann, and Hermann Wilfarth. 1888. 'Untersuchungen über die Stickstoffnahrung der Gramineen und Leguminosen, von H. Hellriegel und H. Wilfarth unter mitwirkung von H. Roemer, R. Günther, H. Moeller und G. Wimmer. (Referent: H. Hellriegel.)'.

Hemmrich, G., B. Anokhin, H. Zacharias, and T. C. Bosch. 2007. 'Molecular phylogenetics in Hydra, a classical model in evolutionary developmental biology', *Mol Phylogenet Evol*, 44: 281-90.

Herfindal, A. M., S. D. C. Rocha, D. Papoutsis, S. K. Bohn, and H. Carlsen. 2022. 'The ROS-generating enzyme NADPH oxidase 1 modulates the colonic microbiota

but offers minor protection against dextran sulfate sodium-induced low-grade colon inflammation in mice', *Free Radic Biol Med*, 188: 298-311.

Herring, Peter J. 1977. 'Bioluminescence of marine organisms', *Nature*, 267: 788-93.

Hinzke, T., M. Kleiner, C. Breusing, H. Felbeck, R. Hasler, S. M. Sievert, R. Schluter, P. Rosenstiel, T. B. H. Reusch, T. Schweder, and S. Markert. 2019. 'Host-Microbe Interactions in the Chemosynthetic Riftia pachyptila Symbiosis', *mBio*, 10.

Hobmayer, B., F. Rentzsch, K. Kuhn, C. M. Happel, C. C. von Laue, P. Snyder, U. Rothbacher, and T. W. Holstein. 2000. 'WNT signalling molecules act in axis formation in the diploblastic metazoan Hydra', *Nature*, 407: 186-9.

Holstein, T. W., R. D. Campbell, and P. Tardant. 1990. 'Identity Crisis', *Nature*, 346: 21-22.

Holstein, T. W., M. W. Hess, and W. Salvenmoser. 2010. 'Preparation techniques for transmission electron microscopy of Hydra', *Methods Cell Biol*, 96: 285-306.

Hong, Y., A. Boiti, D. Vallone, and N. S. Foulkes. 2024. 'Reactive Oxygen Species Signaling and Oxidative Stress: Transcriptional Regulation and Evolution', *Antioxidants (Basel)*, 13.

Hughes, D. T., and V. Sperandio. 2008. 'Inter-kingdom signalling: communication between bacteria and their hosts', *Nat Rev Microbiol*, 6: 111-20.

Human Microbiome Project, Consortium. 2012. 'Structure, function and diversity of the healthy human microbiome', *Nature*, 486: 207-14.

Imlay, J. A. 2019. 'Where in the world do bacteria experience oxidative stress?', *Environ Microbiol*, 21: 521-30.

Iyer, R. B., R. Silaghi-Dumitrescu, D. M. Kurtz, Jr., and W. N. Lanzilotta. 2005. 'High-resolution crystal structures of Desulfovibrio vulgaris (Hildenborough) nigerythrin: facile, redox-dependent iron movement, domain interface variability, and peroxidase activity in the rubrerythrins', *J Biol Inorg Chem*, 10: 407-16.

Jakus, N., N. Blackwell, D. Straub, A. Kappler, and S. Kleindienst. 2021. 'Presence of Fe(II) and nitrate shapes aquifer-originating communities leading to an autotrophic enrichment dominated by an Fe(II)-oxidizing Gallionellaceae sp', *FEMS Microbiol Ecol*, 97.

Jalloul, A., J. L. Montillet, K. Assigbetse, J. P. Agnel, E. Delannoy, C. Triantaphylides, J. F. Daniel, P. Marmey, J. P. Geiger, and M. Nicole. 2002. 'Lipid peroxidation in cotton: Xanthomonas interactions and the role of lipoxygenases during the hypersensitive reaction', *Plant J*, 32: 1-12.

Jantzen, H., M. Hassel, and I. Schulze. 1998. 'Hydroperoxides mediate lithium effects on regeneration in Hydra', *Comp Biochem Physiol C Pharmacol Toxicol Endocrinol*, 119: 165-75.

Jaspers, C., S. Fraune, A. E. Arnold, D. J. Miller, T. C. G. Bosch, C. R. Voolstra, and Participants Consortium of Australian Academy of Science Boden Research Conference. 2019. 'Resolving structure and function of metaorganisms through a holistic framework combining reductionist and integrative approaches', *Zoology (Jena)*, 133: 81-87.

Jenney, F. E., Jr., M. F. Verhagen, X. Cui, and M. W. Adams. 1999. 'Anaerobic microbes: oxygen detoxification without superoxide dismutase', *Science*, 286: 306-9.

Jia, H., C. Bian, and Y. Chang. 2025. 'Exploring the molecular interactions between ferroptosis and the Wnt/beta-catenin signaling pathway: Implications for cancer and disease therapy', *Crit Rev Oncol Hematol*, 210: 104674.

Jones, R. M., C. Desai, T. M. Darby, L. Luo, A. A. Wolfarth, C. D. Scharer, C. S. Ardita, A. R. Reedy, E. S. Keebaugh, and A. S. Neish. 2015. 'Lactobacilli Modulate Epithelial Cytoprotection through the Nrf2 Pathway', *Cell Rep*, 12: 1217-25.

Jones, R. M., L. Luo, C. S. Ardita, A. N. Richardson, Y. M. Kwon, J. W. Mercante, A. Alam, C. L. Gates, H. Wu, P. A. Swanson, J. D. Lambeth, P. W. Denning, and A. S. Neish. 2013. 'Symbiotic lactobacilli stimulate gut epithelial proliferation via Nox-mediated generation of reactive oxygen species', *EMBO J*, 32: 3017-28.

Jones, R. M., J. W. Mercante, and A. S. Neish. 2012. 'Reactive oxygen production induced by the gut microbiota: pharmacotherapeutic implications', *Curr Med Chem*, 19: 1519-29.

Jones, R. M., and A. S. Neish. 2017. 'Redox signaling mediated by the gut microbiota', *Free Radic Biol Med*, 105: 41-47.

Jumper, J., R. Evans, A. Pritzel, T. Green, M. Figurnov, O. Ronneberger, K. Tunyasuvunakool, R. Bates, A. Zidek, A. Potapenko, A. Bridgland, C. Meyer, S. A. A. Kohl, A. J. Ballard, A. Cowie, B. Romera-Paredes, S. Nikolov, R. Jain, J. Adler, T. Back, S. Petersen, D. Reiman, E. Clancy, M. Zielinski, M. Steinegger, M. Pacholska, T. Berghammer, S. Bodenstein, D. Silver, O. Vinyals, A. W. Senior, K. Kavukcuoglu, P. Kohli, and D. Hassabis. 2021. 'Highly accurate protein structure prediction with AlphaFold', *Nature*, 596: 583-89.

Jung, S., A. J. Dingley, R. Augustin, F. Anton-Erxleben, M. Stanisak, C. Gelhaus, T. Gutsmann, M. U. Hammer, R. Podschun, A. M. Bonvin, M. Leippe, T. C. Bosch, and J. Grotzinger. 2009. 'Hydramacin-1, structure and antibacterial activity of a protein from the basal metazoan Hydra', *J Biol Chem*, 284: 1896-905.

Kajla, S., A. S. Mondol, A. Nagasawa, Y. Zhang, M. Kato, K. Matsuno, C. Yabe-Nishimura, and T. Kamata. 2012. 'A crucial role for Nox 1 in redox-dependent regulation of Wnt-beta-catenin signaling', *FASEB J*, 26: 2049-59.

Kawasaki, S., Y. Sakai, T. Takahashi, I. Suzuki, and Y. Niimura. 2009. 'O2 and reactive oxygen species detoxification complex, composed of O2-responsive NADH:rubredoxin oxidoreductase-flavoprotein A2-desulfoferrodoxin operon enzymes, rubperoxin, and rubredoxin, in Clostridium acetobutylicum', *Appl Environ Microbiol*, 75: 1021-9.

Kern, L., S. K. Abdeen, A. A. Kolodziejczyk, and E. Elinav. 2021. 'Commensal inter-bacterial interactions shaping the microbiota', *Curr Opin Microbiol*, 63: 158-71.

Kickstein, E., K. Harms, and W. Wackernagel. 2007. 'Deletions of recBCD or recD influence genetic transformation differently and are lethal together with a recJ deletion in Acinetobacter baylyi', *Microbiology (Reading)*, 153: 2259-70.

Klimovich, A., and T. C. G. Bosch. 2024. 'Novel technologies uncover novel 'anti'-microbial peptides in Hydra shaping the species-specific microbiome', *Philos Trans R Soc Lond B Biol Sci*, 379: 20230058.

Klimovich, A., J. Wittlieb, and T. C. G. Bosch. 2019. 'Transgenesis in Hydra to characterize gene function and visualize cell behavior', *Nat Protoc*, 14: 2069-90.

Knoll, Andrew H. 2015. *Life on a Young Planet* (Princeton University Press: Princeton, N.J.).

Koch, E. J., and M. McFall-Ngai. 2018. 'Model systems for the study of how symbiotic associations between animals and extracellular bacterial partners are established and maintained', *Drug Discov Today Dis Models*, 28: 3-12.

Korswagen, H. C. 2006. 'Regulation of the Wnt/beta-catenin pathway by redox signaling', *Dev Cell*, 10: 687-8.

Kovacevic, G. 2012. 'Value of the Hydra model system for studying symbiosis', *Int J Dev Biol*, 56: 627-35.

Kumar Rajendran, N., B. P. George, R. Chandran, I. M. Tynga, N. Houreld, and H. Abrahamse. 2019. 'The Influence of Light on Reactive Oxygen Species and NF-small ka, CyrillicB in Disease Progression', *Antioxidants (Basel)*, 8.

Kumar, S., G. Stecher, M. Li, C. Knyaz, and K. Tamura. 2018. 'MEGA X: Molecular Evolutionary Genetics Analysis across Computing Platforms', *Mol Biol Evol*, 35: 1547-49.

Kunst, C., S. Schmid, M. Michalski, D. Tumen, J. Buttenschon, M. Muller, and K. Gulow. 2023. 'The Influence of Gut Microbiota on Oxidative Stress and the Immune System', *Biomedicines*, 11.

Kwong, W. K., L. A. Medina, H. Koch, K. W. Sing, E. J. Y. Soh, J. S. Ascher, R. Jaffe, and N. A. Moran. 2017. 'Dynamic microbiome evolution in social bees', *Sci Adv*, 3: e1600513.

Lambeth, J. D., and A. S. Neish. 2014. 'Nox enzymes and new thinking on reactive oxygen: a double-edged sword revisited', *Annu Rev Pathol*, 9: 119-45.

Le, V. V., S. R. Ko, M. Kang, S. Jeong, H. M. Oh, and C. Y. Ahn. 2023. 'Comparative Genome analysis of the Genus Curvibacter and the Description of Curvibacter microcysteis sp. nov. and Curvibacter cyanobacteriorum sp. nov., Isolated from Fresh Water during the Cyanobacterial Bloom Period', *J Microbiol Biotechnol*, 33: 1428-36.

Lengfeld, T., H. Watanabe, O. Simakov, D. Lindgens, L. Gee, L. Law, H. A. Schmidt, S. Ozbek, H. Bode, and T. W. Holstein. 2009. 'Multiple Wnts are involved in Hydra organizer formation and regeneration', *Dev Biol*, 330: 186-99.

Lennicke, C., J. Rahn, R. Lichtenfels, L. A. Wessjohann, and B. Seliger. 2015. 'Hydrogen peroxide - production, fate and role in redox signaling of tumor cells', *Cell Commun Signal*, 13: 39.

Lesaulnier, C. C., C. W. Herbold, C. Pelikan, D. Berry, C. Gerard, X. Le Coz, S. Gagnot, J. Niggemann, T. Dittmar, G. A. Singer, and A. Loy. 2017. 'Bottled aqua incognita: microbiota assembly and dissolved organic matter diversity in natural mineral waters', *Microbiome*, 5: 126.

Li, X. Y., T. Lachnit, S. Fraune, T. C. G. Bosch, A. Traulsen, and M. Sieber. 2017. 'Temperate phages as self-replicating weapons in bacterial competition', *J R Soc Interface*, 14.

Li, X. Y., C. Pietschke, S. Fraune, P. M. Altrock, T. C. Bosch, and A. Traulsen. 2015. 'Which games are growing bacterial populations playing?', *J R Soc Interface*, 12: 20150121.

Li, Y., S. P. Leonard, J. E. Powell, and N. A. Moran. 2022. 'Species divergence in gut-restricted bacteria of social bees', *Proc Natl Acad Sci U S A*, 119: e2115013119.

Lim, S. J., and S. R. Bordenstein. 2020. 'An introduction to phylosymbiosis', *Proc Biol Sci*, 287: 20192900.

Lourenco, M., L. Chaffringeon, Q. Lamy-Besnier, M. Titecat, T. Pedron, O. Sismeiro, R. Legendre, H. Varet, J. Y. Coppee, M. Berard, L. De Sordi, and L. Debarbieux. 2022. 'The gut environment regulates bacterial gene expression which modulates susceptibility to bacteriophage infection', *Cell Host Microbe*, 30: 556-69 e5.

Love, Michael I., Wolfgang Huber, and Simon Anders. 2014. "Moderated estimation of fold change and dispersion for RNA-seq data with DESeq2." In.: Bioconductor.

Lumppio, H. L., N. V. Shenvi, R. P. Garg, A. O. Summers, and D. M. Kurtz, Jr. 1997. 'A rubrerythrin operon and nigerythrin gene in Desulfovibrio vulgaris (Hildenborough)', *J Bacteriol*, 179: 4607-15.

Lumppio, H. L., N. V. Shenvi, A. O. Summers, G. Voordouw, and D. M. Kurtz, Jr. 2001. 'Rubrerythrin and rubredoxin oxidoreductase in Desulfovibrio vulgaris: a novel oxidative stress protection system', *J Bacteriol*, 183: 101-8.

Ma, D., Z. Hao, R. Sun, M. Bartlam, and Y. Wang. 2016. 'Genome Sequence of a Typical Ultramicrobacterium, Curvibacter sp. Strain PAE-UM, Capable of Phthalate Ester Degradation', *Genome Announc*, 4.

Macpherson, A. J., and N. L. Harris. 2004. 'Interactions between commensal intestinal bacteria and the immune system', *Nat Rev Immunol*, 4: 478-85.

Marciano, Francesca, and Pietro Vajro. 2017. 'Oxidative Stress and Gut Microbiota.' in, *Gastrointestinal Tissue*.

Marcum, B. A., and R. D. Campbell. 1978. 'Development of Hydra lacking nerve and interstitial cells', *J Cell Sci*, 29: 17-33.

Margulis, Lynn. 1993. *Symbiosis in cell evolution* (Freeman: New York).

Margulis, Lynn, and René Fester. 1991. *Symbiosis as a source of evolutionary innovation* (MIT Press: Cambridge Mass.).

Marples, M. J. 1969. 'Life on the human skin', *Sci Am*, 220: 108-15.

Martin, V. J., C. L. Littlefield, W. E. Archer, and H. R. Bode. 1997. 'Embryogenesis in hydra', *Biol Bull*, 192: 345-63.

Martinez, D. E. 1998. 'Mortality patterns suggest lack of senescence in hydra', *Exp Gerontol*, 33: 217-25.

Martinez, D. E., A. R. Iniguez, K. M. Percell, J. B. Willner, J. Signorovitch, and R. D. Campbell. 2010. 'Phylogeny and biogeography of Hydra (Cnidaria: Hydridae) using mitochondrial and nuclear DNA sequences', *Mol Phylogenet Evol*, 57: 403-10.

Martins, M., L. F. C. Ramos, J. R. Murillo, A. Torres, S. S. de Carvalho, G. B. Domont, D. M. P. de Oliveira, R. D. Mesquita, F. C. S. Nogueira, R. Maciel-de-Freitas, and M. Junqueira. 2021. 'Comprehensive Quantitative Proteome Analysis of Aedes aegypti Identifies Proteins and Pathways Involved in Wolbachia pipientis and Zika Virus Interference Phenomenon', *Front Physiol*, 12: 642237.

Matziouridou, C., S. D. C. Rocha, O. A. Haabeth, K. Rudi, H. Carlsen, and A. Kielland. 2018. 'iNOS- and NOX1-dependent ROS production maintains bacterial homeostasis in the ileum of mice', *Mucosal Immunol*, 11: 774-84.

McClure, R., D. Balasubramanian, Y. Sun, M. Bobrovskyy, P. Sumby, C. A. Genco, C. K. Vanderpool, and B. Tjaden. 2013. 'Computational analysis of bacterial RNA-Seq data', *Nucleic Acids Res*, 41: e140.

McCord, Joe M., and Irwin Fridovich. 1969. 'Superoxide Dismutase', *Journal of Biological Chemistry*, 244: 6049-55.

McFall-Ngai, M., M. G. Hadfield, T. C. Bosch, H. V. Carey, T. Domazet-Loso, A. E. Douglas, N. Dubilier, G. Eberl, T. Fukami, S. F. Gilbert, U. Hentschel, N. King, S. Kjelleberg, A. H. Knoll, N. Kremer, S. K. Mazmanian, J. L. Metcalf, K. Nealson, N. E. Pierce, J. F. Rawls, A. Reid, E. G. Ruby, M. Rumpho, J. G. Sanders, D. Tautz, and J. J. Wernegreen. 2013. 'Animals in a bacterial world, a new imperative for the life sciences', *Proc Natl Acad Sci U S A*, 110: 3229-36.

McFall-Ngai, M. J. 2002. 'Unseen forces: the influence of bacteria on animal development', *Dev Biol*, 242: 1-14.

McKenzie, V. J., R. M. Bowers, N. Fierer, R. Knight, and C. L. Lauber. 2012. 'Co-habiting amphibian species harbor unique skin bacterial communities in wild populations', *ISME J*, 6: 588-96.

Meireles, D. A., J. F. da Silva Neto, R. M. Domingos, T. G. P. Alegria, L. C. M. Santos, and L. E. S. Netto. 2022. 'Ohr - OhrR, a neglected and highly efficient antioxidant system: Structure, catalysis, phylogeny, regulation, and physiological roles', *Free Radic Biol Med*, 185: 6-24.

Meyer-Abich, A. 1943. *Beiträge zur Theorie der Evolution der Organismen* (Brill).

———. 1950. *Beiträge zur Theorie der Evolution der Organismen* (Brill Archive).

Meyer-Abich, Adolf. 1948. *Naturphilosophie auf neuen Wegen* (Hippokrates Verlag).

———. 1963. *Gesitesgeschichtliche Grundlagen der Biologie* (G. Fischer).

Miklos, M., K. Cseri, L. Laczko, G. Kardos, S. Fraune, and J. Tokolyi. 2023. 'Environmental bacteria increase population growth of hydra at low temperature', *Front Microbiol*, 14: 1294771.

Miller, D. J., G. Hemmrich, E. E. Ball, D. C. Hayward, K. Khalturin, N. Funayama, K. Agata, and T. C. Bosch. 2007. 'The innate immune repertoire in cnidaria--ancestral complexity and stochastic gene loss', *Genome Biol*, 8: R59.

Minten-Lange, Timo, and Sebastian Fraune. 2020. 'Hydra and Curvibacter.' in Thomas C. G. Bosch and Michael G. Hadfield (eds.), *Cellular Dialogues in the Holobiont* (CRC Press).

Minten, Timo. 2017. 'Establishment of AHL-sensitive Curvibacter bioreporters', Christian-Albrechts-Universität zu Kiel.

Miyamoto, S., G. E. Ronsein, F. M. Prado, M. Uemi, T. C. Correa, I. N. Toma, A. Bertolucci, M. C. Oliveira, F. D. Motta, M. H. Medeiros, and P. D. Mascio. 2007. 'Biological hydroperoxides and singlet molecular oxygen generation', *IUBMB Life*, 59: 322-31.

Möbius, Karl August. 1877. *Die Auster und die Austernwirthschaft* (Verlag von Wiegandt, Hemple & Parey Berlin: Berlin).

Moeller, A. H., A. Caro-Quintero, D. Mjungu, A. V. Georgiev, E. V. Lonsdorf, M. N. Muller, A. E. Pusey, M. Peeters, B. H. Hahn, and H. Ochman. 2016. 'Cospeciation of gut microbiota with hominids', *Science*, 353: 380-2.

Mone, Y., D. Monnin, and N. Kremer. 2014. 'The oxidative environment: a mediator of interspecies communication that drives symbiosis evolution', *Proc Biol Sci*, 281: 20133112.

Mongkolsuk, S., and J. D. Helmann. 2002. 'Regulation of inducible peroxide stress responses', *Mol Microbiol*, 45: 9-15.

Mongkolsuk, S., W. Praituan, S. Loprasert, M. Fuangthong, and S. Chamnongpol. 1998. 'Identification and characterization of a new organic hydroperoxide resistance

(ohr) gene with a novel pattern of oxidative stress regulation from Xanthomonas campestris pv. phaseoli', *J Bacteriol*, 180: 2636-43.

Montillet, Jean-Luc, Jean-Pierre Agnel, Michel Ponchet, Fabienne Vailleau, Dominique Roby, and Christian Triantaphylidès. 2002. 'Lipoxygenase-mediated production of fatty acid hydroperoxides is a specific signature of the hypersensitive reaction in plants', *Plant Physiology and Biochemistry*, 40: 633-39.

Morgan, M. J., and Z. G. Liu. 2011. 'Crosstalk of reactive oxygen species and NF-kappaB signaling', *Cell Res*, 21: 103-15.

Mukherjee, S., and B. L. Bassler. 2019. 'Bacterial quorum sensing in complex and dynamically changing environments', *Nat Rev Microbiol*, 17: 371-82.

Murillo-Rincon, A. P., A. Klimovich, E. Pemoller, J. Taubenheim, B. Mortzfeld, R. Augustin, and T. C. G. Bosch. 2017. 'Spontaneous body contractions are modulated by the microbiome of Hydra', *Sci Rep*, 7: 15937.

Murugadas, A., M. Zeeshan, K. Thamaraiselvi, S. Ghaskadbi, and M. A. Akbarsha. 2016. 'Hydra as a model organism to decipher the toxic effects of copper oxide nanorod: Eco-toxicogenomics approach', *Sci Rep*, 6: 29663.

Muscatine, L., and H. M. Lenhoff. 1963. 'Symbiosis: On the Role of Algae Symbiotic with Hydra', *Science*, 142: 956-8.

———. 1965. 'Symbiosis of hydra and algae. Ii. Effects of limited food and starvation on growth of symbiotic and aposymbiotic Hydra', *The Biological bulletin*, 129: 316-28.

Nawroth, J. C., C. Giez, A. Klimovich, E. Kanso, and T. C. G. Bosch. 2023. 'Spontaneous body wall contractions stabilize the fluid microenvironment that shapes host-microbe associations', *Elife*, 12.

Neish, A. S. 2013. 'Redox signaling mediated by the gut microbiota', *Free Radic Res*, 47: 950-7.

Nicholson, J. K., E. Holmes, J. Kinross, R. Burcelin, G. Gibson, W. Jia, and S. Pettersson. 2012. 'Host-gut microbiota metabolic interactions', *Science*, 336: 1262-7.

Nyholm, S. V., B. Deplancke, H. R. Gaskins, M. A. Apicella, and M. J. McFall-Ngai. 2002. 'Roles of Vibrio fischeri and nonsymbiotic bacteria in the dynamics of mucus secretion during symbiont colonization of the Euprymna scolopes light organ', *Appl Environ Microbiol*, 68: 5113-22.

Nyholm, S. V., and M. J. McFall-Ngai. 2003. 'Dominance of Vibrio fischeri in secreted mucus outside the light organ of Euprymna scolopes: the first site of symbiont specificity', *Appl Environ Microbiol*, 69: 3932-7.

———. 2004. 'The winnowing: establishing the squid-vibrio symbiosis', *Nat Rev Microbiol*, 2: 632-42.

———. 2021. 'A lasting symbiosis: how the Hawaiian bobtail squid finds and keeps its bioluminescent bacterial partner', *Nat Rev Microbiol*, 19: 666-79.

Nyholm, S. V., E. V. Stabb, E. G. Ruby, and M. J. McFall-Ngai. 2000. 'Establishment of an animal-bacterial association: recruiting symbiotic vibrios from the environment', *Proc Natl Acad Sci U S A*, 97: 10231-5.

O'Hara, A. M., and F. Shanahan. 2006. 'The gut flora as a forgotten organ', *EMBO Rep*, 7: 688-93.

Ochsner, U. A., D. J. Hassett, and M. L. Vasil. 2001. 'Genetic and physiological characterization of ohr, encoding a protein involved in organic hydroperoxide resistance in Pseudomonas aeruginosa', *J Bacteriol*, 183: 773-8.

Pacheco, A. R., and V. Sperandio. 2009. 'Inter-kingdom signaling: chemical language between bacteria and host', *Curr Opin Microbiol*, 12: 192-8.

Pan, X., G. Zhou, J. Wu, G. Bian, P. Lu, A. S. Raikhel, and Z. Xi. 2012. 'Wolbachia induces reactive oxygen species (ROS)-dependent activation of the Toll pathway to control dengue virus in the mosquito Aedes aegypti', *Proc Natl Acad Sci U S A*, 109: E23-31.

Pande, A., T. C. Veale, and A. Grove. 2018. 'Gene Regulation by Redox-Sensitive Burkholderia thailandensis OhrR and Its Role in Bacterial Killing of Caenorhabditis elegans', *Infect Immun*, 86.

Paone, P., and P. D. Cani. 2020. 'Mucus barrier, mucins and gut microbiota: the expected slimy partners?', *Gut*, 69: 2232-43.

Perez, S., R. Talens-Visconti, S. Rius-Perez, I. Finamor, and J. Sastre. 2017. 'Redox signaling in the gastrointestinal tract', *Free Radic Biol Med*, 104: 75-103.

Pessione, E. 2020. 'The Russian Doll Model: How Bacteria Shape Successful and Sustainable Inter-Kingdom Relationships', *Front Microbiol*, 11: 573759.

Petersen, C., I. K. Hamerich, K. L. Adair, H. Griem-Krey, M. Torres Oliva, M. P. Hoeppner, B. J. M. Bohannan, and H. Schulenburg. 2023. 'Host and microbiome jointly contribute to environmental adaptation', *ISME J*, 17: 1953-65.

Peterson, L. W., and D. Artis. 2014. 'Intestinal epithelial cells: regulators of barrier function and immune homeostasis', *Nat Rev Immunol*, 14: 141-53.

Philpott, Delbert E., Alfred B. Chaet, and Allison L. Burnett. 1966. 'A study of the secretory granules of the basal disk of hydra', *Journal of Ultrastructure Research*, 14: 74-84.

Pietschke, C., C. Treitz, S. Foret, A. Schultze, S. Kunzel, A. Tholey, T. C. G. Bosch, and S. Fraune. 2017. 'Host modification of a bacterial quorum-sensing signal induces a phenotypic switch in bacterial symbionts', *Proc Natl Acad Sci U S A*, 114: E8488-E97.

Pietschke, Cleo I. 2015. 'Inter-kingdom communication: quorum sensing and quorum quenching in the metaorganism Hydra', Christian-Albrechts-Universität zu Kiel.

Poole, L. B., and H. R. Ellis. 1996. 'Flavin-dependent alkyl hydroperoxide reductase from Salmonella typhimurium. 1. Purification and enzymatic activities of overexpressed AhpF and AhpC proteins', *Biochemistry*, 35: 56-64.

Previato-Mello, M., D. A. Meireles, L. E. S. Netto, and J. F. da Silva Neto. 2017. 'Global Transcriptional Response to Organic Hydroperoxide and the Role of OhrR in the Control of Virulence Traits in Chromobacterium violaceum', *Infect Immun*, 85.

Rahat, M., and C. Dimentman. 1982. 'Cultivation of bacteria-free Hydra viridis: missing budding factor in nonsymbiotic hydra', *Science*, 216: 67-8.

Reedy, A. R., L. Luo, A. S. Neish, and R. M. Jones. 2019. 'Commensal microbiota-induced redox signaling activates proliferative signals in the intestinal stem cell microenvironment', *Development*, 146.

Rince, A., J. C. Giard, V. Pichereau, S. Flahaut, and Y. Auffray. 2001. 'Identification and characterization of gsp65, an organic hydroperoxide resistance (ohr) gene encoding a general stress protein in Enterococcus faecalis', *J Bacteriol*, 183: 1482-8.

Rocha, B. S., and J. Laranjinha. 2020. 'Nitrate from diet might fuel gut microbiota metabolism: Minding the gap between redox signaling and inter-kingdom communication', *Free Radic Biol Med*, 149: 37-43.

Roffman, B., and H. M. Lenhoff. 1969. 'Formation of polysaccharides by hydra from substrates produced by their endosymbiotic algae', *Nature*, 221: 381-2.

Rohwer, F., V. Seguritan, F. Azam, and N. Knowlton. 2002. 'Diversity and distribution of coral-associated bacteria', *Marine Ecology Progress Series*, 243: 1-10.

Ros-Rocher, N., A. Perez-Posada, M. M. Leger, and I. Ruiz-Trillo. 2021. 'The origin of animals: an ancestral reconstruction of the unicellular-to-multicellular transition', *Open Biol*, 11: 200359.

Rosenberg, E., G. Sharon, and I. Zilber-Rosenberg. 2009. 'The hologenome theory of evolution contains Lamarckian aspects within a Darwinian framework', *Environ Microbiol*, 11: 2959-62.

Rosenberg, E., and I. Zilber-Rosenberg. 2011. 'Symbiosis and development: the hologenome concept', *Birth Defects Res C Embryo Today*, 93: 56-66.

———. 2016. 'Microbes Drive Evolution of Animals and Plants: the Hologenome Concept', *mBio*, 7: e01395.

Rudzka, D. A., J. M. Cameron, and M. F. Olson. 2015. 'Reactive oxygen species and hydrogen peroxide generation in cell migration', *Commun Integr Biol*, 8: e1074360.

Ruhland, B. R., and M. L. Reniere. 2019. 'Sense and sensor ability: redox-responsive regulators in Listeria monocytogenes', *Curr Opin Microbiol*, 47: 20-25.

Ruhlemann, M. C., C. Bang, J. F. Gogarten, B. M. Hermes, M. Groussin, S. Waschina, M. Poyet, M. Ulrich, C. Akoua-Koffi, T. Deschner, J. J. Muyembe-Tamfum, M. M. Robbins, M. Surbeck, R. M. Wittig, K. Zuberbuhler, J. F. Baines, F. H. Leendertz, and A. Franke. 2024. 'Functional host-specific adaptation of the intestinal microbiome in hominids', *Nat Commun*, 15: 326.

Saikolappan, S., K. Das, and S. Dhandayuthapani. 2015. 'Inactivation of the organic hydroperoxide stress resistance regulator OhrR enhances resistance to oxidative stress and isoniazid in Mycobacterium smegmatis', *J Bacteriol*, 197: 51-62.

Salem, H., and M. Kaltenpoth. 2022. 'Beetle-Bacterial Symbioses: Endless Forms Most Functional', *Annu Rev Entomol*, 67: 201-19.

Samatha Jain, M., M. K. Makalakshmi, Dikshita Deka, Surajit Pathak, and Antara Banerjee. 2022. 'Therapeutic Strategies Targeting Wnt/β-Catenin Signaling Pathway in Stem Cells for ROS-Induced Cancer Progression.' in, *Handbook of Oxidative Stress in Cancer: Therapeutic Aspects*.

Sarras, M. P., Jr., M. E. Madden, X. M. Zhang, S. Gunwar, J. K. Huff, and B. G. Hudson. 1991. 'Extracellular matrix (mesoglea) of Hydra vulgaris. I. Isolation and characterization', *Dev Biol*, 148: 481-94.

Sato, Y., M. Kameya, S. Fushinobu, T. Wakagi, H. Arai, M. Ishii, and Y. Igarashi. 2012. 'A novel enzymatic system against oxidative stress in the thermophilic hydrogen-oxidizing bacterium Hydrogenobacter thermophilus', *PLoS One*, 7: e34825.

Schauder, S., and B. L. Bassler. 2001. 'The languages of bacteria', *Genes Dev*, 15: 1468-80.

Schenkelaars, Q., D. Perez-Cortes, C. Perruchoud, and B. Galliot. 2020. 'The polymorphism of Hydra microsatellite sequences provides strain-specific signatures', *PLoS One*, 15: e0230547.

Schieber, M., and N. S. Chandel. 2014. 'ROS function in redox signaling and oxidative stress', *Curr Biol*, 24: R453-62.

Schneider, Karl Canmillo. 1890. 'Histologie von Hydra fusca mit besonderer Berücksichtigung des Nervensystems der Hydropolypen', *Archiv für Mikroskopische Anatomie*, 35: 321-79.

Schröder, K., and T. C. Bosch. 2016. 'The Origin of Mucosal Immunity: Lessons from the Holobiont Hydra', *mBio*, 7.

Schwentner, M., and T. C. Bosch. 2015. 'Revisiting the age, evolutionary history and species level diversity of the genus Hydra (Cnidaria: Hydrozoa)', *Mol Phylogenet Evol*, 91: 41-55.

Shea, R. J., and M. H. Mulks. 2002. 'ohr, Encoding an organic hydroperoxide reductase, is an in vivo-induced gene in Actinobacillus pleuropneumoniae', *Infect Immun*, 70: 794-802.

Shostak, S. 1974. 'The complexity of Hydra: homeostasis, morphogenesis, controls and integration', *Q Rev Biol*, 49: 287-310.

Si, M., T. Su, C. Chen, J. Liu, Z. Gong, C. Che, G. Li, and G. Yang. 2018. 'OhsR acts as an organic peroxide-sensing transcriptional activator using an S-mycothiolation mechanism in Corynebacterium glutamicum', *Microb Cell Fact*, 17: 200.

Si, Y., D. Guo, S. Deng, X. Lu, J. Zhu, B. Rao, Y. Cao, G. Jiang, D. Yu, Z. Zhong, and J. Zhu. 2020. 'Ohr and OhrR Are Critical for Organic Peroxide Resistance and Symbiosis in Azorhizobium caulinodans ORS571', *Genes (Basel)*, 11.

Siebert, S., J. A. Farrell, J. F. Cazet, Y. Abeykoon, A. S. Primack, C. E. Schnitzler, and C. E. Juliano. 2019. 'Stem cell differentiation trajectories in Hydra resolved at single-cell resolution', *Science*, 365.

Sies, H., V. V. Belousov, N. S. Chandel, M. J. Davies, D. P. Jones, G. E. Mann, M. P. Murphy, M. Yamamoto, and C. Winterbourn. 2022. 'Defining roles of specific reactive oxygen species (ROS) in cell biology and physiology', *Nat Rev Mol Cell Biol*, 23: 499-515.

Sies, H., and B. Chance. 1970. 'The steady state level of catalase compound I in isolated hemoglobin-free perfused rat liver', *FEBS Lett*, 11: 172-76.

Sies, H., and D. P. Jones. 2020. 'Reactive oxygen species (ROS) as pleiotropic physiological signalling agents', *Nat Rev Mol Cell Biol*, 21: 363-83.

Sies, Helmut. 2022. 'Oxidativer Stress, Eustress und Distress: H2O2 als Signalmolekül', *BIOspektrum*, 28: 685-90.

Silva, Rcmc, I. B. Ramos, L. H. Travassos, A. P. G. Mendez, and F. M. Gomes. 2024. 'Evolution of innate immunity: lessons from mammalian models shaping our current view of insect immunity', *J Comp Physiol B*, 194: 105-19.

Smirnoff, N., and D. Arnaud. 2019. 'Hydrogen peroxide metabolism and functions in plants', *New Phytol*, 221: 1197-214.

Smith, R. S., S. G. Harris, R. Phipps, and B. Iglewski. 2002. 'The Pseudomonas aeruginosa quorum-sensing molecule N-(3-oxododecanoyl)homoserine lactone contributes to virulence and induces inflammation in vivo', *J Bacteriol*, 184: 1132-9.

Sperandio, V., A. G. Torres, B. Jarvis, J. P. Nataro, and J. B. Kaper. 2003. 'Bacteria-host communication: the language of hormones', *Proc Natl Acad Sci U S A*, 100: 8951-6.

Spooner, R., and O. Yilmaz. 2011. 'The role of reactive-oxygen-species in microbial persistence and inflammation', *Int J Mol Sci*, 12: 334-52.

Staehlke, S., F. Haack, A. C. Waldner, D. Koczan, C. Moerke, P. Mueller, A. M. Uhrmacher, and J. B. Nebe. 2020. 'ROS Dependent Wnt/beta-Catenin Pathway and Its Regulation on Defined Micro-Pillars-A Combined In Vitro and In Silico Study', *Cells*, 9.

Steele, R. E. 2002. 'Developmental signaling in Hydra: what does it take to build a "simple" animal?', *Dev Biol*, 248: 199-219.

Sun, M., M. Lyu, Y. Wen, Y. Song, J. Li, and Z. Chen. 2018. 'Organic Peroxide-Sensing Repressor OhrR Regulates Organic Hydroperoxide Stress Resistance and Avermectin Production in Streptomyces avermitilis', *Front Microbiol*, 9: 1398.

Sun, W., Z. Lu, Z. Zhang, Y. Zhang, B. Shi, and H. Wang. 2022. 'Ozone and Fenton oxidation affected the bacterial community and opportunistic pathogens in biofilms and effluents from GAC', *Water Res*, 218: 118495.

Sun, Y., X. Wang, L. Li, C. Zhong, Y. Zhang, X. Yang, M. Li, and C. Yang. 2024. 'The role of gut microbiota in intestinal disease: from an oxidative stress perspective', *Front Microbiol*, 15: 1328324.

Sztukowska, M., M. Bugno, J. Potempa, J. Travis, and D. M. Kurtz, Jr. 2002. 'Role of rubrerythrin in the oxidative stress response of Porphyromonas gingivalis', *Mol Microbiol*, 44: 479-88.

Tamura, K. 1992. 'Estimation of the number of nucleotide substitutions when there are strong transition-transversion and G+C-content biases', *Mol Biol Evol*, 9: 678-87.

Taubenheim, J., M. Miklos, J. Tokolyi, and S. Fraune. 2022. 'Population Differences and Host Species Predict Variation in the Diversity of Host-Associated Microbes in Hydra', *Front Microbiol*, 13: 799333.

Taubenheim, J., D. Willoweit-Ohl, M. Knop, S. Franzenburg, J. He, T. C. G. Bosch, and S. Fraune. 2020. 'Bacteria- and temperature-regulated peptides modulate beta-catenin signaling in Hydra', *Proc Natl Acad Sci U S A*, 117: 21459-68.

Theis, K. R., N. M. Dheilly, J. L. Klassen, R. M. Brucker, J. F. Baines, T. C. Bosch, J. F. Cryan, S. F. Gilbert, C. J. Goodnight, E. A. Lloyd, J. Sapp, P. Vandenkoornhuyse, I. Zilber-Rosenberg, E. Rosenberg, and S. R. Bordenstein. 2016. 'Getting the Hologenome Concept Right: an Eco-Evolutionary Framework for Hosts and Their Microbiomes', *mSystems*, 1.

Tjaden, B. 2015. 'De novo assembly of bacterial transcriptomes from RNA-seq data', *Genome Biol*, 16: 1.

———. 2020. 'A computational system for identifying operons based on RNA-seq data', *Methods*, 176: 62-70.

Torres, M. A. 2010. 'ROS in biotic interactions', *Physiol Plant*, 138: 414-29.

Trembley, Abraham. 1744. 'Mémoires pour servir à l'histoire d'un genre de polypes d'eau douce, à bras en forme de cornes'.

Tursch, A., N. Bartsch, M. Mercker, J. Schluter, M. Lommel, A. Marciniak-Czochra, S. Ozbek, and T. W. Holstein. 2022. 'Injury-induced MAPK activation triggers body

axis formation in Hydra by default Wnt signaling', *Proc Natl Acad Sci U S A*, 119: e2204122119.

Ulrich, L., C. Giez, L. X. Steiner, U. Hentschel, and T. Lachnit. 2022. 'Adaptive lifestyle of bacteria determines phage-bacteria interaction', *Front Microbiol*, 13: 1056388.

UniProt, Consortium. 2025. 'UniProt: the Universal Protein Knowledgebase in 2025', *Nucleic Acids Res*, 53: D609-D17.

van der Post, S., G. M. H. Birchenough, and J. M. Held. 2021. 'NOX1-dependent redox signaling potentiates colonic stem cell proliferation to adapt to the intestinal microbiota by linking EGFR and TLR activation', *Cell Rep*, 35: 108949.

Vandermaesen, J., B. Lievens, and D. Springael. 2017. 'Isolation and identification of culturable bacteria, capable of heterotrophic growth, from rapid sand filters of drinking water treatment plants', *Res Microbiol*, 168: 594-607.

Varadi, M., S. Anyango, M. Deshpande, S. Nair, C. Natassia, G. Yordanova, D. Yuan, O. Stroe, G. Wood, A. Laydon, A. Zidek, T. Green, K. Tunyasuvunakool, S. Petersen, J. Jumper, E. Clancy, R. Green, A. Vora, M. Lutfi, M. Figurnov, A. Cowie, N. Hobbs, P. Kohli, G. Kleywegt, E. Birney, D. Hassabis, and S. Velankar. 2022. 'AlphaFold Protein Structure Database: massively expanding the structural coverage of protein-sequence space with high-accuracy models', *Nucleic Acids Res*, 50: D439-D44.

Visick, K. L., J. Foster, J. Doino, M. McFall-Ngai, and E. G. Ruby. 2000. 'Vibrio fischeri lux genes play an important role in colonization and development of the host light organ', *J Bacteriol*, 182: 4578-86.

Volker, U., K. K. Andersen, H. Antelmann, K. M. Devine, and M. Hecker. 1998. 'One of two osmC homologs in Bacillus subtilis is part of the sigmaB-dependent general stress regulon', *J Bacteriol*, 180: 4212-8.

Voolstra, C. R., J. B. Raina, M. Dorr, A. Cardenas, C. Pogoreutz, C. B. Silveira, A. R. Mohamed, D. G. Bourne, H. Luo, S. A. Amin, and R. S. Peixoto. 2024. 'The coral microbiome in sickness, in health and in a changing world', *Nat Rev Microbiol*, 22: 460-75.

Wang, H. W., C. H. Chung, T. Y. Ma, and H. C. Wong. 2013. 'Roles of alkyl hydroperoxide reductase subunit C (AhpC) in viable but nonculturable Vibrio parahaemolyticus', *Appl Environ Microbiol*, 79: 3734-43.

Wei, S. L., and R. E. Young. 1989. 'Development of symbiotic bacterial bioluminescence in a nearshore cephalopod, Euprymna scolopes', *Marine Biology*, 103: 541-46.

Wein, T., T. Dagan, S. Fraune, T. C. G. Bosch, T. B. H. Reusch, and N. F. Hulter. 2018. 'Carrying Capacity and Colonization Dynamics of Curvibacter in the Hydra Host Habitat', *Front Microbiol*, 9: 443.

Werren, J. H., L. Baldo, and M. E. Clark. 2008. 'Wolbachia: master manipulators of invertebrate biology', *Nat Rev Microbiol*, 6: 741-51.

Wittlieb, J., K. Khalturin, J. U. Lohmann, F. Anton-Erxleben, and T. C. Bosch. 2006. 'Transgenic Hydra allow in vivo tracking of individual stem cells during morphogenesis', *Proc Natl Acad Sci U S A*, 103: 6208-11.

Wong, Z. S., J. C. Brownlie, and K. N. Johnson. 2015. 'Oxidative stress correlates with Wolbachia-mediated antiviral protection in Wolbachia-Drosophila associations', *Appl Environ Microbiol*, 81: 3001-5.

Wu, T., E. Hu, S. Xu, M. Chen, P. Guo, Z. Dai, T. Feng, L. Zhou, W. Tang, L. Zhan, X. Fu, S. Liu, X. Bo, and G. Yu. 2021. 'clusterProfiler 4.0: A universal enrichment tool for interpreting omics data', *Innovation (Camb)*, 2: 100141.

Xu, H., G. Xuan, H. Liu, H. Liu, Y. Xia, and L. Xun. 2022. 'Sulfane Sulfur Is an Intrinsic Signal for the Organic Peroxide Sensor OhrR of Pseudomonas aeruginosa', *Antioxidants (Basel)*, 11.

Xu, S., E. Hu, Y. Cai, Z. Xie, X. Luo, L. Zhan, W. Tang, Q. Wang, B. Liu, R. Wang, W. Xie, T. Wu, L. Xie, and G. Yu. 2024. 'Using clusterProfiler to characterize multiomics data', *Nat Protoc*, 19: 3292-320.

Yang, L., D. Han, D. Jin, J. Zhang, Y. Shan, M. Wan, Y. Hu, and W. Jiao. 2023. 'Soil physiochemical properties and bacterial community changes under long-term polycyclic aromatic hydrocarbon stress insitu steel plant soils', *Chemosphere*, 334: 138926.

Yu, G., L. G. Wang, Y. Han, and Q. Y. He. 2012. 'clusterProfiler: an R package for comparing biological themes among gene clusters', *OMICS*, 16: 284-7.

Zeeshan, M., A. Murugadas, S. Ghaskadbi, R. B. Rajendran, and M. A. Akbarsha. 2016. 'ROS dependent copper toxicity in Hydra-biochemical and molecular study', *Comp Biochem Physiol C Toxicol Pharmacol*, 185-186: 1-12.

Zeeshan, M., A. Murugadas, S. Ghaskadbi, B. R. Ramaswamy, and M. A. Akbarsha. 2017. 'Ecotoxicological assessment of cobalt using Hydra model: ROS, oxidative stress, DNA damage, cell cycle arrest, and apoptosis as mechanisms of toxicity', *Environ Pollut*, 224: 54-69.

Zhao, J., F. Zhao, J. Yuan, H. Liu, and Y. Wang. 2023. 'Gut microbiota metabolites, redox status, and the related regulatory effects of probiotics', *Heliyon*, 9: e21431.

Zheng, R., Q. Wang, R. Wu, P. N. Paradkar, A. A. Hoffmann, and G. H. Wang. 2023. 'Holobiont perspectives on tripartite interactions among microbiota, mosquitoes, and pathogens', *ISME J*, 17: 1143-52.

Zhou, K., T. Zhang, X. W. Chen, Y. Xu, R. Zhang, and P. Y. Qian. 2024. 'Viruses in Marine Invertebrate Holobionts: Complex Interactions Between Phages and Bacterial Symbionts', *Ann Rev Mar Sci*, 16: 467-85.

Zhou, T., Y. Hu, Y. Chen, K. K. Zhou, B. Zhang, G. Gao, and J. X. Ma. 2010. 'The pathogenic role of the canonical Wnt pathway in age-related macular degeneration', *Invest Ophthalmol Vis Sci*, 51: 4371-9.

Zilber-Rosenberg, I., and E. Rosenberg. 2008. 'Role of microorganisms in the evolution of animals and plants: the hologenome theory of evolution', *FEMS Microbiol Rev*, 32: 723-35.

ZoBell, Claude Ephraim. 1946. *Marine microbiology, a monograph on hydrobacteriology, by Claude E. ZoBell ... Foreword by Selman A. Waksman* (Chronica Botanica Company: Waltham, Mass.).

Acknowledgments

An dieser Stelle möchte ich mich vor allem bei Professor Sebastian Fraune bedanken. Seit Beginn meiner Masterarbeit in Kiel hat er mich mit seiner Fachkompetenz und seiner ansteckenden Begeisterung für die Wissenschaft motiviert und inspiriert - und diese Arbeit überhaupt möglich gemacht. In all den Jahren, in denen ich mit ihm zusammenarbeiten durfte, hat er nicht nur mich, sondern das gesamte Team, stets in jeder Hinsicht unterstützt und uns in unserer wissenschaftlichen Entwicklung gefördert. Ich bin ihm für seine Betreuung und Unterstützung in jeder Situation unendlich dankbar.

Mein Dank gilt ebenfalls Professor Martin Beye, der nicht nur die Mentorenrolle während meiner Zeit in Düsseldorf übernommen hat, sondern auch die Rolle des Zweitgutachters.

Mein ganz besonderer Dank gilt außerdem Hanna Domin, die mich ebenfalls seit meiner Zeit in Kiel begleitet hat. Ohne ihre emotionale, aber auch kritische, fachliche Unterstützung, sowie ihre außergewöhnliche Ruhe und Gelassenheit, wenn sie ein ums andere Mal zu lange Schachtelsätze lesen musste, in denen ich viel zu viele Kommata benutze, wäre diese Arbeit wohl niemals fertig, oder halbwegs lesbar geworden.

Ebenfalls danke ich der gesamten OrgInt-Arbeitsgruppe, insbesondere Jay, Nida, Gaby, Lukas und Liam. Die freundschaftliche Atmosphäre, die fachlichen Diskussionen und die Frage, ob jemand mit mir bouldern kommen möchte, werden mir immer eine schöne Erinnerung bereiten.

Besonderer Dank gilt natürlich auch meinen Eltern und meinem Bruder, die diesen Weg hierhin überhaupt erst möglich gemacht haben. Ich schätze mich sehr glücklich, eine so wundervolle Familie hinter mir zu wissen.

Eidesstattliche Erklärung

Ich versichere an Eides Statt, dass die Dissertation von mir selbständig und ohne unzulässige fremde Hilfe unter Beachtung der „Grundsätze zur Sicherung guter wissenschaftlicher Praxis an der Heinrich-Heine-Universität Düsseldorf“ erstellt worden ist.

Ferner erkläre ich, dass ich in keinem anderen Dissertationsverfahren mit oder ohne Erfolg versucht habe, diese Dissertation einzureichen.

Düsseldorf, den _____